Università degli Studi di Padova

Studies on a new Magnetic Energy Storage and Transfer system: application to the European DEMO Fusion Reactor

RELATORE
PROF. PAOLO BETTINI
UNIVERSITÀ DI PADOVA

CORRELATORE
DOTT. ING. ALBERTO MAISTRELLO
CONSORZIO RFX

LAUREANDO
IACOPO SPRESIAN

ii

A TE,
CHE SEMPRE SARAI NELLA MIA MENTE
E NEL MIO CUORE.

iv

Abstract

The increasing demand for energy to raise the level of well-being of the population and the ever greater quantity of carbon dioxide present in the air that compromises the various life cycles on Earth, require large and zero-emission energy sources. One of the possible solution that may help the humanity in this area is nuclear fusion, the energy of stars. International Tokamak Experiment Reactor (ITER) and European DEMOnstration Fusion Reactor (DEMO) are those experiments that will probably lead us towards this great step of being able to use this carbon free energy source.

DEMO is the first reactor with net production of electricity and, like ITER, is a tokamak type rector where plasma is confined by magnetic field generated by currents in the order of tens of kilo Amperes that flow through superconducting coils. Therefore DEMO besides being a source of electricity is also an enormous load, which requires an active power peak of $\approx 1{,}2 \cdot 10^9$ W. If thyristor converters are used, a reactive power problem arises when the required voltage is low. Indeed, it is estimated that the reactive power demand is $\approx 2 \cdot 10^9$ VAR.

In this thesis these two problems, of peak active power and reactive power, are faced in DEMO, analysing a new system of coils power supply that could replace thyristor converters: MEST system (Magnetic Energy Storage and Transfer system). It consists in having a superconducting coil that stores energy before reactor operations and that during the various phases releases it or takes it to/from the magnets according to the needs of the tokamak. This method allows a certain degree of decoupling from the grid in order to reduce the amount of active and reactive power absorbed by the grid.

The study of MEST is divided into three parts: the first describes the operation principle (chapter 3, section 3.1 and 3.2); the second presents the equations which describe the analytical model of the system and the design of MEST components (chapter 3, section 3.3 and 3.4); in the third part a Simulink® model developed in order to verify the applicability of MEST system to one of the DEMO coils is presented (section 4.1 and 4.3); finally the simulation results are commented highlighting the critical issues (section 4.4) and the advantages of MEST with respect to the traditional thyristors converters power supplies in terms of active and reactive power demand (section 4.5).

Sommario

La sempre maggior richiesta di energia per innalzare il livello di benessere della popolazione e la sempre maggior quantità di anidride carbonica presente nell'aria che compromette i diversi cicli vitali della Terra, richiedono fonti di energia di grossa entità e a emissioni zero. Una delle possibili soluzione a lungo termine che potrà essere d'aiuto all'umanità in questo ambito è la fusione nucleare. International Tokamak Experiment Reactor (ITER) e European DEMOnstration Fusion Reactor (DEMO) sono quegli esperimenti che probabilmente ci porteranno verso questo grande passo di riuscire a imbrigliare l'energia delle stelle.

DEMO è il primo reattore con una produzione netta di elettricità e, come ITER, è un rettore di tipo tokamak dove il plasma è confinato da un campo magnetico prodotto da correnti enormi dell'ordine di decine di kilo Amperes che attraversano le bobine superconduttorici. La potenza necessaria per questo tipo di funzionamento è elevatissima e perciò DEMO prima di essere una fonte di energia elettrica è anche un carico estremamente grande che richieda come picco di potenza attiva una quantità di $1{,}2 \cdot 10^9$ W. Se venissero usati i convertitori a tiristori nascerebbe un problema di potenza reattiva quando la tensione richiesta è esigua. Infatti in DEMO è stato stimato che utilizzando la stessa tecnologia di ITER la domanda di potenza reattiva ammonterà a $2 \cdot 10^9$ VAR.

In questa tesi si affrontano in DEMO questi due problemi, di picco di potenza attiva e della potenza reattiva, analizzando un nuovo sistema di alimentazione delle bobine che potrebbe soppiantare i convertitori a tiristori: il MEST (Magnetic Energy Storage and Transfer system). Consiste nell'avere una bobina superconduttore che immagazzina energia prima del funzionamento del reattore e che durante le varie fasi la rilascia o la prende ai/dai magneti in base alla necessità della macchina. Questo metodo permette un certo grado di disaccoppiamento dalla rete così da ridurre le quantità di potenza attiva e reattiva assorbite dalla rete.

Lo studio del MEST è suddiviso in quattro parti: nella prima parte si descrive il principio di funzionamento (capitolo 3, sezioni 3.1 e 3.2); nella seconda parte si presentano le equazioni che descrivono il modello analitico del sistema e si progettano i componenti del MEST applicati a DEMO (capitolo 3, sezioni 3.3 e 3.4); nella terza parte è presentato il modello Simulink® sviluppato per verificare la fattibilità del MEST applicato a DEMO e sono mostrati i risultati delle simulazioni con le forme d'onda richieste dal tokamak (section 4.1 and 4.3); infine vengono discussi i risultati delle simulazioni identificando gli aspetti critici (section 4.4) e i vantaggi del MEST in confronto all'alimentazione fornita dai convertitori a tiristori in termini di potenza attiva e reattiva richiesta (section 4.5).

Contents

Listing of figures

Listing of tables

Listing of acronyms

AFE . . . . Active Front End

BD . . . . BreakDown phase

CCS . . . . Carbon Capture and Storage

CPSS . . . . Coils Power Supply System

CS . . . . Central Solenoid

DC . . . . Direct Current

DEMO . . . . European DEMOnstration Fusion Reactor

DT . . . . Dwell Time phase

DTT . . . . Divertor Tokamak Test

ESS . . . . Energy Storage System

FDU . . . . Fast Discharge Unit

FTU . . . . Frascati Tokamak Upgrade

FW . . . . First Wall

GHG . . . . Green House Gasses

HB . . . . Hysteresis Band

HV . . . . High Voltage

IFMIF . . . . International Fusion Materials Irradiation Facility

IGCT . . . . Integrated Gate-Commutated Thyristor

ITER . . . . International Tokamak Experiment Reactor

JET . . . . Joint European Torus

JT-60SA . . . . Japan Tokamak 60 Super Advanced

KCL . . . . Kirchhoff's Current Law

LB . . . . Lower Bond

LV . . . . Low Voltage

MEST . . . . Magnetic Energy Storage and Transfer system

MV . . . . Medium Voltage

NBI . . . . Neutral Beam Injectors

PES . . . . Plant Electrical System

PF . . . . Poloidal Field coils

PPEN . . . . Pulsed Power Electrical Network

PS . . . . Power Supply

PSS . . . . Power Supply System

QPC . . . . Quench Protection Circuit

RCHG . . . . Recharge phase

RD . . . . Ramp-Down phase

RPC&HF . . . . . . Reactive Power Compensation and Harmonic Filter

RU . . . . Ramp-Up phase

SMES . . . . Superconducting Magnetic Energy Storage

SNU . . . . Switching Network Unit

TC . . . . Tank Coil

TF . . . . Toroidal Field coils

UB . . . . Upper Bond

1

Energy problems and the role of fusion

1.1   INTRODUCTION

The climate change is one of the most critic difficulties which the human being has to oppose in this century to allow his own survival on the Earth.

It is well known that rising temperature, ocean acidification, sea level rise and other many changes are due to the anthropogenic effect. The figure 1.1 represents how the temperature had been increased until 2000 and the measurements of some different reasons which could be responsible of this growth: the anthropogenic influence is the reasonable first choice to be added as the main cause to the temperature growth. The problem did not end in 2000, like someone could understand from the figure 1.1, but it continues up to now with heavier intensity [1].

Emissions of greenhouse gasses (GHG), cause of temperature changes, are mostly due to the fossil fuel combustion, which is widespread in the human activities, like energy production or transport. Focusing on the energy generation, the figure 1.2 shows the plants type mix and it is not cheering: more than half Watts-per-hour are produced by fossil fuels . Moreover the steadily increasing demand for new electric energy does not help to reduce the emissions of GHG but instead enhances the problem because there are very few options to generate electric power in a environmentally friendly way and all these manners have their own disadvantages:

1. Hydroelectric plants are a good resources of green energy due to their large amounts
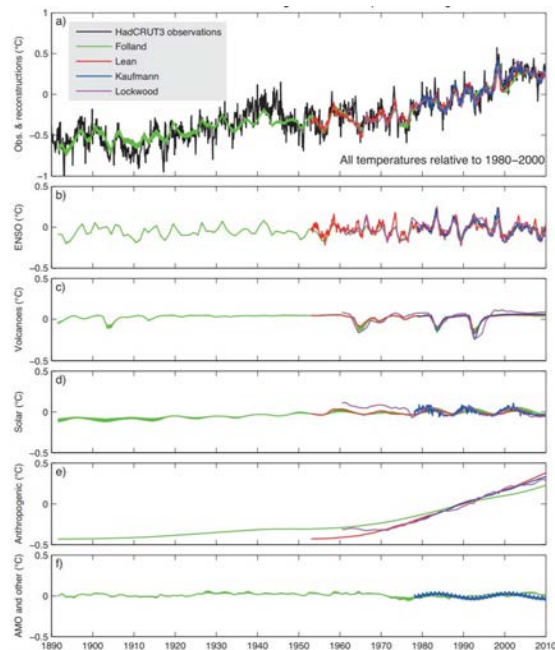
Figure 1.1: Variation of the observed global mean surface temperature [1]

of power generated, they can produce continuously for the base load and the reserves are actually infinite; in the other hand most of the suitable sites are already used and new dams could have some environmental issues (flooding lands, hydrogeological instability).

2. Solar power (photovoltaic cells and concentrating solar power plants) is unreliable and is not clearly predictable because of its weather dependence; its power density is very low; it is expensive; the photovoltaic use (as a big power plant) reduces the stability of the grid. Associated to some sort of energy storage (chemical or flow batteries, flywheels), it could be an important CO_2 free source but the integration in the grid is not ready yet.

3. Wind power presents the same solar power disadvantages but another one has to be added to the list: the power range; indeed too much o too little wind does not permit electric generation. Moreover modern windmills are noisy and could be not aesthetically accepted by general public.

4. Nuclear power by fissioning of the uranium isotope U^{235} is the best option to substitute fuel fossil plants as base load. Nevertheless nowadays it does not represent the main energy source because of its political issues: with the right technology any government (dictatorship, group of terrorist, unstable democracy) could create a nuclear

bomb; moreover in some countries the population does not accept it for its danger-
ousness (which the technology has already largely reduced).

Scientists are trying to think new paradigms to overcome the GHG emissions: carbon
capture and storage (CCS), smart grid (where electric vehicles, buildings, energy production
are integrated together by a central control unit to reach the maximum efficiency), energy
from tides and sea currents and waves, *etc.* [14]. All this new technologies are solutions to
reduce CO_2 emissions today or in the near future, however they could not be the solution
to long-term electric energy demand. *Thermonuclear fusion*, instead, could have its chances
to reset human dangerous emissions (not only GHG but also particulate and other harmful
substances) and to fulfil a large part of the world energy demand.
The human race have done a lots to reach this worrying situation, avoiding evident signals of
environmental changes, and nowadays new generations must put the human condition right.
Fusion technology will not be ready until 2060 (if everything goes right) and it will take lots
more years to built reactors and to substitute entirely fossil fuel plants, so that a transition
period must be considered: nuclear fission energy could become a mandatory resource, effi-
ciency should be improved, all type of CO_2 free energy generation should be integrated in
the present mix.
Nuclear power by fusing atoms, the stars power, is probably the best chance for human race
to avoid the climate change in long term future and for that reason it will be discussed in the
next section.
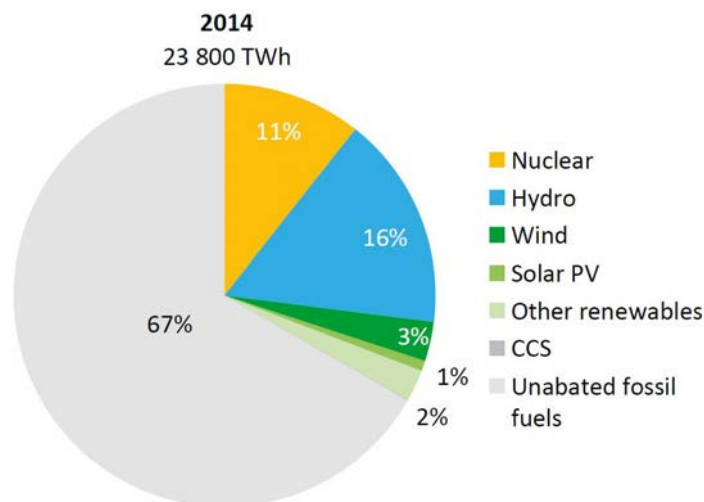
Figure 1.2: Power generation mix in 2014 [2]

To understand how the fusion reaction works, firstly it is necessary to comprehend what the *binding energy* is, secondly why the binding energy has the shape it does and finally which quantities are important to evaluate the power reaction [3].

What the binding energy is   Each elements in the periodic table with mass number A, whose nucleus contains N neutrons e Z protons, present a mass difference:

$$Nm_n + Zm_p > m_a \tag{1.1}$$

This mass difference is transformed in what is called *binding energy* (Einstein's equation $E = mc^2$ explains how this transformation is possible): it is the force which holds the nucleus together and it is the quantity which has to be overcome to break it apart into its components. This type of force classifies into three groups the chemical elements: heavy, light and stable atoms. The latter group has the highest value of energy and with these type of atoms any nuclear reaction is rather impossible due to the difficulties to initialised the reaction (binding energy is too high) and due to the very small energy released. Uranium belongs to the first group, which is positioned at the end of curve of binding energy, and it can be used to produce a fission nuclear reaction. Hydrogen and Helium join the light atoms and they can be used to produce a fusion nuclear reaction. Light and heavy atoms are suitable to nuclear reactions because of their simpler initialisation (binding forces are weaker than those of stable elements) and because they release more energy.

It is possible to quantify the power emitted by a reaction making use of the Einstein's equation. Indeed if the reactants are named A_k, with k goes from 1 to n number of reactants, and the products are named B_h, with h goes from 1 to s number of products, the released energy will be:

$$E = \left(\sum_{k=1}^{n} m_{Ak} - \sum_{h=1}^{s} m_{Bh} \right) c^2 \tag{1.2}$$

where m_{Ak} are the masses of the reactants, m_{Bh} are the masses of the products and c is the speed of light. An example of fusion reaction is D-T reaction in which a deuterium and a tritium (isotope of hydrogen respectively H^2 and H^3) are involved:

$$D + T \longrightarrow \alpha + n + 17.6 \text{ MeV} \tag{1.3}$$
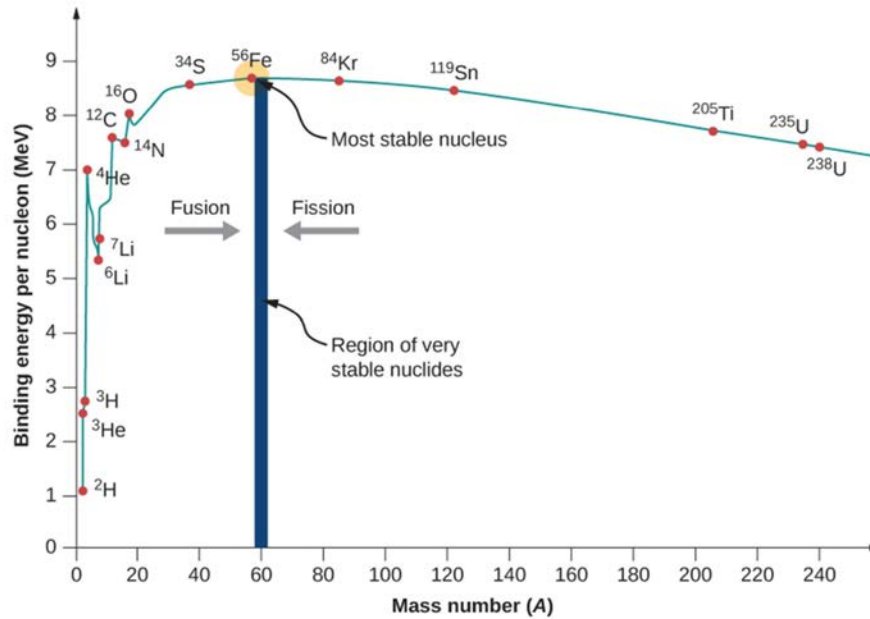
Figure 1.3: Binding Energy per nucleon mass against mass number

where α is $_2\text{He}^4$ and n is a neutron. The released energy corresponds to a 3.52 MeV per nucleon and macroscopically to $338 \cdot 10^6$ MJ/kg with a gain of a factor $\approx 10^7$ compared to gasoline (40 MJ/kg).

BINDING ENERGY CURVE SHAPE   Binding energy per nucleon is represented in figure 1.3 and it has the shape it does (with the maximum corresponding to iron with $A \approx 56$) because of two different forces acting on the particles of the nucleus: the strong short-range nuclear force and the weak long-range Coulomb force.

To make a fusion reaction happen it is necessary that the nuclei of two elements are very close to each other, more or less within a nuclear diameter. Nevertheless the ions we would like to fuse are positive, thus the Coulomb force occurs and the two charges repulse each other. What helps us to reach the fusion is that within a certain distance, named r_m, the strong short-range nuclear force becomes dominant and overcomes the repulsive force making it opposite, i.e. attractive. The figure 1.4 explains the evolution of the relation between the Coulomb and strong nuclear force.

The figure 1.5 represents the potential energy and shows glaringly the so called *Coulomb barrier*. It is the needed energy (the maximum in the graph) to let the strong force be prevalent
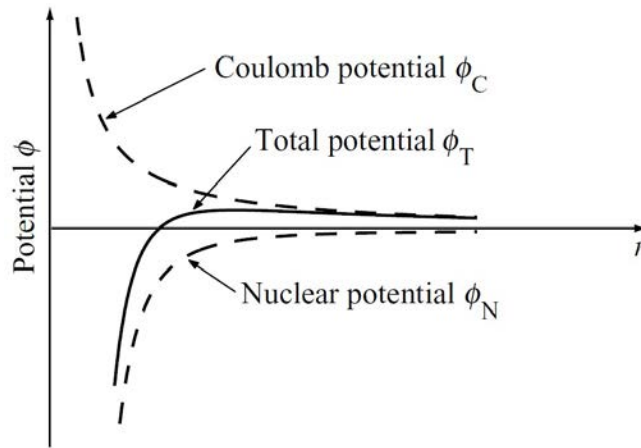
Figure 1.4: The Coulomb, nuclear and total potential against radius [3]

and, with the classic electrostatic theory, it can be calculated by the following equation:

$$U(r) = \frac{Z_1 Z_2 e^2}{4\pi \epsilon_0 r} \tag{1.4}$$

where Z_1 and Z_2 are the respective charge or atomic number, e is the unit charge, ϵ_0 is the dielectric constant into the void and r is the distance between the centres of the charges. If $r = r_m \approx 5 \cdot 10^{-15}$ m the potential energy is the Coulomb barrier and for a D-T reaction, where $Z_1 = Z_2 = 1$, is equal to $U(r_m) \approx 288\,\text{keV}$.

THE MAIN QUANTITIES OF THE NUCLEAR REACTION   There are four main quantities which characterize the nuclear reaction: cross section, mean free path and collision frequency describe the microscopic physics; reaction rate describes the macroscopic physics.

The cross section represents, in a certain way, the likelihood that two atoms will undergo a nuclear fusion reaction. It is said in the previous paragraph that the strong nuclear force acts within a distance. Now you think to a target particle (a sphere) surrounded by a sort of spherical field and a incident particle with its velocity v, like in the figure 1.6. The section of the field of the target particle perpendicular to v is the cross section σ. If the incident particle goes through it then a nuclear reaction occurs, in the other cases, it is too far from the target atom or if collides with the target atom, no reaction takes place. But the value of σ is not easy to calculate because of its dependence on the relative velocity of the two atoms. The figure 1.7 (where 1 barn $= 10^{-24}$ cm^2) shows the trend of σ, function of the kinetic deuteron energy

6
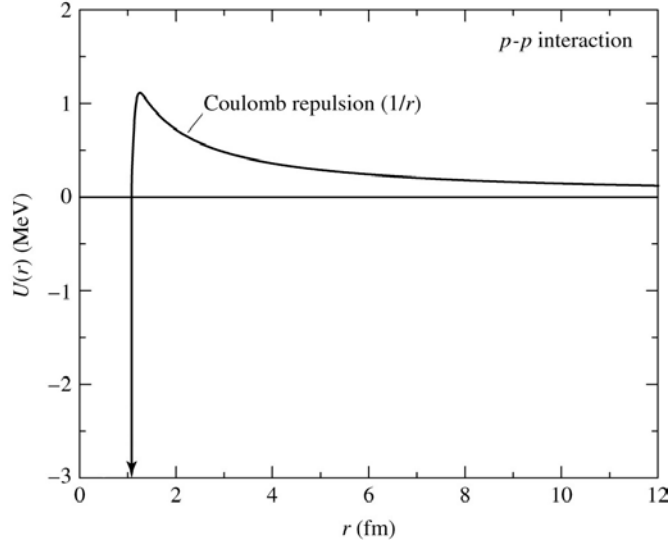
Figure 1.5: The Coulomb barrier

(i.e. the velocity of the incident particle).

The mean free path, indicated with λ_m, can be easily calculated [vedi 3] and its value is $\lambda_m = 1/n_1\sigma$ where n_1 is the number density of the target particles. It has the meaning of the average distance which a incident particle covers before a collision occurs and, moreover, it indicates the decay constant of the incident particles flux which has not reacted yet (the relation is $\Gamma = \Gamma_0 \exp^{-x/\lambda_m}$).

The collision frequency, and its inverse the collision time (or better the average time between collisions), are simply:

$$\tau_m = \frac{\lambda_m}{v} = \frac{1}{n_1\sigma v} \qquad \nu_m = \frac{1}{\tau_m} = n_1\sigma v \tag{1.5}$$

where v is the incident particle velocity. The evaluation of ν_m serves to indicate how much the reaction is difficult to be produced.

These three quantities are included in the concept of the reaction rate R_{12}: it indicates the number of fusion collisions per unit volume per unit time. It can be easily calculated by thinking of a incident particles ($n_2 A dx$) which pass through the target volume in a time $dt = dx/v$. Denoting with dF the total area blocked by target particle, calculated by $dF = \sigma N_1/A = \sigma n_1 dx$ (where N_1 is the particles number, A is the cross sectional area),

7
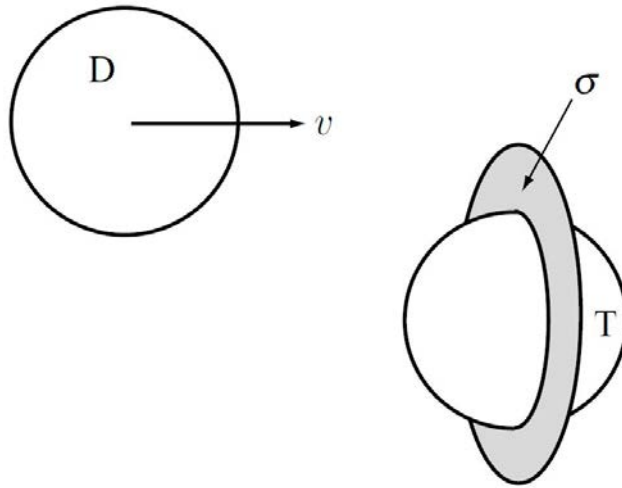
Figure 1.6: The cross section σ [3]
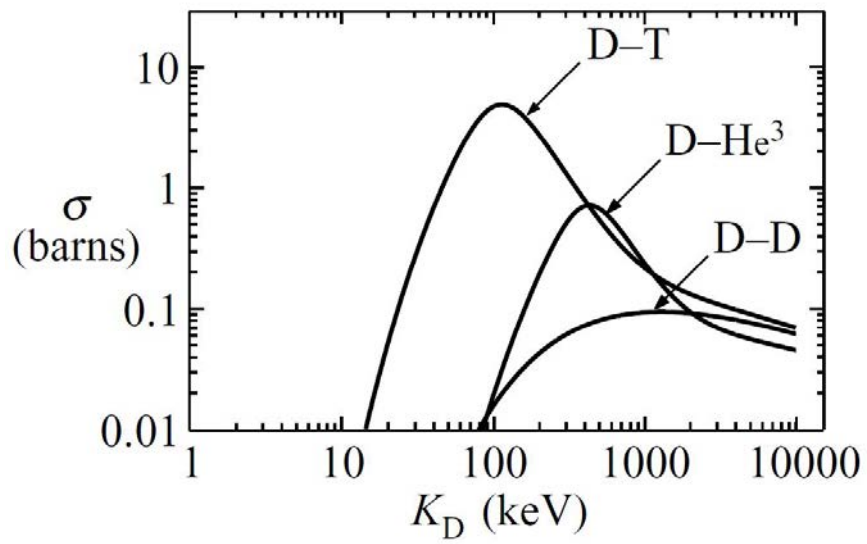
Figure 1.7: The cross section σ against kinetic deuteron energy ($K_D = m_d v_d^2/2$) [3]

the collision number is computed by dFn_2Adx and, thus, the reaction rate is:

$$R_{12} = \frac{dFn_2Adx}{Adxdt} = \sigma n_1 n_2 \frac{dx}{dt} = n_1 n_2 \sigma v \qquad (1.6)$$

The equation 1.6 could be made more detailed taking into account that the target particles have their own velocity, so that the speed used in the equations should be the relative speed between target and incident particles. Moreover the cross section (as said before) depends on the relative velocity $\sigma = \sigma(|\boldsymbol{v_1} - \boldsymbol{v_2}|)$, so that the mean value $\langle \sigma v \rangle$ has to be considered in the reaction rate equation. It is important to underline that, with a fixed density $n = n_1 + n_2$, the maximum reaction rate is reached when $n_1 = n_2 = n/2$.

NUCLEAR REACTION   To conclude, the first point to underline is that the nuclear reaction is an event which has a likelihood to occur only under certain constrained conditions of velocity and of cross section and which two atoms fuse in together to generate another element and to release particles. These parameters are achieved through the utilization of a plasma with its density (n), with a characteristic time τ_e (indicating the lost energy for transport) and at a temperature (20 keV) hotter than the core of the Sun. The product of the three mentioned quantities is the so called *triple product*. It has to be $\approx 6 \cdot 10^{19}$ m^3 s keV to reach the breakeven condition (condition in which thermal power is equal to the external power -for more details see [3, cap. 4]-).
The second and last point is the energy: the released energy is the mass difference between the reactants and the products (is calculated in 1.2). Thus, from the evaluation of the energy, the thermonuclear power can be computed through the reaction rate. The power estimate lets us make a thermal equilibrium between the losses and the sources, which brings to the evaluation of the characteristic time.
Studying and understanding physic of fusion was a step to a fusion nuclear reactor, another one is to take advantage of and control the reaction.

1.3   FUSION ON EARTH

Fusion on Earth, as seen above, can occur only if the triple product of plasma is very high, above all if the temperature is higher than sun core temperature. For this fusion reaction can be operated only in some special reactors, whose differences depend on diverse type of plasma confinement. Those most studied are: magnetic mirror, stellarator and tokamak. The first (figure 1.8a) is an open plasma confinement, that is a straight machine in which ion-

ized particles go from an edge to another. Magnetic field on edges have to be more intense than in the centre area and have to be intense enough to inverse particles speed. Nevertheless this plasma confinement has a low efficiency because lots of ions are lost at the machine edges.

The second (figure 1.8b) is a closed plasma confinement, that is a machine with torus geometry. It is very close to the tokamak but differs for how the confining magnetic field is reached: stellarator uses helical coils. The largest reactors of this type are the Large Helical Device (LHD) in Japan and the Wendelstein 7-X (W7-X) in Germany. It is not the first choice to adopt in next future as fusion reactor because of its complexity and because the machine structure is bigger than a tokamak for the same plasma volume.

The last (figure 1.8c) is a closed plasma confinement like stellarator but it presents Toroidal Field (TF) and Poloidal Field (PF) coils to control and to confine the conductor gas. Both the tokamak and stellarator use a Central Solenoid (CS) to induce current into the plasma: CS works as a transformer, with flux variation it induces a voltage on plasma considered as secondary winding. TF coils need to provide the magnetic field which creates the elliptic trajectory of ions and which tries to prevent the particles from crashing into the first wall following torus geometry; PF coils need to provide the magnetic field which compensates the vertical stability (to elaborate on why there are so many instabilities see [3, cap 8]).

Between the three alternatives, tokamak reactor is the most promising machine to reach a fusion nuclear plant. The beginning of tokamak is dated 1950 and since then scientists have designed and built reactors bigger and bigger (Joint European Torus -JET- in United Kingdom, Frascati Tokamak Upgrade -FTU- in Italy, Japan Tokamak 60 Super Advanced - JT-60SA - in Japan must be cited). The last designed project is ITER (International Thermonuclear Experimental Reactor) and it is under construction in Cadarache, France. It should be functional in 2025 and its aim is to produce net power. Table 1.1 sums up the main quantities to describe ITER. At the same time as the construction of ITER, another project is being studied, that is DEMO, which will be described in section 2.

Tokamak operation is very complex and comprehends lots systems which have to be integrated together. All systems aim to maximize the likelihood that fusion reaction occurs. For this reason a certain plasma conditions, dictated by the triple product, must be reached. For example, in ITER tokamak temperature must arrive to $150\,°C$ and for entire operation this value must be maintained to extract energy. It is necessary to heat so much the plasma to get to these conditions that one single heating source can not supply such energy. Main heating sources are: plasma itself because, being a conductor, it has its resistance, thus the first heat-

ing contribution is ohmic losses; Neutral Beam Injectors (NBI) provides a very high energy uncharged beam which, by collisions between neutral particles coming from NBI and ions, exchange its power to plasma charged particles; high-frequency electromagnetic heating system uses resonance frequency of ions (40 to 50 MHz) and electrons (170 GHz) to transfer energy to particles [15].

An important thing not mentioned up to now is that the nuclear reaction can only take place in an environment without impurities, *i.e.* only in the presence of deuterium and tritium because other molecules would negatively affect the reaction. This provides the possibility of introducing a fundamental system, which is the vacuum system (VS). VS has the task of ensuring an exceptional initial vacuum degree (10^{-5} Pa), of introducing reaction products (as fuel) and of eliminating impurities when they are formed due to the interactions between plasma and first wall. In addition, the vacuum system is integrated with the cryogenics plant, which cools and maintains the supercapacitors at about (between 5 and 20 K).

Another component to consider in the description of a tokamak is the first wall (FW). FW is the structure that faces the plasma and its first aim is safety, that is to protect the outside of the vacuum chamber from radiation and plasma energy. Moreover, in contact with the plasma (when gas is not perfectly confined) it must be able not to melt and must not have chemical reactions that can introduce into the plasma impurities. Furthermore, its other functions are to recover the energy of the plasma and exchange it with a fluid that then generates electricity (this operation is carried out by the divertor); to provide tritium necessary for fusion through the deuterium-lithium reaction; finally it must be optimized to contain the plasma and all the systems necessary for reactor operation.

All these systems serve to produce energy by fusion reaction, but initially they need power, so that they are loads for the grid. Therefore, a plant electrical system is necessary both to get and to supply energy from and to the grid (respectively). It will be discussed in more detail in next chapter.

Fusion is by itself a difficult reaction to occur; fusion on Earth is a project so complex that it seems to be impossible. But with ITER first and DEMO after, humanity could reach stars power.

Table 1.1: ITER main parameters

	value
Total fusion power	$500\ MW$
Q (fusion power/input power)	≥ 10
Average neutron wall loading	$0.57\ MW/m^2$
Plasma inductive burn time	$\geq 400\ s$
Plasma major radius	$6.2\ m$
Plasma minor radius	$2.0\ m$
Plasma current	$19\ MA$
Plasma volume	$837\ m^3$
Plasma surface	$678\ m^2$
Installed auxiliary heating	$73\ MW$
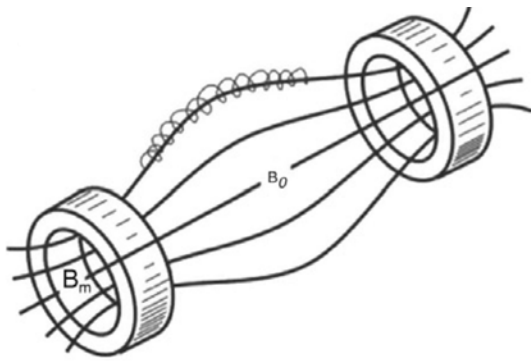
(a) Magnetic mirror machine
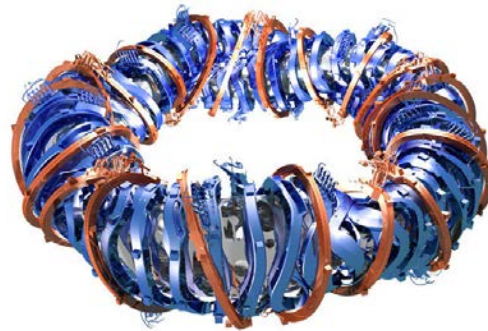
(b) Stellarator machine
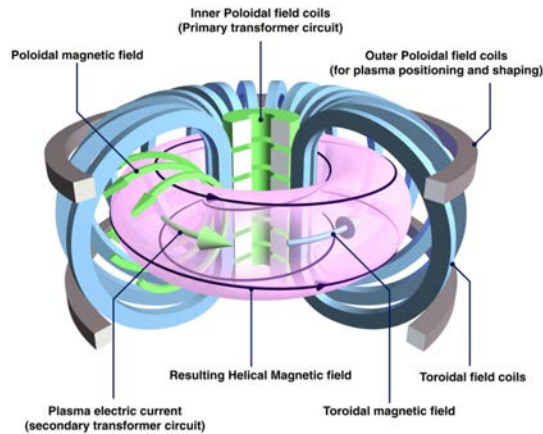
(c) Tokamak machine

2

The European DEMOnstration Fusion Reactor

The European DEMOnstration Fusion Reactor (DEMO*) is a EU agency EUROfusion research project which aims to produce electric energy by the nuclear fusion reaction and to deliver that generated power to the grid by 2060. DEMO will be the intermediate fusion plant between ITER and a first-of-a-kind commercial fusion plant. ITER is going to study deeply the physic behind the fusion reaction and should prove the feasibility of the production of net electric energy; DEMO should deliver the net energy produced to the grid and should give input to verify the economical convenience. The roadmap [4] fixes the path for the fusion research and the goals of DEMO, which can be summed up with the following list [5]:

- Conversion of fusion heat into electric energy (≈ 500 MWe)

- Operating with tritium self-sufficiency

- Reasonable availability up to several full power years

- Minimize activation waste, no long-term activated materials storage

- DEMO as a pathfinder to the first fusion power plant

---

*In the world there are many projects named DEMO and are all independent; this thesis refers strictly to the European project.

Reaching these goals means to solve some essential issues, which are the foundation of all other systems because they influence the design and the feasibility of DEMO. Some of these fundamental components are described.

The divertor is that component which is in the bottom of the vessel and has to remove heat and impurity particles. Thermal load would be so high that its peak could reach 20 MW/m². Divertor problems are the development of a novel structure and testing new materials (such as W or CuCrZr alloy) [16].

Another essential challenge is the breeding blanket, which comprehends those components facing the plasma and those immediately behind. Together with the first wall (facing-plasma component), it should permit tritium self-production, power extraction and radiation protection. The first two tasks have never been tested in any previous experiments, so that you understand the importance of studying this component. The breeding blanket should bear to an environment extremely dangerous due to high magnetic field, high energy neutrons, high pressure, etc.; it should hold up a very high thermal load with sharp gradient; it should provide tritium self-sufficiency. Also other objectives are related to the breeding blanket, but the theme is not concerning to this thesis and they are not discussed (to elaborate on see [17] and [18]).

These challenges are so complex to fully understand that EUROfusion agency came up with a design approach to DEMO which is constituted by three phases (figure 2.1): a pre-conceptual design phase, which should evaluate and develop more possible options and should end in 2020; a conceptual design phase, which should upgrade and validate the main ideas of the previous phase and should end in 2027; a engineer design phase, which should improve precisely the design and should start the major procurement activities. The figure 2.1 fixes the idea of what the design approach is. Obviously DEMO project is not isolated but interacts actively with ITER and the other fusion experiments in the world (JET, JT-60SA, FTU, new experiment on divertor -DTT- and other tokamak facilities which contribute to the research of single parts of a reactor, such as IFMIF – International Fusion Materials Irradiation Facility- or MITICA -which is a NBI-).

2.1 Main features of DEMO project

DEMO is a project which should overcome ITER both with further tasks to be obtained (already seen above) and size to be increased. Table 2.1 shows the main features and performances to be obtained in this plant [12] which characterize the size of DEMO. In particular
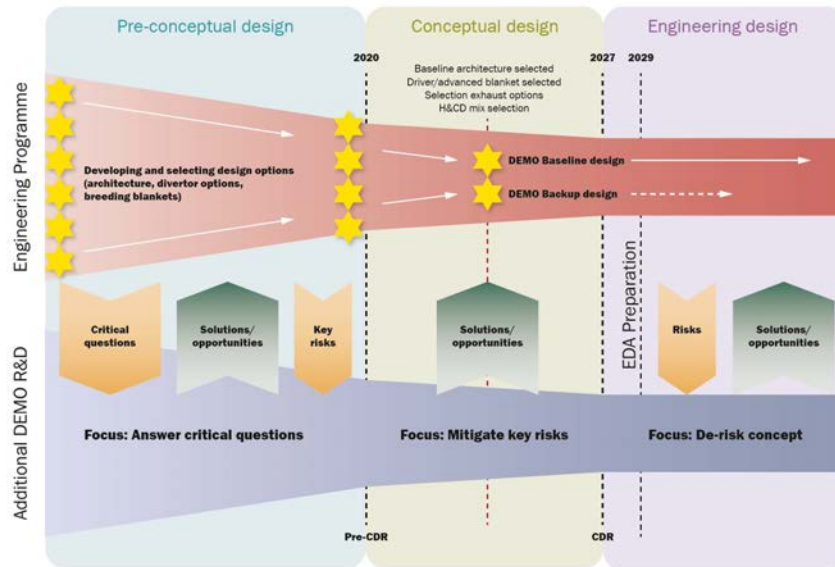
Figure 2.1: DEMO design approach [4]

from figure 2.2, you can notice the difference of plasma volume of different tokamaks: DEMO plasma volume should be bigger two times than ITER one and 30 times than JET (the biggest tokamak currently in operation). Consequently this feature implies a bigger vacuum vessel and a bigger plasma confinement and equilibrium system (magnets). To give an idea of its size, in table 2.2 size and coils positions are presented (referring to figure 2.3), where R is the abscissa of middle point of magnet considered, DR is the width of coils take into account, Z is the vertical axis of middle point of magnet considered and DZ is the height of coils taken into account. In figure 2.4 are shown schematic poloidal and toroidal cross sections of DEMO built by PROCESS.

Magnets systems (coils) is a part of the Plant Electrical System, that will be described in next section for its important role in this thesis.

As for DEMO operation, its main goal is that of providing constant energy output, which means to operate in a steady state functioning. Actually, today, this task can not be considered feasible for technological reasons, mostly for limits of materials, which can not bear all neutrons energy of fusion reaction [19]. Thus pulsed operation is current field of studies and those phases that concern this thesis are described below:

- Ramp-Up (RU), in which in the first few seconds plasma is activated (sub-phase called BreakDown -BD-) and then a voltage is induced in the plasma to let its current grow until the current value for the next phase is reached;
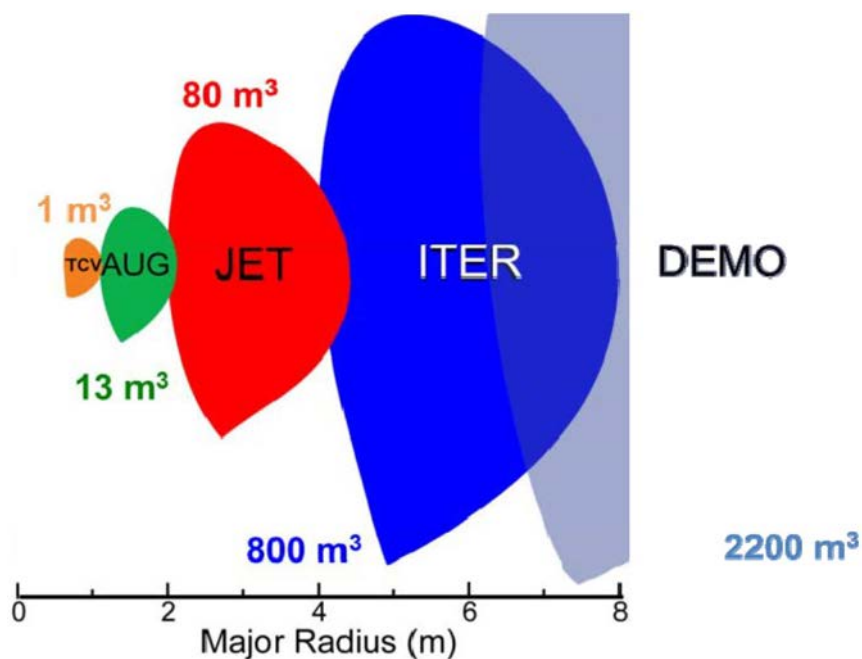
Figure 2.2: Sizes of major radius and plasma volume of different tokamaks [5]

Table 2.1: DEMO main parameters [12]

Characteristics	Value
Aspect ratio	3.1
Major/minor radius (m)	9.0/2.9
Plasma current (MA)	18.0
Elongation/triangularity (95%)	1.59/0.33
Toroidal field, axis/coil-peak (T)	5.9/ > 12.5
Auxiliary heating power – flat top (MW)	50

Performance	Value
Fusion power (MW)	2000
Electric Output (MW)	500
Neutron wall loading (MW/m²)	1.04
Volt-sec capability/Volt-sec for burn (Vs)	728/365
Loop voltage (V)	0.048
Av. electron temperature (keV)	12.6
Av. electron density (10^{20}m³)	0.73
Plasma stored energy (GJ)	1.181
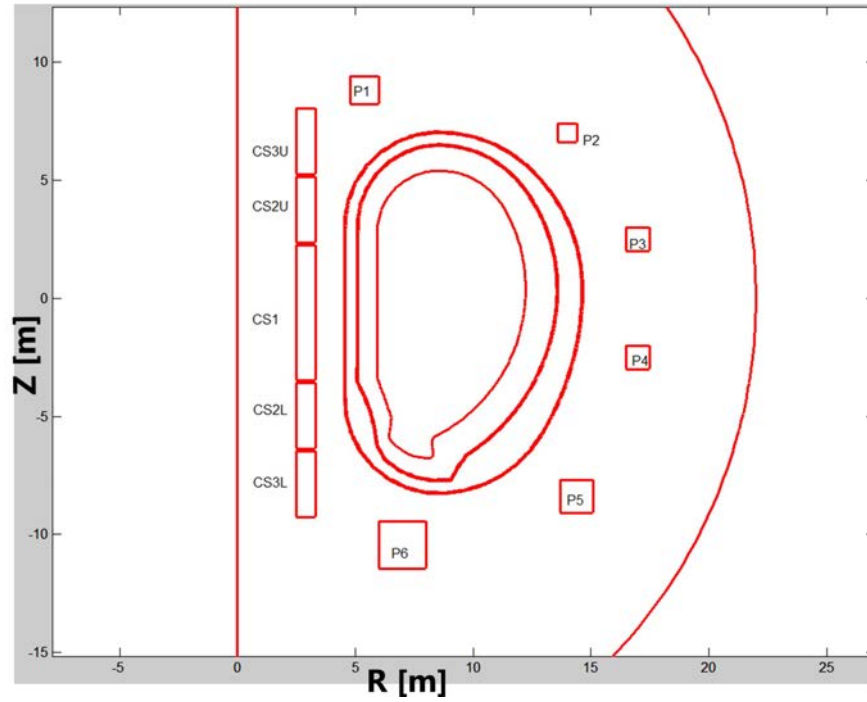
Figure 2.3: DEMO poloidal cross section with coils position [6]

Table 2.2: Coils position referring to figure 2.3 [6]

	R [m]	Z [m]	DR [m]	DZ [m]	Area [m2]	Turns
CS3U	2,900	6,6574	0,8000	2,8072	2,2458	630
CS2U	2,900	3,7503	0,8000	2,8072	2,2458	630
CS1	2,900	-0,6105	0,8000	5,7143	4,5714	1260
CS2L	2,900	-4,9713	0,8000	2,8072	2,2458	630
CS3L	2,900	-7,8784	0,8000	2,8072	2,2458	630
P1	5,400	8,8200	1,2000	1,2000	1,4400	400
P2	14,000	7,0000	0,8000	0,8000	0,6400	200
P3	17,000	2,5000	1,0000	1,0000	1,0000	280
P4	17,000	-2,5000	1,0000	1,0000	1,0000	280
P5	14,400	-8,4000	1,4000	1,4000	1,9600	545
P6	7,000	-10,4500	2,0000	2,0000	4,0000	1100

(a) Poloidal cross section of DEMO

(b) Toroidal cross section
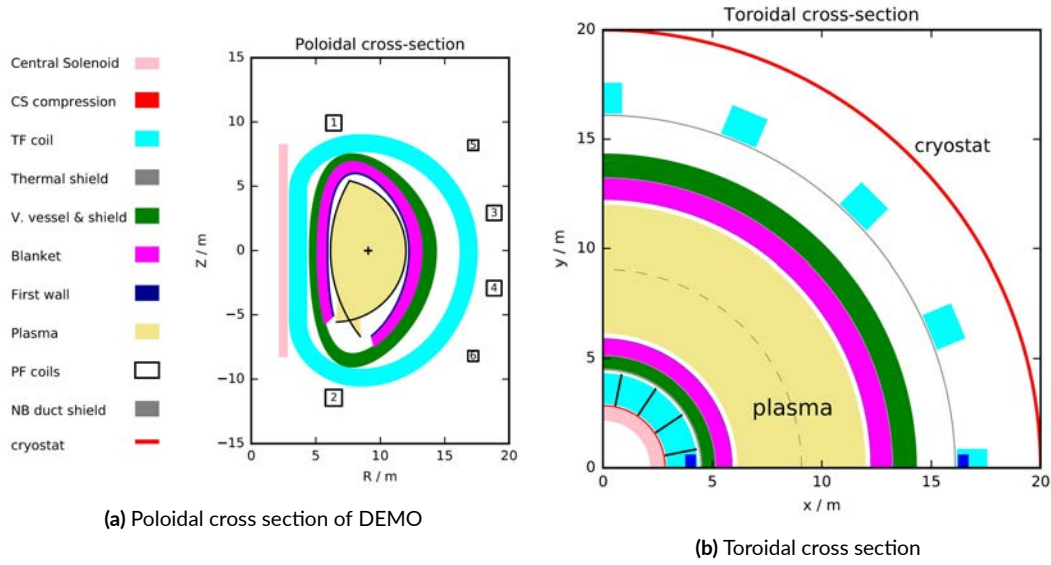
Figure 2.4: DEMO poloidal and toroidal cross sections by PROCESS

Table 2.3: Time of operation phases of DEMO

	Breakdown	Ramp-up	Flat-top	Ramp-down	Dwell time
time [s]	1.44	146	7200	146	600

- Flat-Top (FT), in which the plasma current remains constant and the voltage induced on it serves to compensate for power necessary to increase temperature (caused by internal resistance);

- Ramp-Down (RD), it is the opposite phase to the RU but plasma current returns to initial conditions from FT value, *i.e.* it is the shutdown of plasma;

- Dwell Time (DT) or Recharge phase (RCHG), it is a waiting phase in which all systems must return to the initial state and they must prepare for the next pulse.

The times required for individual DEMO phases are shown in the table 2.3.

2.2 PLANT ELECTRICAL SYSTEM

Plant Electrical System (PES) is all about supplying loads and feeding the generated power into the grid. In other words, it is the whole system that allows the transfer of power from the grid to users, from generators to the grid and from generators to loads. The PES scheme
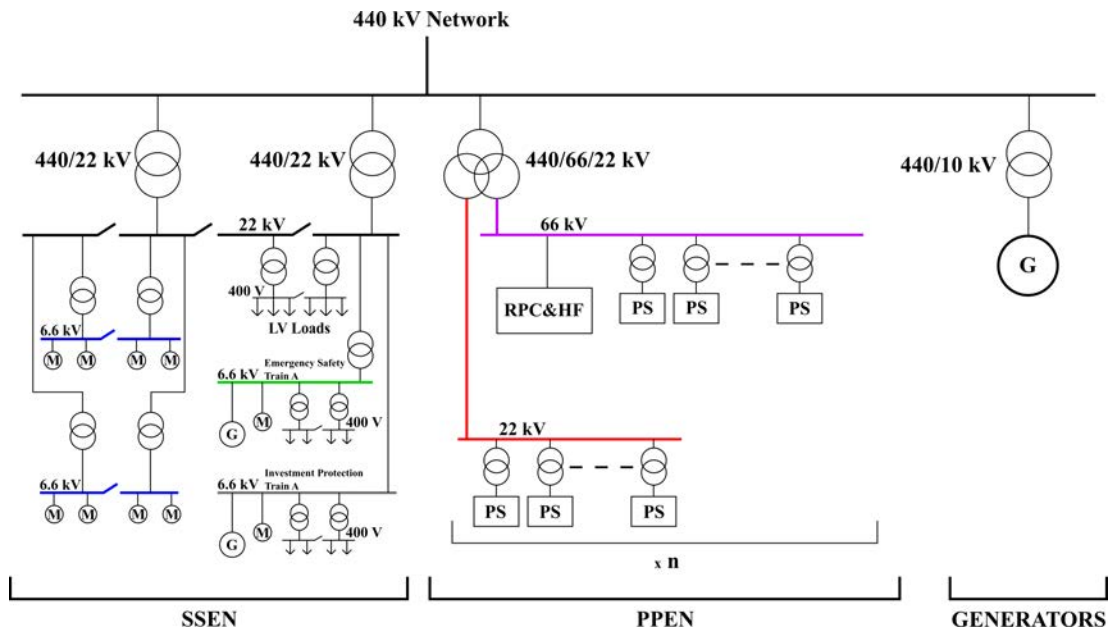
Figure 2.5: DEMO plant electrical system [7]

is shown in figure 2.5 and is divided into three parts: that of continuous loads, pulsed loads and generators. Pulsed loads are connected to the Pulsed Power Electrical Network (PPEN) while the continuous loads are connected by what is called Steady State Electrical Network. Everything is connected to the grid by a 440 kV bar and then voltage is reduced at 22 kV and 66 kV by HV/MV transformers depending on the power to be supplied to the different loads. The medium voltage bars are attached directly to the loads or there are other transformers that still reduce the voltage to 400 V. The main loads are shown in figure 2.6. The whole system is similar to the one already studied in ITER, but what changes is the presence of the generators.

For development of this thesis, the focus is on the PPEN and in particular on the magnet circuits of central solenoid and of poloidal field coils.

2.2.1 COILS CIRCUITS AND POWER SUPPLY SYSTEM

Among the loads of the Pulsed Power Electrical Network, as can be seen from the figure 2.6, there are the magnets systems: Central Solenoid (CS), Poloidal Field (PF) coils and Toroidal Field (TF) coils. The first two are the subject of the thesis and will be described below.

In figure 2.7 an attempt to reproduce the circuit for CS is shown. CS magnet is a vertical stack in the centre of vacuum chamber and is divided into six sectors (CS1U, CS2U, CS3U
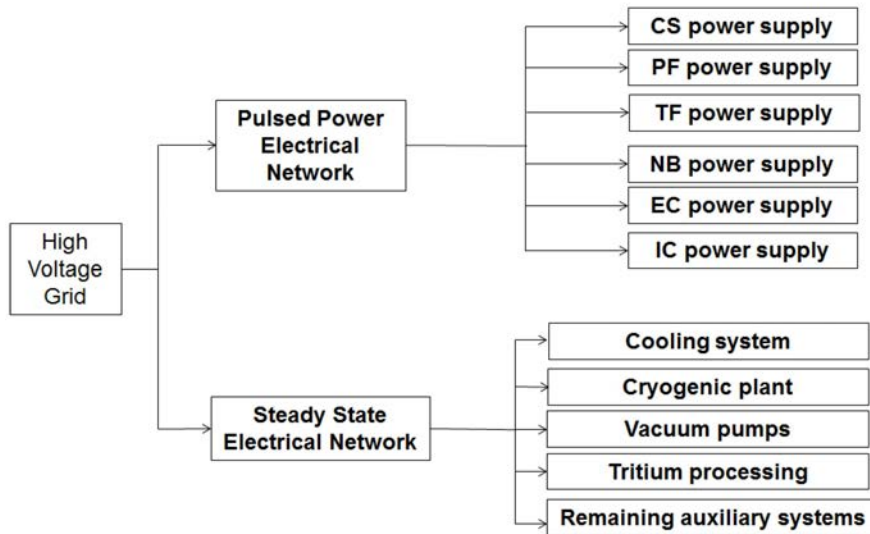
Figure 2.6: DEMO main loads [7]

and CS1L, CS2L, CS3L, where U is upper and L is lower; see also figure 2.4), where CS1U and CS1L are connected in series because currents in those coils should be identical, as in ITER. It provides the flux variation needed to rise plasma current to the maximum value during ramp-up and to maintain that value during flat-top.

In figure 2.8 an attempt to reproduce the circuit for PF coils is shown. PF magnets are six coils, positioned around the vacuum chamber, and they provide overall the vertical plasma stability, but also contribute in a small part to magnetic flux variation of CS. Only PF1 and PF6 coils are isolated, while the others are in parallel to each other and to a Vertical Stability (VS) power supply, which serves to generate differential voltage and current to stabilize vertically the plasma.

How you can see from figures 2.7 and 2.8, circuits are similar for each coils and they present a power supply, a Switching Network Unit (SNU) and a Quench Protection Circuits (QPCs; this unit will be named Fast Discharge Unit -FDU- because it serves not only for quench but also for other events). These units will be discussed in next section.

As it has been said before CS and PF are used to have variations of the flux that modify the magnetic field for certain tasks, previously described. To obtain these flux variations it is necessary to have current variations in the magnets, which are caused by the voltage imposed on the coils. These voltages are obtained by CREATE consortium or software such as PROCESS, which, given plasma position and determined evolution, calculate the induc-
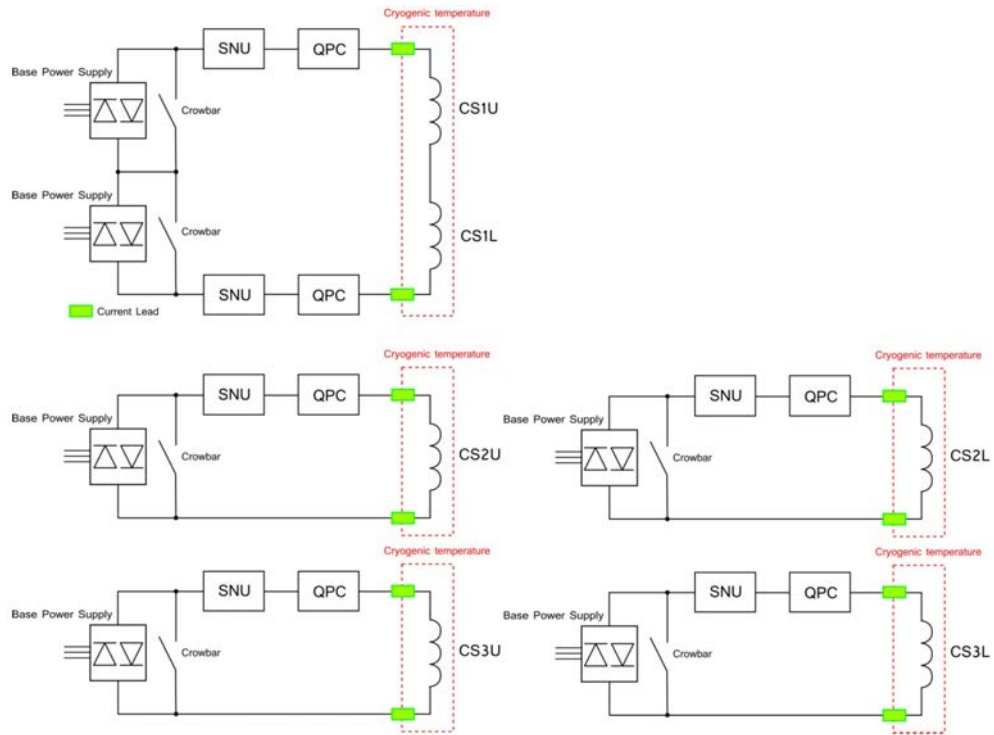
Figure 2.7: Tentative sketch of circuits for CS [7]

Table 2.4: Inductance matrix [H]

	CS3U	CS2U	CS1	CS2L	CS3	PF1	PF2	PF3	PF4	PF5	PF6	plasma
CS3U	2.002	0.634	0.272	0.100	0.072	0.534	0.036	0.121	0.237	0.464	0.413	0.001
CS2U	0.633	2.008	0.949	0.145	0.085	0.163	-0.050	0.007	0.156	0.413	0.424	0.001
CS1	0.267	0.946	5.716	0.873	0.214	0.184	0.022	-0.095	-0.112	-0.016	0.309	0.001
CS2L	0.099	0.144	0.874	1.999	0.644	0.139	0.169	0.141	0.017	-0.012	0.420	0.001
CS3L	0.072	0.086	0.216	0.645	2.023	0.111	0.166	0.186	0.100	0.177	1.138	0.000
PF1	0.535	0.164	0.186	0.140	0.112	2.457	0.229	0.382	0.505	0.844	0.695	0.002
PF2	0.042	-0.044	0.009	0.166	0.171	0.239	2.788	1.873	1.490	1.794	1.239	0.002
PF3	0.134	0.014	-0.148	0.127	0.196	0.411	1.932	7.517	3.477	3.173	1.743	0.003
PF4	0.248	0.158	-0.175	-0.001	0.108	0.536	1.585	3.572	7.147	3.766	1.450	0.002
PF5	0.472	0.411	-0.076	-0.030	0.183	0.871	1.901	3.324	3.836	17.05	3.460	0.002
PF6	0.415	0.427	0.307	0.420	1.140	0.697	1.230	1.697	1.391	3.399	21.68	0.002
plasma (μH)	98.14	114	148	57.48	52.05	157	275	380	275	298	304	1.127
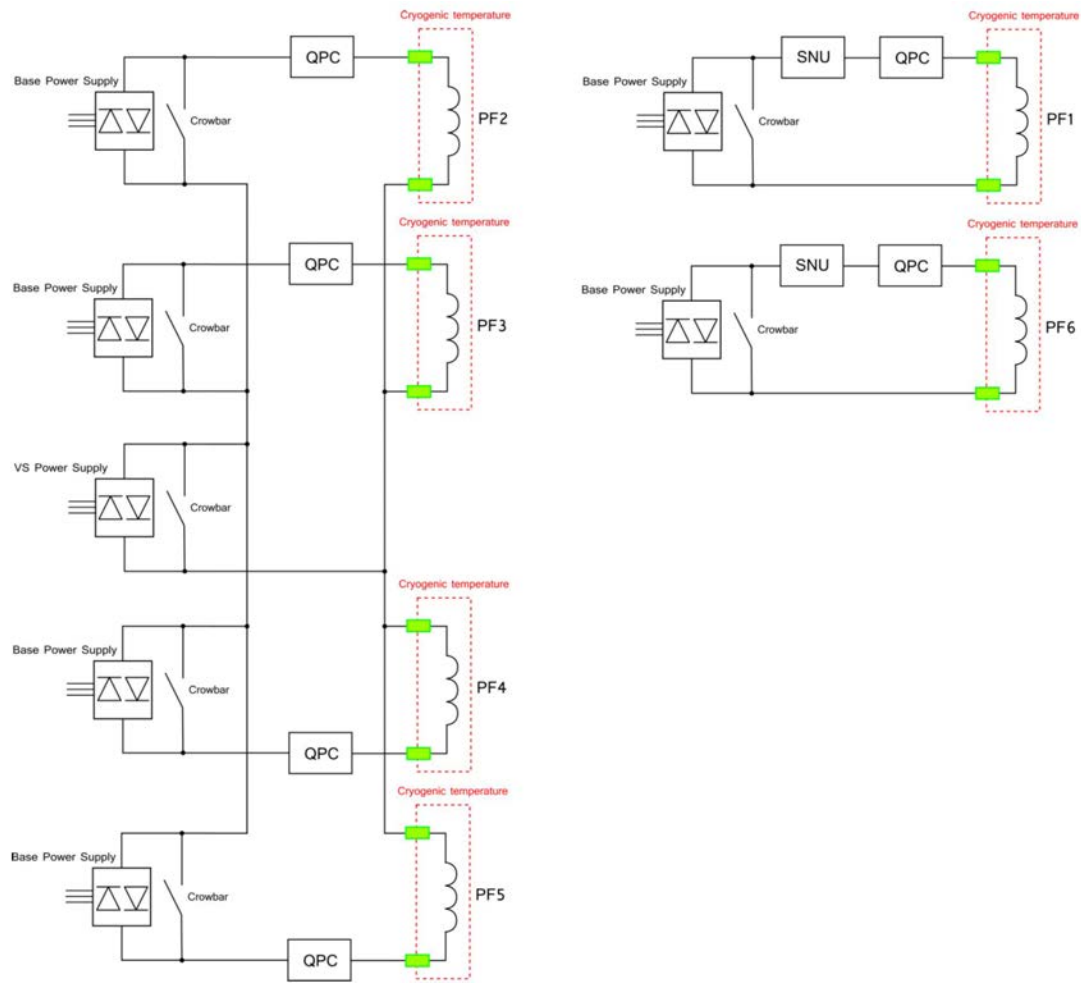
Figure 2.8: Tentative sketch of circuits for PF coils [7]

tance matrix of the whole system (coils coupled to each other, to the plasma and to the passive elements of the vacuum chamber) and they get the voltages to be imposed on magnets. This voltage waveforms (that would change in the future because depend on others systems) serves to understand what voltage variations the coils have to support (conductors have their maximum dv/dt) and to design power supply converter performance. Moreover these voltages together with needed currents give an idea of necessary power. The most challenging waveforms are those of the breakdown (see appendix A) and some example of those voltages applied to CS1, PF1, PF2 and PF3 are presented in the figures 2.9. Making some examples for fast transients and high voltages, in less than a second in one coil it is required to go from $+9\,\text{kV}$ to 0 or in another magnet from $-10\,\text{kV}$ to $+10\,\text{kV}$. Also magnets currents magnitude can not be neglected. Indeed some sectors of central solenoid are crossed by current which reaches $+45\,\text{kA}$, while maximum PF current is $+9\,\text{kA}$. As for requested power, an example of the first instant calculated for CS1 is shown: current is $i = 40 \cdot 10^3$ A, voltage is $v = 12 \cdot 10^3$ V, so that active power is $P = 480 \cdot 10^6$ W. These challenging features (high currents, high voltage) must be provided by Power Supply System (PSS).

Another physic behaviour, which concerns magnets, is that the central solenoid sectors and the poloidal field coils are magnetically coupled. As it is known by Faraday-Neumann-Lenz law, a magnetic flux variation in time through the surface enclosed by a coil induces an electromotive force in that coil. This means that all the magnets (and the plasma, because it is a conductor itself) affect others coils voltage depending on self currents variation (which induces a magnetic flux fluctuation). To take into account this phenomenon mutual and auto inductances have to be known. Also the plasma is coupled with CS and PF and, as its geometrical configuration varies during the pulse, auto and mutual inductances change during the pulse. Specific algorithm are used to estimate the flux variation require to control the plasma position and shape then to calculate the required current and voltage waveforms. This algorithm calculates also inductances matrix and Table 2.4 represents the matrix of auto and mutual inductances between coils and plasma (the inductances of the passive elements are not listed, since they do not significantly affect the studies of this thesis).

2.3 First design approach for power supply system of DEMO superconducting coils

First design approach for PSS is realized with traditional converters, those utilized also in ITER (thyristors converter), with SNU and FDU. Thyristor converters are consolidated, be-

(a) CS1 voltage trend

(b) PF1 voltage trend

(c) PF2 voltage trend
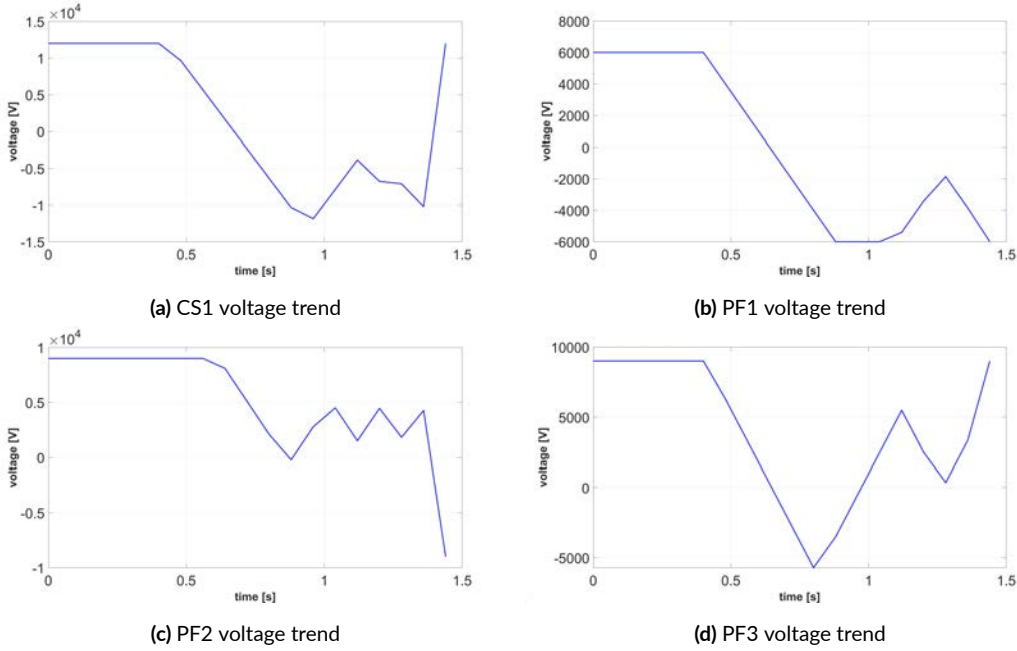
(d) PF3 voltage trend

Figure 2.9: Some of the most challenge voltage trends to perform in coils

cause they are already used in many fusion reactors (JET, Reversed Field eXperiment modified - RFX-mod -, JT60-U, FTU, etc.).

With the use of thyristor converters, the voltages reached during BD are provided with the introduction of SNUs. These units in series with the power supplies of the coils of CS and of PF1 and PF6 are used to ensure a high voltage drop. This unit is composed by a DC interrupting switch and some resistors in parallel. The SNU has to increase voltage drop on coil which it belongs to and to achieve its task it has to interrupt a very high current (± 45 kA), which is exploited by passing through resistances (causing additional voltage drop), inserted in the circuit thanks to the switching of particular mechanical and electrical switches [20] [21]. Usually SNU has two different resistor banks in parallel (each bank has many resistors in parallel), so that when a voltage reduction needs the second bank is inserted in the circuit. The interruption of a current in DC of 45 kA is anything but trivial and indeed the development of SNU is focused on increasing its service life, as the electric arches that are formed deteriorate heavily the device (for ITER, latest version of SNU should bear 30000 plasma pulses). Another highlight of SNUs is the reaction time, *i.e.* how long it takes the unit to interrupt DC current and to supply the required voltage (for ITER few ms). SNU, which will be used for ITER, should be the same of DEMO (if thyristor converter would be utilized) because

24
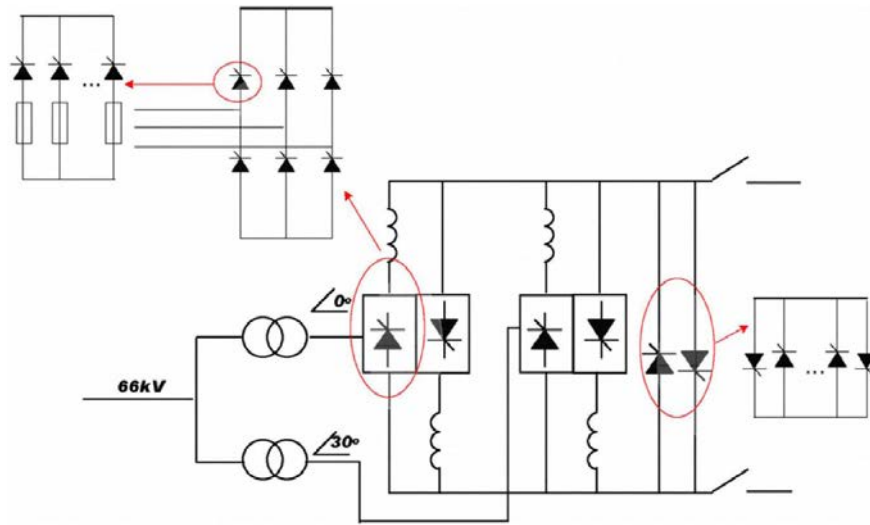
Figure 2.10: PF/CS ITER converter topology [8]

voltage and current ratings are equal. It is important to underline that dissipated energy per coil system in normal operation is up to 700 MJ [22]. Finally, when ramp-up finishes SNU is bypassed and current regulation is provided only by power supply.

In case of faults, Fast Discharge Units are the protection of superconducting coils. Similar to switching network units, FDU consists of a mechanical and electrical switches with a resistor bank in parallel and its task is to dissipate energy stored in magnets. Dissipated energy on resistors bank for CS and PF coils turns around few GJ in a period of tens of seconds. This leads to an important issue that is disposing of the heat produced by resistors. For FDUs the most challenging circuits are those of toroidal coils, due to the very high currents that have to be interrupted ($68 \cdot 10^3$ A, energy dissipated $34{,}4 \cdot 10^9$ J) [23].

As for converter, ITER thyristor converter is the most recent design example to compare with, thus it is important to analyse its topology and operation. ITER ac/dc converter is based on modular approach to satisfy high voltage output. The basic modular unit comprehends four six-pulse bridge carrying out four-quadrant operation, fed by two phase-shifted transformers, so that a twelve-pulse operation is provided. Fuses are in series to every thyristors in all the bridges. The crowbar is formed by external thyristor so that, in case of converter fault, coil current continues to circulate through the coil. Figure 2.10 shows how a thyristor converter is composed.

A first tentative design for DEMO CPSS was done in [7], using the same approach of ITER: modular units connected in series and parallel to reach the required voltage and current.

Table 2.5: DEMO tentative configuration of magnet base converter [13]

Load	On-load voltage rating [kV]	Current rating [kA]	Thyristors in parallel	Units in series
CS1U, CS1L CS2U, CS2L CS3U, CS3L	±8	±45	12	8
PF1, PF6	±8	±45	12	8
PF2, PF3, PF4, PF5	±10	±45	12	10

The basic unit is a 12-pulse 4-quadrant converter, made with four three-phase 6-pulse basic bridge, realized with the parallel connection of some thyristors (the number of parallel depends on the magnet system considered, CS or PF or TF coils). Adopting the ITER technology in DEMO, table 2.5 presents the number of parallel/series connections and the current/voltage ratings.

2.4 MAIN ISSUES OF FIRST DESIGN APPROACH FOR POWER SUPPLY SYSTEM DESIGN

The approach with thyristors converter presents two important issues: the first one is about active power (P); the second one is about reactive power (Q).

DEMO should produce electric energy, so that it should be seen by the grid as a generator. Nevertheless its goal is not to became a real fusion power plant, but it is still an experiment so that it will be also a huge load. All systems in figure 2.6 require lot of active power, overall magnets power supply systems during breakdown and ramp-up phases. As for coils system, ITER peak of active power reaches 600 MW [8] (figure 2.11a); for DEMO it would be much greater than ITER (it would be almost 1 GW [13], figure 2.11b). Peaks of these kind are very difficult to be supplied by whatever grid, considering also that grids are going to be weaker than before due to renewable sources expansion and distributed energy sources.

The second problem is the reactive power. Thyristor technology has an important issue due to its nature: by default it introduces a phase displacement between current and voltage and the delay is amplified when low voltage and high current are requested. This causes a presence of reactive power and it increases when the delay angle increases (that is when low voltage is requested). Figure 2.11a (red curve) shows the reactive power required by ITER power supply system and how much Q is demanded to the grid (green curve). Difference between the two curves is very big and so it is necessary a compensation system: it is called

Reactive Power Compensation and Harmonic Filter system (RPC&HF). It is designed to provide 750 MVAR [24]. For DEMO, which is bigger than ITER, the issue becomes bigger (2 GVAR [13], figure 2.11b). Solution of this problem could be RPC&HF or Active Front End (AFE) converters [13] or the alternative solution, which will be discussed in the next chapter.
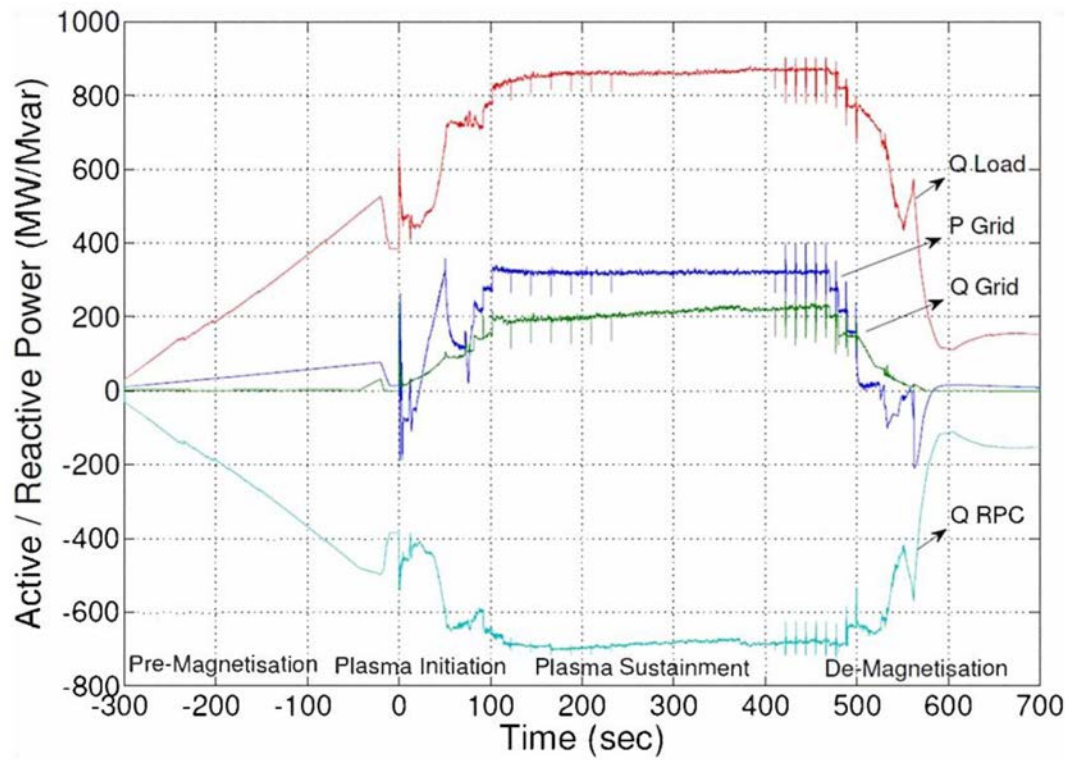
(a) Active and reactive power profile for ITER and compensation by RPC&HF system [24]
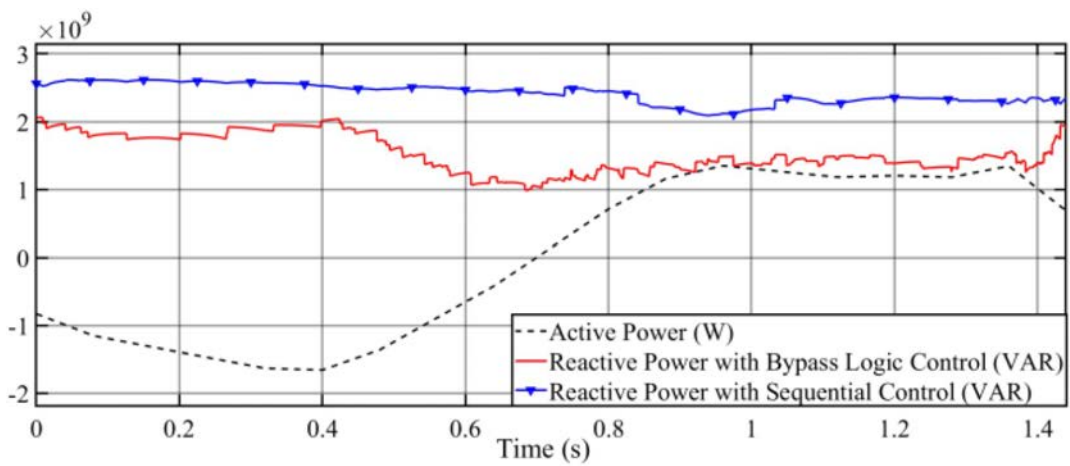
(b) Active and reactive power profile for DEMO with two types of control in the breakdown phase [13]

Figure 2.11: Active and reactive power profiles for main fusion reactor experiments, ITER and DEMO

3

MEST: alternative design solution for DEMO coils power supply

Magnetic Energy Storage and Transfer system (MEST) is an alternative solution that should give some degree of decoupling between the grid and the magnets, that means that coils requests are not instantly supplied by the network. It would substitute thyristors converter, implementing also SNU function (so that efficiency increases respect to PSS with SNUs), and would be used as Electric Storage System (ESS) for that energy necessary to the coils. To decouple grid and coils this system stores energy before DEMO operation (Magnetic Energy Storage) and provides/receives the power to/from magnets when it needs (Transfer). This permits to separate magnets and the grid because most of the power, which would have been requested to the grid, will be supplied by the MEST.

This alternative system is meant to solve active and reactive power issues. The first problem can be easily understand because, instead of supplying instantly the coils, the grid charges MEST system and therefore the energy for active power peak is distributed in a longer time. The reactive power issue depends on converter integrated in MEST system. This converter, also called power supply (do not consider now what type of technology it has), is the link with the grid; it serves to charge MEST and the coils and to compensate losses in the circuit and power needed for plasma sustainment. The power supply is what influences reactive power absorption, which depends on converter technology and voltage to be supplied. In the next chapter it will be shown that in any case reactive power with MEST is less than that
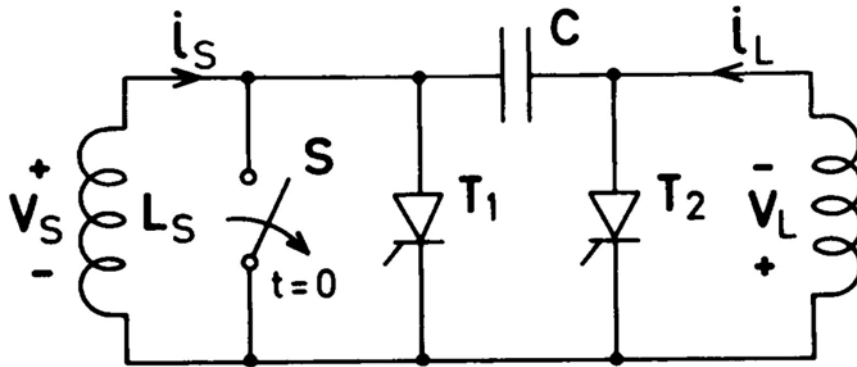
Figure 3.1: Magnetic energy transfer using flying capacitor [9]

required with first approach design.

Instead in this chapter MEST system will be explained from which idea it comes from to its conceptual design for DEMO.

3.1 MAGNETIC ENERGY STORAGE AND MEST

In the field of fusion research, a magnetic energy storage system with superconductor had been studied between the seventies and eighties. It was considered due to its power density and its release time. Nowadays another important reason is that almost fusion devices have a cryogenic plant, thus costs to cool down the coils is inferior than in the past.

Different types of circuits had been proposed and all of them were integrated in the circuit with thyristors, the main device for power electronics. Two of the most interesting are presented below.

The first one is shown in figure 3.1 and its operation is a simple use of the switching thyristors T1 and T2 (which are complementary): considering C and L_L uncharged, T2 is closed (T1 is opened) to let L_S charge C until the imposed maximum value of V_C is reached; whereupon T1 is fired (T2 is opened), shorting L_S, V_C is seen by L_L, discharging the capacitor and increasing i_L; when V_C reaches the minimum imposed value, T1 is opened and T2 is fired, thus the cycle restarts. With i_L and i_S less than zero and with the same use of thyristors, the circuit allows to reverse the energy direction. Taking into account value of inductances and thyristor switching time (duty cycle), C has a minimum value which has to be exceeded [9].

The second circuit [10] is shown in the figure 3.2. It presents a power source converter, which connects the grid with the superconductor L_o, a converter dc/ac/dc three phase 6-pulse, which connects L_o with a pure inductive load L_1. Focusing on the power flow, energy
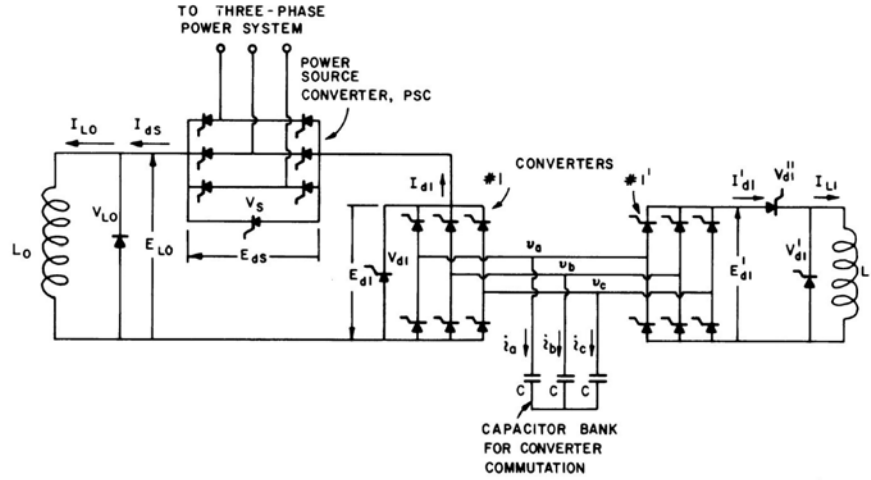
Figure 3.2: Basic circuit of superconducting inductor-converter unit [10]

can pass from the grid to the superconductor, from L_o to L_1 and vice versa depending only on the switches control. Moreover this type of configuration can be multiplied, i.e. more loads (with their own dc/ac/dc converter) can be added.

For this thesis another circuit is studied [11] and is shown in figure 3.3. The proposed model is still theoretical, so that it could be referred to an hypothetical unique CS or to a single sector or to PF coil. It is composed of four fully controllable switches S1...S4, a superconducting inductor named Tank Coil (TC) with equal inductance of CS, a Power Supply (PS) and a capacitor (C); CS, the central solenoid, is the load of MEST system. PS serves to provide the initial energy of the tank coil and of the central solenoid before the beginning of pulse and to compensate switches losses and the power needed to increase and sustain the plasma current against resistive dissipation; the capacitor has a main role as it is necessary to move energy from/to TC to/from coil; TC is energy storage system. More detailed operation will be discussed further on. It is important to say that the basic idea behind the MEST system is that energy would be transferred between TC and CS when it needs to obtain those currents and voltages waveforms which are necessary for plasma ignition and equilibrium.

Figure 3.4 shows the ideal waveforms of TC, CS and plasma currents (no losses are considered). From zero to t_1 TC and CS are charged to starting values, which should be equal. During ramp-up CS has to provide a magnetic flux variation needed for plasma ignition and to rise its current up to the flat-top value. To achieve this task, in the time $(t_2 - t_1)$ CS current decreases and CS energy is transferred from CS to TC, where it is stored. In the last part of ramp-up $(t_3 - t_2)$, where $i_{CS} < 0$, and during the flat-top $(t_4 - t_3)$ TC releases its stored
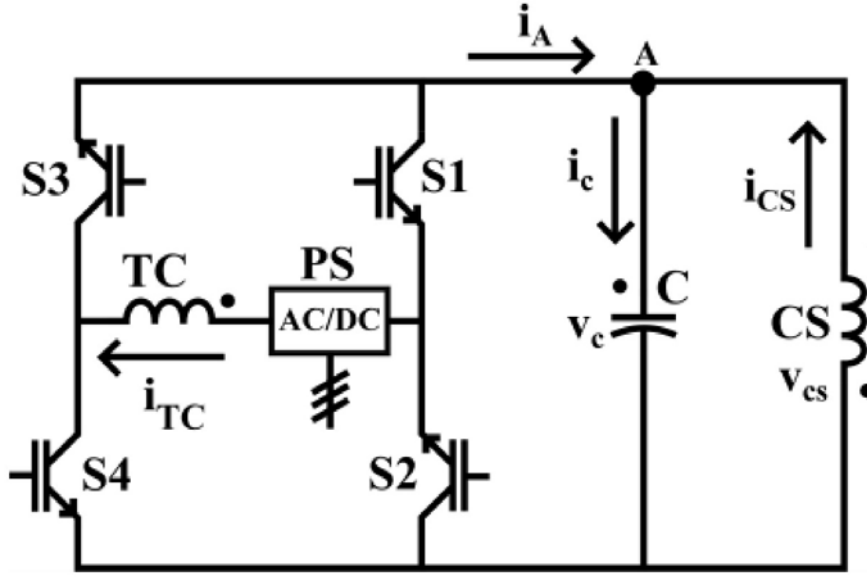
Figure 3.3: MEST converter with power supply [11]

energy to CS to fulfil magnetic flux variation request. During ramp-down $(t_5 - t_4)$ CS recovers plasma energy which is transferred to the tank coil. In the time $(t_6 - t_5)$ energy moves from CS to TC. Finally from t_6 to t_7 recharge of CS is completed with stored energy of TC and initial values are restored, so that another cycle could restart or a whole shutdown could be initialized discharging both TC and CS coils (in the last case energy would be dissipated or transferred to the grid depending on the PS technology).

3.2 PRINCIPLE OF OPERATION

3.2.1 IDEAL CIRCUIT SCHEME

The circuit diagram for MEST model without plasma coupling is presented in figure 3.3 and physically it means that no gas is introduced in the vacuum chamber during flux variation. This condition is used sometimes for some tests and for this thesis it serves to understand the MEST principle operation and the four allowed circuit topologies provided by diverse combinations of switches (states). The possible states are shown in table 3.1. For the discussion of operating principle, the power losses are neglected. Operation inputs are: L_{TC}, L_{CS} and di_{CS}/dt needed to provide a magnetic flux variation for current plasma rising. A certain voltage (reference voltage) serves to produce a current derivative on a inductor and this voltage is supplied by the capacitor. Switches have to manage v_C as near as possible to the
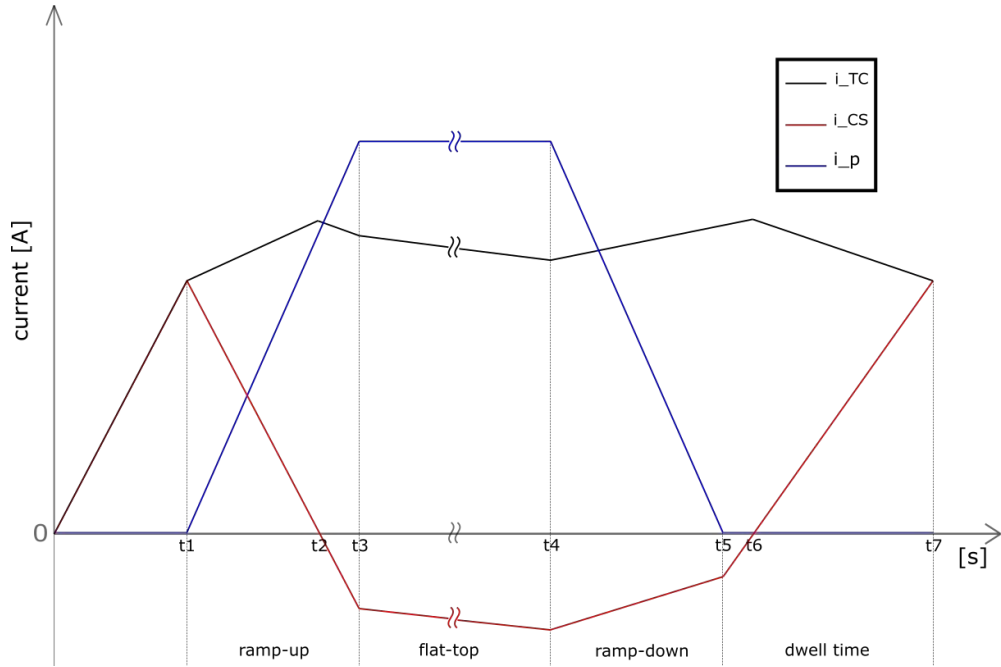
Figure 3.4: Ideal waveforms of TC, CS and plasma currents

Table 3.1: Possible state of MEST system and trends of main quantities

	S1	S2	S3	S4	i_{CS}	i_{TC}	v_C
state	1	0	0	1	> 0	$\uparrow$	$\downarrow$
	0	1	0	1	> 0	$-$	$\uparrow$
	1	0	1	0	< 0	$-$	$\downarrow$
	0	1	1	0	< 0	$\downarrow$	$\uparrow$

(a) State [0101]

(b) State [1001]

(c) State [0110]

(d) State [1010]
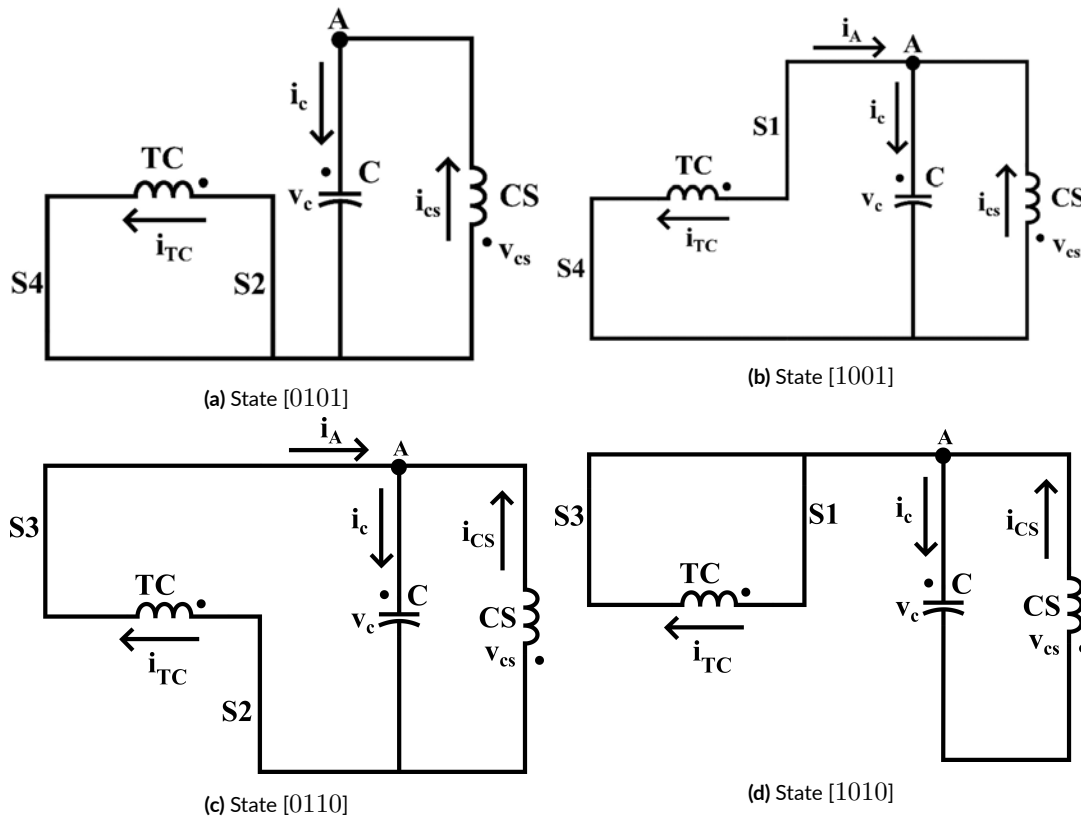
Figure 3.5: All possible states of MEST system [11]

reference, so that di_{CS}/dt is performed.

Switches control system provides the signals needed to commute in the right moment and it is divided in two parts: one for S1 and S2, and the other for S3 and S4. Both the couples are complementary, so that if S1 is on S2 is off and vice-versa; the same occurs for S3 and S4. The first couple switches in relation to a hysteresis band(there are an Upper Bond -UB- and a Lower Bond -LB-) on capacitor voltage; instead the second one refers to CS current and it depends on the sign of i_{CS}.

Initial conditions are: $i_{CS} > 0$, $i_{TC} = i_{CS} = i_0$, v_C is zero, S4 and S2 are closed. In this case, state [0101] (figure 3.5a), TC and CS are isolated and no energy exchange occurs between the two coils: i_{TC} should remain constant because TC is a superconducting coil, v_C increases due to i_{CS} (it is positive so that it charges the capacitor, using references of figure 3.3).

 When capacitor voltage arrives at UB, S2 is opened, S1 is fired and the state becomes [1001] (figure 3.5b) so that v_C reverses its trend and remains near voltage reference. Indeed in this
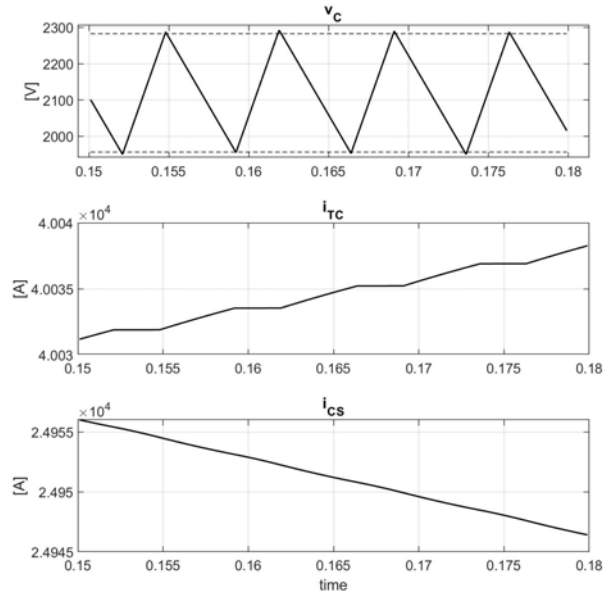
Figure 3.6: Waveforms of v_C, i_{TC} and i_{CS} in a short time period with $i_{CS} > 0$ (states $[0101]$ and $[1001]$)

case the v_C decreases and i_{TC} increases, indeed the voltage imposed by C on TC is positive; in other words, energy is transferred from CS to TC and i_C is negative (respect to the agreement of figure 3.3) so that voltage capacitor is reduced. State $[1001]$ ends when capacitor voltage reaches LB and then state $[0101]$ restarts, making another duty cycle begins. The switch S4 is closed until i_{CS} is equal or higher than zero, then S3 is closed. For the states $[0110]$ and $[1010]$ (figure 3.5c and 3.5d) the control of S1 and S2 is already described above with hysteresis control. However in these cases, capacitor voltage increases when the two mashes are linked (state $[0110]$, figure 3.5c) and it decreases when TC and CS are decoupled (state $[1010]$, figure 3.5d). In state $[0110]$ the voltage imposed by C on TC is negative, so that i_{TC} decreases, that means that the energy moves from TC to CS. In figure 3.6 voltage and current waveform are shown as example on how strategy control works when i_{CS} is greater than zero (switching from state $[1001]$ to state $[0101]$ and vice versa).

The most important constrain to take care of is that i_{TC} must be always greater than $|i_{CS}|$ otherwise the control system can not operate as described previously. Indeed if $|i_{CS}| > i_{TC}$ and $i_{CS} < 0$ then in state $[0110]$ for the KCL, $i_C < 0$ so v_C decreases instead of increasing. Thus there would not be commutation from state $[0110]$ to $[1010]$ and a trend of resonant circuit will occur. With $i_{CS} > 0$ a similar situation occurs, but in state $[1010]$

35

v_C increases instead of decreasing.

3.2.2 CIRCUIT SCHEME WITH PLASMA COUPLING

The MagnetoHydroDynamics (MHD) theory explains behaviours of fluid conductors, such as plasma. It combines the equations of mass, momentum and energy conservation with Maxwell's equations, making its comprehension not so simple. Nevertheless for thesis purpose, a plasma detailed representation is not necessary and only the fluid and coupling characteristics, which affect magnets behaviours, are taking into consideration.

As already said in section 2.2.1, Plasma is coupled to six sectors of CS and to six PF coils and the coupling is the same of a transformer: the superconducting (CS and PF) coils play the role of a primary winding (also called multi-turns side), which provide the flux variation, and the plasma plays the role of a single conductor secondary winding (also called single-turn side), in which a voltage is induced. Coupling with vacuum chamber is neglected. This phenomenon on plasma voltage can be written as:

$$v_p = M_{p,i}\frac{di_i}{dt} + \sum_{\substack{j=1 \\ j \neq i}}^{n} M_{p,j}\frac{di_j}{dt} + L_p\frac{di_p}{dt} \tag{3.1}$$

where v_p is plasma voltage, $M_{p,i}$ is mutual inductance between coil i and plasma, $M_{p,j}$ is mutual inductance between coil j and plasma and L_p is plasma auto-inductance. The first addend is out of the sum because it is the coil which is taken into account in the circuit.

It is also important to consider that every coil (both CS and PF) is coupled to the others and thus each coil current influences the voltage of the other coils (this is explained by equation 3.2) in the same way as they affect plasma:

$$v_{coil_i} = L_i\frac{di_i}{dt} + \sum_{\substack{j=1 \\ j \neq i}}^{n} M_{i,j}\frac{di_j}{dt} + M_{i,p}\frac{di_p}{dt} \tag{3.2}$$

where v_{coil_i} is voltage of coil i, n is number of coils, L_i ia auto-inductance of coil i, $M_{i,j}$ is mutual inductance between coil i and j, $M_{i,p}$ is mutual inductance between coil i and plasma and $\frac{di}{dt}$ is the current derivative of the relative subscript.

The complexity and the difficulty to implement a system with so many couplings between coils-plasma and coils-coils are overcame using two equivalent voltage sources, one on multi-turns side ($v_{eq_{CS}}$) and the other on single-turn side (v_{eq_p}). These two voltage sources are

necessary because they serve to reproduce the voltage induced in the considered coil by variation of the currents in the plasma and in the other coils; if they are not taken into account and if the voltage reference is provided to the capacitor, i_{CS} will be different to those current waveforms which are requested.

Considering equations 3.1 and 3.2 and taking into account the sum of all couplings with other coils ($\sum M_{p,j} \frac{di_j}{dt}$ and $\sum M_{i,j} \frac{di_j}{dt}$), the summations can be substituted by a controlled voltage sources, which generate an equivalent voltage such as the induced one by couplings. In other words, in the model the coupling between magnet under consideration and plasma is built as a transformer with two windings, each with its own auto-inductance (L_i and L_p) and a mutual inductances (where $M_{coil,p} = M_{p,coil}$), and the contribution of coupling of other coils (j from $1 \rightarrow n$) with plasma and with considered coil (i) is built as two voltage sources. No coil is specified as primary winding (*i.e.* the subscript i in equations 3.1 and 3.2 is not fixed), therefore it is possible to vary the parameters (auto and mutual inductance and controlled voltage sources) to change the coil under observation. How the value of these equivalent sources are explained in section 3.4.

Regarding conductor fluid characteristics, simplifying, plasma can be associated to a single conductor with its impedance which comprehends a small resistance, a negligible capacitance and an inductance. Plasma impedance depends on inner proprieties, such as temperature, presence of impurity etc., and on geometrical quantities, such as the position of plasma, vacuum chamber geometry, coils position etc. Most of inner parameters vary during time and so it is very difficult to model it precisely. In the model the plasma is simplified: its resistance is variable and it has four values for different phases of pulse operation; the inductances (auto and mutual) are kept constant for all the operations. Values are taken from a linear model using finite elements method dated 2015 built by CREATE consortium. Also currents and voltages data of different scenarios are imported by CREATE model (appendix A). Data could change in the future models because DEMO project is in its pre-conceptual design phase, thus improvements could be added further on in the future.The figure 3.7 shows a simple circuit of a CS sector coupled with the plasma, including equivalent voltage sources that take into account coupling with other CS sectors and PF coils.

As plasma has its resistance and its current, power losses are generated. This power is necessary to increase plasma temperature but, however, it has to be compensated by a Power Supply (PS). Moreover it should compensate ohmic losses in the circuit, but in this thesis this power is not considered (the circuit is ideal). There are many methods to balance losses and, firstly, integral mode is chosen. Thus PS voltage value is imposed to be constant and
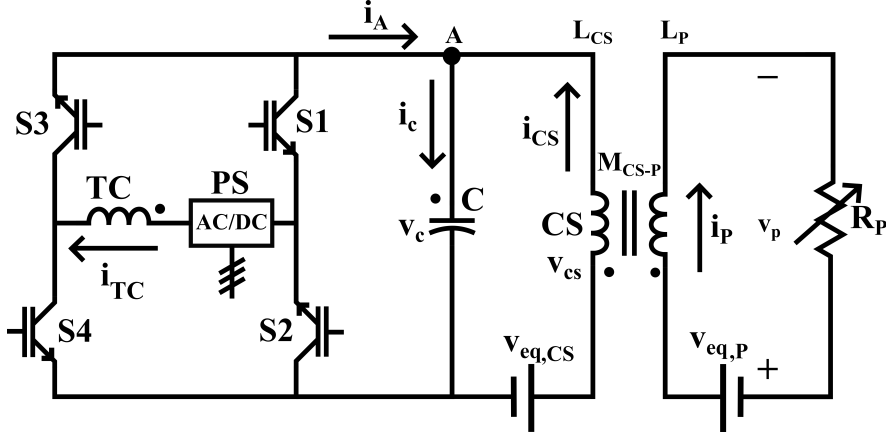
Figure 3.7: Circuit scheme of a single CS sector including plasma and other coils couplings

can be obtained as following.

Energy losses are

$$E_{R_{loss}} = \int_0^\tau R_p(t) i_p^2(t) dt \tag{3.3}$$

where τ is the pulse duration and $R_p(t)$ and $i_p(t)$ are known. Energy of power supply is calculated easily as:

$$E_{PS} = \int_0^\tau V_{DC_{PS}} i_{TC} dt = V_{DC_{PS}} \int_0^\tau i_{TC} dt \tag{3.4}$$

where $V_{DC_{TC}}$ is power supply voltage. TC current integer is got numerically by a simulation without losses, or equivalently with compensated losses. As PS energy should counterbalance ohmic losses, from the 3.3 and 3.4 equations PS voltage is:

$$V_{DC_{PS}} = \frac{E_{R_{loss}}}{\int_0^\tau i_{TC} dt} \tag{3.5}$$

From equation 3.5 the mean necessary voltage is calculated. Nevertheless it is possible to make a piecewise constant waveform of voltage that has the same mean value and nothing would change. Varying PS voltage permits variation of power direction and therefore it is possible to reduce peak current in tank coil. Others way to control power supply will be discussed further on in section 3.4.

3.3 MEST ANALYTICAL MODEL

3.3.1 EQUATIONS OF THE MODEL

Referring to the circuit scheme with plasma coupling (figure 3.7), the following assumptions must be added: ideal switches are considered (no switching or operation losses, instant commutations) and voltage power supply is set to zero.

Waveforms are not linear, neither the equations that describe all quantities. At every commutations the equations system varies and, as the circuit has four switches, four topologies have to be studied (they correspond to the four states). Systems of differential equations, which will follow in the description of the model, are derived by Kirchhoff's laws, for voltage and for current, and by component equations [25]. Systems which represent Kirchhoff's laws are the following:

$$
\text{State } [0101]
\begin{cases}
i_{TC} = const \\
i_C = i_{CS} \\
v_C = v_{eq_{CS}} - v_{CS} \\
v_{eq_p} = v_{L_p} + v_{R_p}
\end{cases}
\text{(a)} \quad
\text{State } [1001]
\begin{cases}
i_C = i_{CS} - i_{TC} \\
v_{TC} = v_C \\
v_C = v_{eq_{CS}} - v_{CS} \\
v_{eq_p} = v_{L_p} + v_{R_p}
\end{cases}
\text{(b)} \quad (3.6)
$$

$$
\text{State } [0110]
\begin{cases}
i_C = i_{CS} + i_{TC} \\
v_{TC} = -v_C \\
v_C = v_{eq_{CS}} - v_{CS} \\
v_{eq_p} = v_{L_p} + v_{R_p}
\end{cases}
\text{(a)} \quad
\text{State } [1010]
\begin{cases}
i_{TC} = const \\
i_C = i_{CS} \\
v_C = v_{eq_{CS}} - v_{CS} \\
v_{eq_p} = v_{L_p} + v_{R_p}
\end{cases}
\text{(b)} \quad (3.7)
$$

System which represent components equations is the following:

$$
\begin{cases}
v_{TC} = L_{TC}\dfrac{di_{TC}}{dt} \\[2mm]
v_{CS} = L_{CS}\dfrac{di_{CS}}{dt} + M_{CS,p}\dfrac{di_p}{dt} \\[2mm]
i_C = C\dfrac{dv_C}{dt} \\[2mm]
v_{L_p} = M_{p,CS}\dfrac{di_{CS}}{dt} + L_p\dfrac{di_p}{dt} \\[2mm]
v_{R_p} = R_p i_p
\end{cases}
\quad (3.8)
$$

To describe analytically each state, the system corresponding to the examined state and the system 3.8 have to be utilized. From CREATE i_{CS} and i_p are piecewise linear functions and their derivatives are known, thus the overall system has nine unknowns and nine equations.

- State [0101]

The voltages on inductances and on resistance are easily obtained, by the second, the forth and the fifth equations of 3.8; for v_C a brief operation must be done:

$$i_C = i_{CS} = C\frac{dv_C}{dt} \rightarrow \int_{v_C(t_1)}^{v_C(t)} dv_C = v_C(t) - v_C(t_1) = \frac{1}{C}\int_{t_1}^{t} i_{CS}dt \qquad (3.9)$$

In this state $i_{CS} > 0$, therefore the integral of equation 3.9 is positive, and, as expected, it increases capacitor voltage. Remembering that waveforms are not linear but are piecewise functions, the meanings of time and $v_C(t)$ must be explained: t_1 is always 0 because it is the moment after the commutation, *i.e.* when the circuit state changes; thus $v_C(t_1) = v_0(0)$, that is the initial value of capacitor voltage, which, in this state, is the lower limit value of hysteresis control, V_{LB} (see figure 3.6); the equation 3.9 is valid until the upper limit value of hysteresis control is reached, therefore $v_C(t_{max})$ (that is V_{UB}) is known and t_{max} is easily obtained. Then equivalent voltages in both sides (multi-turns and single-turn) are calculated by the third and fourth equations of system 3.6a.

- State [1001]

The voltages on inductances and on resistance are easily obtained, by the second, the forth and the fifth equations of 3.8; to obtain v_C more complex operations have to be carried out: from the first equation of system 3.6b i_{TC} is derived, and with the second of the same system and with the first of 3.8 you get

$$\frac{d^2v_C}{dt^2} + \frac{v_C}{L_{TC}C} = \frac{1}{C}\frac{di_{CS}}{dt} \qquad (3.10)$$

a non-homogeneous second order differential equation, whose solution is the sum of homo-

geneous and particular solutions:

$$v_{C_{homog}} = c_1 \cos\left(t\sqrt{\frac{1}{L_{TC}C}}\right) + c_2 \sin\left(t\sqrt{\frac{1}{L_{TC}C}}\right) \tag{3.11}$$

$$v_{C_{part}} = L_{TC}\frac{di_{CS}}{dt}$$

The coefficients c_1 and c_2 of 3.11 are obtained by initial conditions:

$$v_C(0) = v_C(t_{max}) = V_{UB}$$

$$\left.\frac{dv_C}{dt}\right|_{t=0} = \frac{i_C(0)}{C} = \frac{i_{CS}(t_{max})}{C}$$

where $v_C(t_{max})$ is capacitor voltage of the previous state in the moment before switching commutation, that is the upper limit of hysteresis band (also it can be obtained from 3.9), and $i_{CS}(t_{max})$ is CS current of the previous state in the moment before switching commutation. Finally the overall function of capacitor voltage for state $[1001]$ is:

$$v_C(t) = \left(v_C(0) - L_{TC}\frac{di_{CS}}{dt}\right)\cos\left(t\sqrt{\frac{1}{L_{TC}C}}\right) +$$

$$+ i_C(0)\sqrt{\frac{L_{TC}}{C}}\sin\left(t\sqrt{\frac{1}{L_{TC}C}}\right) + L_{TC}\frac{di_{CS}}{dt} \tag{3.12}$$

The trend of v_C of equation 3.12 strongly depends on initial conditions. To verify equation 3.12, i_{TC} and i_C are calculated utilizing voltage from equation 3.12, and it should result that i_{CS} is the sum of the two currents. Getting TC current from

$$i_{TC}(t) - i_{TC}(0) = \frac{1}{L_{TC}}\int_0^t v_C dt$$

$$= \sqrt{\frac{C}{L_{TC}}}\left(v_C(0) - L_{TC}\frac{di_{CS}}{dt}\right)\sin\left(t\sqrt{\frac{1}{L_{TC}C}}\right) + \tag{3.13}$$

$$- i_C(0)\cos\left(t\sqrt{\frac{1}{L_{TC}C}}\right) + i_{CS}$$

and getting capacitor current from

$$i_C = C\frac{dv_C}{dt} = -\sqrt{\frac{C}{L_{TC}}}\left(v_C(0) - L_{TC}\frac{di_{CS}}{dt}\right)\sin\left(t\sqrt{\frac{1}{L_{TC}C}}\right)$$
$$+ i_C(0)\cos\left(t\sqrt{\frac{1}{L_{TC}C}}\right) \qquad (3.14)$$

CS current is obtained by the sum of 3.13 and 3.14 and, as expected, it results equal to i_{CS}. Thus the validity of equation 3.12 is verified.

- State $[1010]$

It is similar to state $[0101]$ and the equation of v_C is the same of 3.9. But in this case, $v_C(0)$ is V_{UB} and i_{CS} is less than zero, therefore the voltage decrease (as it should be).

- State $[0110]$

It is similar to state $[1001]$ despite of KCL on node A and despite that tank coil voltage is opposite to v_C. The overall equation is similar to 3.12 but voltage initial condition is different: $v_C(0)$ is V_{LB}.

3.3.2 FREQUENCY EVALUATION

In MEST system the switching frequency is not fixed due to the hysteresis control: a band limits the functional region, but the voltage derivative of capacitor (its current, which affects the period of duty cycle and so the frequency) depends on the circuit characteristics. Thus to evaluate the frequency of commutations, the variables of frequency function have to be known. Qualitatively, as the equation of a capacitor is $i = C\frac{dv}{dt}$, therefore the velocity depends linearly on i_C and inversely on C. Capacitor current is fixed from the KCL on node A in the figure 3.3, $i_A + i_{CS} = i_C$; i_A and i_{CS} are fixed by the request of plasma control waveform. Instead the capacitance C does not have any constrain and it is a degree of freedom. Moreover also the band of the hysteresis control affects the frequency and it is another degree of freedom.

As the switching frequency is variable, it is essential to fix a reasonable maximum value, so that MEST components would be designed adequately to reality. This maximum value depends on switches technology: the switch should undergo to high voltages (some kV) and

to very high current (some tens of kA) and it should commutate at frequency of hundreds of Hz. Moreover a part of switch losses are due to the switching frequency and they are important to design power supply because PS has to compensate all type of losses. However in this thesis these losses are neglected.

Quantitatively the switching frequency can be evaluated assuming some simplifications:

- v_C is considered constant and equals to the reference V_C;

- i_{TC} and i_{CS} are considered constant.

These simplifications are actually very similar to the real functioning, indeed the inductances CS and TC are so big (in order of some [H]) that the angular frequency is very low and so the current varies slowly and TC and CS see only the mean voltage value, which is the reference value. The idea to calculate the switching frequency is to find the duty cycle of S1 (t_{1off} and t_{1on}) then the frequency, considering that $f_{sw} = \frac{1}{t_{1on}+t_{1off}}$. To evaluate the duty cycle energy and power of capacitor in different states are needed. CS current is imposed firstly positive and then negative.

- Positive CS Current

State [0101]: To find the energy stored in a capacitor is:

$$W_C = \int_0^\tau v i \, dt = \int_{Q_0}^{Q_\tau} \frac{q}{C} dq = \frac{1}{2}\left(\frac{Q_\tau^2}{C} - \frac{Q_0^2}{C}\right) \tag{3.15}$$

where v and i are respectively capacitor voltage and current, $q = q(t)$ is a function which describes the charges state, Q_t is the charge at time t and Q_0 is the initial charge. Knowing that $q(t) = Cv(t)$ and using equation 3.15, the energy needed to rise the capacitor voltage to the upper limit of hysteresis control is:

$$\Delta W_C = \frac{1}{2}C\left[\left(V_C + b\right)^2 - \left(V_C - b\right)^2\right] \tag{3.16}$$

where b is half of the total hysteresis band, $V_C + b = V(\tau)$ and $V_C - b = V(0)$. The power entering in capacitor is:

$$P_{in} = V_C i_{CS}$$

Then time in which S1 is open (S2 is closed) is:

$$t_{1off} = \frac{\Delta W_C}{P_{in}}$$

State [1001]: the energy to decrease the capacitor voltage to the lower limit of hysteresis control is the same in equation 3.16. The power outgoing from the capacitor is:

$$P_{out} = V_C(i_{CS} - i_{TC})$$

P_{out} is negative how it should be by the agreement. Then time in which S1 is closed (S2 is open) is:

$$t_{1on} = \frac{\Delta W_C}{|P_{out}|}$$

Finally the switching frequency is calculated by:

$$f_{sw} = \frac{1}{t_{1on} + t_{1off}} = \frac{1}{\frac{\Delta W_C}{|P_{out}|} + \frac{\Delta W_C}{P_{in}}} = \frac{2V_C i_{CS}(|i_{CS} - i_{TC}|)}{C\left[(V_C + b)^2 - (V_C - b)^2\right]i_{TC}} \qquad (3.17)$$

- Negative CS Current

Incoming and outgoing power and KCL in the node A change with negative CS current. State [0110]: energy equation 3.16 remains valid. The incoming power is:

$$P_{in} = V_C(i_{TC} + i_{CS})$$

Then time in which S1 is open (S2 is closed) is:

$$t_{1off} = \frac{\Delta W_C}{P_{in}}$$

State [1010]: energy equation 3.16 remains valid. The outgoing power is:

$$P_{out} = V_C i_{CS}$$

P_{out} is negative how it should be by the agreement. Then time in which S1 is closed (S2 is open) is:

$$t_{1on} = \frac{\Delta W_C}{|P_{out}|}$$

Finally the switching frequency is calculated by:

$$f_{sw} = \frac{1}{t_{1on} + t_{1off}} = \frac{1}{\frac{\Delta W_C}{|P_{out}|} + \frac{\Delta W_C}{P_{in}}} = \frac{2V_C |i_{CS}| (i_{TC} + i_{CS})}{C\left[(V_C + b)^2 - (V_C - b)^2\right] i_{TC}} \tag{3.18}$$

Considering that the condition $i_{TC} > |i_{CS}|$ must be respected, that in the equation 3.17 $i_{CS} > 0$ and that in the equation 3.18 $i_{CS} < 0$, the two equations are equal.

3.3.3 EQUIVALENT VOLTAGES EVALUATION

As said in section 3.2, an equivalent controlled voltage sources are necessary to take into account the coupling of other coils with plasma and with the examined magnet. Referring to figure 3.7 to calculate controlled voltage source in multi-turns side ($V_{eq_{CS}}$), second equation of 3.8 and third equation of 3.6a have to be used. CS voltage is obtained by current derivatives (both of i_{CS} and of i_p), v_C is fixed so that $V_{eq_{CS}}$ is easily calculated. Controlled voltage source in single-turn side (V_{eq_p}, referring to figure 3.7) results immediately by combination of fourth and fifth equations of 3.8 and fourth equation of 3.6a. These controlled voltage sources are not constant because depend on voltage reference and current derivatives (which are piecewise function), so that it is not possible to obtain a single value.

Table 3.2: IGCT ABB® 5SHY42L6500 main characteristics

V_{DRM}	V_{DC}	I_{TGQM}	$I_{max}\big|_{f=500}$	$t_{on,min}$	$t_{off,min}$
6500 [V]	4000 [V]	3800 [A]	1500 [A]	40 [μs]	40 [μs]

3.4 MEST COMPONENTS DESIGN

The main quantities to be assessed for the design of MEST are: power supply voltage, capacitance of the capacitor C, inductance of the tank coil L_{TC} and technology of the switching devices and number of parallel and series swittching device per MEST switch. The IGCT ABB® 5SHY42L6500, whose characteristics are listed in table 3.2*, was selected as switching device since it is fully controllable, as required for the application, and its ratings are suitable to reduce the number of parallel and series components for an individual switch of MEST. The first components to design is power supply voltage because it affects currents behaviours,

---

*V_{DRM} is repetitive peak off-state voltage and I_{TGQM} is max. controllable turn-off current

which influence frequency trend and so the capacitor design.

The initial idea of how to use PS is to compensate plasma losses as said in section 3.2 (integral method). Firstly energy losses have to be evaluated: equation 3.3 can be calculated in ramp-up, flat-top and ramp-down phases where $i_p \neq 0$. This brings to divide the equation into three parts:

$$E_{R_{loss}} = \int_{ru} R_{p,ru} i_{p,ru}^2(t)dt + \int_{ft} R_{p,ft} I_{p,ft}^2 dt + \int_{rd} R_{p,rd} i_{p,rd}^2(t)dt$$

Knowing the overall plasma current waveform (tables 5.5 and 5.3 in Appendix A) and plasma resistances (table 4.1), $E_{R_{loss}}$ can be easily evaluated and it becomes:

$$E_{R_{loss}} = \int_{ru} R_{p,ru}\big(kt + i_{p,ru}(0)\big)^2 dt + \int_{ft} R_{p,ft} I_{p,ft}^2 dt + \int_{rd} R_{p,rd}\big(i_{p,rd}(0) - kt\big)^2(t)dt =$$

$$= 5{,}55 \cdot 10^8 + 8{,}08 \cdot 10^9 + 5{,}55 \cdot 10^9 = 14{,}185 \cdot 10^9 \, \text{J}$$

where k is plasma current derivative ($= 0{,}1 \cdot 10^6$ A) and $i_p(0)$ are initial of relative phases (for RU $= 5 \cdot 10^6$ A; for RD $= 19{,}6 \cdot 10^6$ A). Then PS voltage can be obtained by equation 3.5 using an iterative method because i_{TC} is affected by $V_{DC_{PS}}$ in a non linear proportion. Indeed v_C reference for flat-top is similar to $V_{DC_{PS}}$ and so when the switches S1 and S2 switch voltage conditions on TC vary consistently.

However this method does not work because maintaining PS voltage constant does not satisfy the constrain of $i_{TC} > |i_{CS}|$ during ramp-down phase. A second way, used to simulate the model, is to satisfy the constraint, *i.e.* to take the worst condition for i_{TC} (maximum mandatory stored energy), and to modulate the trend of i_{TC} according to the conditions set by the scenarios. In other words, design of PS is based on modelling the trend of tank coil current according to the i_{CS} minimum point. From data $i_{CS}|_{min} = -45$ kA in ramp-down at 25 seconds after the beginning of the phase (or at 7371 seconds from start of operation) with reference voltage of 1297 V; so that with a little security margin i_{TC} is imposed ($i_{TC} = |i_{CS}| + \epsilon = 45.1$ kA). As reference voltage is maintained constant during those 25 seconds i_{TC} variation can be approximate with a linear one with good accuracy; so that initial

condition of RD can be easily found with

$$v_{TC} = L_{TC}\frac{di_{TC}}{dt} = -v_C = const \rightarrow \int_0^t V_C dt = L_{TC} \int_{i_{TC}(0)}^{i_{TC}(t)} di$$

$$\frac{V_C t}{L_{TC}} = i_{TC}(t) - i_{TC}(0)$$

$$i_{TC}(0) = 45{,}1 \cdot 10^3 + \frac{1297 \cdot 25}{5.716} = 50{,}77 \cdot 10^3$$

where $i_{TC}(0)$ is the value when the phase starts and it is the goal which PS has to get to in flat-top phase. Initial conditions of flat-top are obtained by ramp-up phase, so that, knowing initial and final energy in TC, it can be possible to find a $V_{DC_{PS}}$ which can supply the difference (ΔE_{TC}). TC current remains affected by PS voltage in a non linear proportion due to the circuit topology, therefore a iterative method has to be used:

$$\Delta E_{TC,analytic} = \int v_{TC,sim} i_{TC,sim} dt \quad \begin{cases} if \int \pm\epsilon > \Delta E_{TC,analytic}, V_{DC_{PS}} \downarrow \\ if \int \pm\epsilon < \Delta E_{TC,analytic}, V_{DC_{PS}} \uparrow \end{cases}$$

where ϵ is the accuracy, $\int$ after braces is an abbreviation of the whole integral, which is calculated by the use of numerical model built in Simulink® and presented in chapter 4, and $\Delta E_{TC,analytic}$ is

$$\Delta E_{TC,analytic} = \frac{1}{2}L_{TC}\left[\left(i_{TC}(t)\right)^2 - \left(i_{TC}(0)\right)^2\right] = 1{,}269 \cdot 10^9 \, J$$

With an accuracy of $\epsilon = 1 \cdot 10^6$ J (that is 0.08% of ΔE_{TC}), after some iterations, it results $V_{DC_{PS}} = 13.67$ V.

As for the capacitor, equation 3.17 has to be used and frequency and hysteresis band have to be fixed. Maximum switching frequency is fixed by the choice of switch and in this case it is 500 Hz. Hysteresis band is variable and a trade-off between hysteresis width and capacitor size have to be done. Indeed if you increase capacitance you can reduce hysteresis band, and vice-versa. Capacitance cost and volume depends on its magnitude, so that it should be as small as possible; moreover capacitance value affects respond times, bigger is the capacitor, lower is its maximum derivative; hysteresis limits can not be too high because inductances will be affected by variable voltage. Therefore hysteresis band is fixed to $2b = 600$ V. In equation 3.17

47

there is also another factor depending on currents, that is $m = |i_{CS}|(i_{TC} - |i_{CS}|)/i_{TC}$. Currents do not depend on capacitance neither on hysteresis band (if it is small enough) but only on voltage across inductances, which is already fixed by scenarios. Thus it is possible to simulate the model with the fixed band and with a casual capacitance, so that the worst case for m is obtained: maximum value of m for each phase (except RU in which i_{TC} is lower than in others) are $12,09 \cdot 10^3$ A for FT, $14,60 \cdot 10^3$ A for RD, $14,83 \cdot 10^3$ A for RCHG. The mandatory value of m which can not be modified by alternative control of PS is flat-top value, therefore $m = 12,09 \cdot 10^3$ A is chosen to design the capacitor. So that you obtain:

$$C = \frac{m}{2fb} = 40{,}3 \cdot 10^{-3} \text{F}$$

Regarding L_{TC}, there are technological and constructive constraints. In this model L_{TC} is equal to L_{CS} because it is known the possibility to build such structure. However building a bigger tank coil to increase its inductance could not be so difficult, also because it could be a different shape and position respect to central solenoid.

As for the number of parallel of IGCT, data sheet of ABB® 5SHY 42L6500 provides a graph of maximum turn-off current vs. frequency depending on temperature. To maintain temperature below 80 C (limited losses) with frequency 500 Hz, $I_{IGCT_{max}}$ is written in table 3.2. A different design has to be achieved for the couple S1-S2 and for the couple S3-S4. Indeed the latter one commutes only when i_{CS} changes its sign and it happens only twice during the pulse. A simulation is carried out with imposed voltage and right inductance to obtain the maximum obligatory current value that crosses the switch ($50{,}77 \cdot 10^3$ A). Model with losses must be taken into consideration because power supply affects TC current, making it increase during flat-top phase (as it is explained in next chapter). As for S1-S2 the current at maximum frequency value has to be considered (see table 3.2) and so the number of parallel is

$$n_{paral_{1,2}} = \frac{I_{max}}{I_{IGCT_{max}}|_{f=500}} = 33.58 \approx 34$$

where n_{paral} is the number of parallel in a single switch, I_{max} is maximum current through the switch and $I_{IGCT_{max}}|_{f=500}$ is the current at 500 Hz in data sheet of IGCT. As for S3-S4 maximum controllable turn-off current can be used:

$$n_{paral_{3,4}} = \frac{I_{max}}{I_{IGCT_{TCQM}}} = 13.36 \approx 14$$

A trade-off between size of L_{TC} and parallel of IGCT could be studied due to the fact that increasing the inductance reduces the current because needed energy remains the same. Number of series of switches depends on maximum reference voltage value, which occurs in BD phase ($12 \cdot 10^3$ V). Reference value has to be compared with IGCT characteristics. IGCTs have two different maximum values, one for repetitive peak, V_{DRM}, and the other for DC, V_{DC}. For safety reasons number of series of switches is the highest value between the ratio of reference value and V_{DRM} or V_{DC}. For series number there are no differences between couple S1-S2 and couple S3-S4 because they have to bear the same voltage drop. So that:

$$n_{series,DRM} = \frac{V_{max}}{V_{DRM}} = 1.85 \approx 2$$
$$n_{series,DC} = \frac{V_{max}}{V_{DC}} = 3$$

Total number of IGCTs needed for MEST converter is:

$$n_{tot} = \left(n_{paral_{1,2}} + n_{paral_{3,4}}\right)n_{series,DC}n_{switch} = 288$$

where $n_{switch} = 2$ is the number of MEST switches in a couple. In table 3.2 time in which IGCT can not change its status (from *on* to *off*, or vice-versa) are reported. Nevertheless for imposed frequency of operation this margin can not be reached in any case.

4

Numerical MEST model

To verify the correct MEST operation and the design presented in section 3.4, a numerical model of MEST has been developed applied to the CS1 sector of DEMO with Simulink®. In the next section the MEST numerical model will be introduced explaining the functioning of the parts that compose it: switches control, plasma model, the blocks to take into account the magnetic coupling with the other sectors of CS and PF. The model will be used to simulate the waveforms required by the plasma in the various phases of the pulse according to the reference scenario (figure 3.4, table 2.3) and the results obtained will be commented on. Finally, the advantages and critical issues of MEST will be discussed, in particular the power requests will be explained in comparison with those of a traditional power supply with thyristor converters.

4.1 Simulink® model

In this section Simulink® model will be presented and some blocks operation will be explained. The overall model is shown in figure 4.1 in which five parts are highlighted and will be discussed individually: the red square comprehends TC and switches; the green square comprehends the capacitor, the equivalent controlled voltage source in multi-turns side and CS1 sector; the blue square comprehends plasma resistances and inductance and the equivalent controlled voltage source in single-turn side; the magenta square comprehends the block in which switches signals for S1...S4 are built; the light blue square comprehends the block
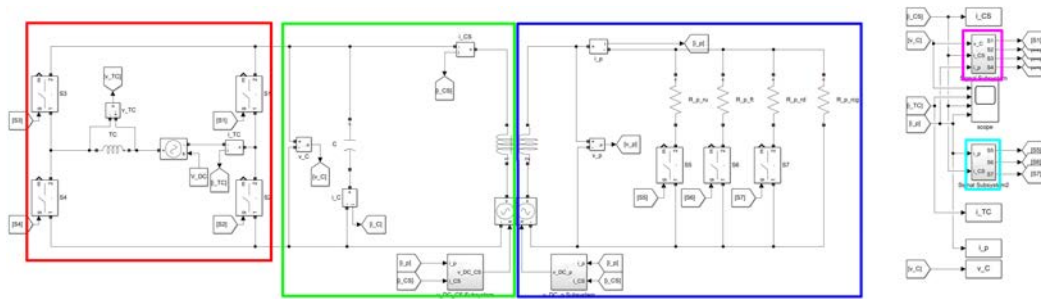
Figure 4.1: Overall Simulink® model of MEST system coupled with plasma

in which switches signals for S5...S7 are built. In figure 4.2 MEST converter is shown and it is composed with four ideal switches, an inductance L_{TC} and a voltage waveforms source as power supply. Signals connected to the switches are built with a subsystem shown in figure 4.3. In this subsystem there are two possibilities: one is for the phases of flat-top and dwell time (reference voltage is constant and calculated previously); the other, indicated with the blocks named *D*, is for breakdown, ramp-up, and ramp-down phases (voltage is provided by the scenario). The block *Hysteresis Function* is the following Matlab® function:

```
function [sign_ref,k_out] = fcn(ref,v_C,k_in)
if ref>=0
        if v_C>=(ref*1.1)% or (ref+b) where b=300 (fixed band)
                sign_ref=1;
                k_out=1;
        elseif v_C<=(ref*0.9)% or (ref-b) (fixed band)
                sign_ref=0;
                k_out=0;
        else
                sign_ref=k_in;
                k_out=k_in;
        end
else
        if v_C>=(ref*0.9)% or (ref+b) (fixed band)
                sign_ref=1;
                k_out=1;
        elseif v_C<=(ref*1.1)% or (ref-b) (fixed band)
                sign_ref=0;
                k_out=0;
```

```matlab
        else
                sign_ref=k_in;
                k_out=k_in;
        end
end
```

where *k_out* and *k_in* are used to maintain the signal status of the previous step. This function serves to build signals for switches S1 and S2. In the block named *CS_scenario* voltage breakdown waveforms of all CS and PF coils are stored. In figure 4.4 coils part is shown. The interior part of *v_DC_CS subsystem* is presented in figure 4.5. Simulink® block of Matlab® function named *v_DC_CS Function* takes into account that the derivative of i_{CS} remains constant for a while and then changes to another constant value (there are six period in RU). The block is built specifically for those scenarios and the code is:

```matlab
function v_DC_CS = fcn(ref)
a=load('v_CS1_ru.mat','CS1');
b=load('i_CS1_ru.mat','ICS1');
b.ICS1=b.ICS1*1e3;
time=[0 25 50 75 100 125 146]';
if ref==-a.CS1(1)
        dics = (b.ICS1(1)-b.ICS1(1+1))/(time(1)-time(1+1));
        vcs = 5.716*dics + 1.4e-3*0.1e6;
        v_DC_CS = vcs + ref;
elseif ref==-a.CS1(2)
        dics = (b.ICS1(2)-b.ICS1(2+1))/(time(2)-time(2+1));
        vcs = 5.716*dics + 1.4e-3*0.1e6;
        v_DC_CS = vcs + ref;
elseif ref==-a.CS1(3)
        dics = (b.ICS1(3)-b.ICS1(3+1))/(time(3)-time(3+1));
        vcs = 5.716*dics + 1.4e-3*0.1e6;
        v_DC_CS = vcs + ref;
elseif ref==-a.CS1(4)
        dics = (b.ICS1(4)-b.ICS1(4+1))/(time(4)-time(4+1));
        vcs = 5.716*dics + 1.4e-3*0.1e6;
        v_DC_CS = vcs + ref;
elseif ref==-a.CS1(5)
        dics = (b.ICS1(5)-b.ICS1(5+1))/(time(5)-time(5+1));
```

```matlab
        vcs = 5.716*dics + 1.4e-3*0.1e6;
        v_DC_CS = vcs + ref;
elseif ref==-a.CS1(6)
        dics = (b.ICS1(6)-b.ICS1(6+1))/(time(6)-time(6+1));
        vcs = 5.716*dics + 1.4e-3*0.1e6;
        v_DC_CS = vcs + ref;
else
        v_DC_CS=0;
end
```

Figure 4.6 shows plasma model (already described in section 3.2), in which each resistance is inserted in the circuit only when its phase is occurring, while *R_p_rcg* is always connected because is much greater than the others (nine order of magnitude) and it does not influence the circuit during operation. Figure 4.8 shows switches signal subsystem which builds signals for plasma resistances. The block *v_DC_p subsystem* (figure 4.7) is similar to *v_DC_CS subsystem* and an identical Matlab® function is used for ramp-down, except for loaded file .mat which contains RD parameters.
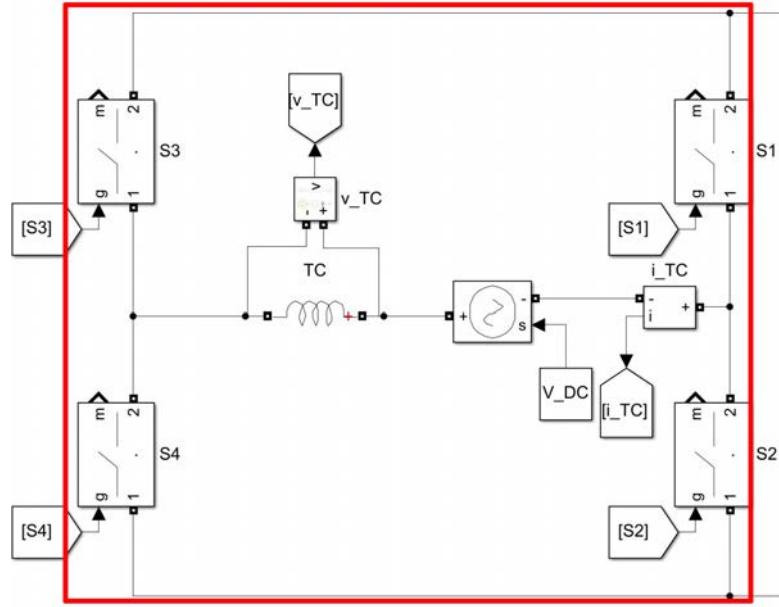
Figure 4.2: Simulink® model of MEST converter system
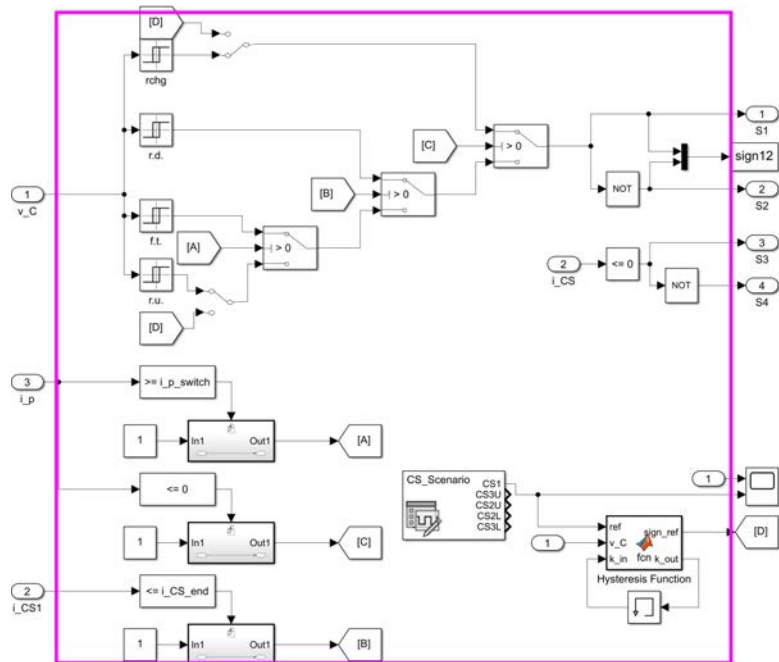
Figure 4.3: Simulink® subsystem utilized to build switches signals for converter
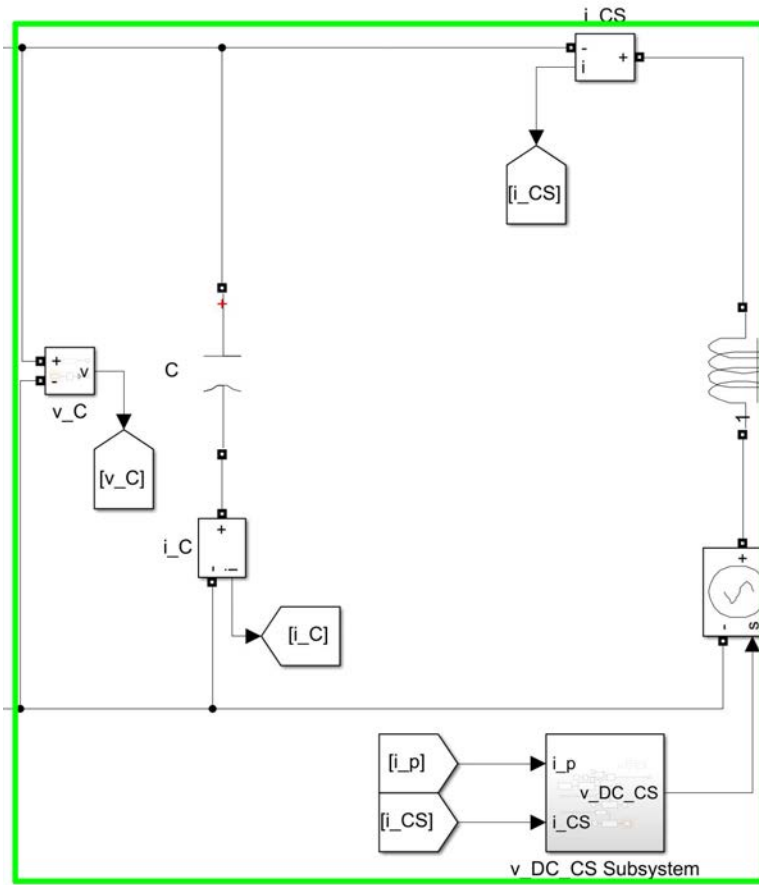
Figure 4.4: Simulink® blocks of capacitor, magnet coil and equivalent voltage controlled source of multi-turns side
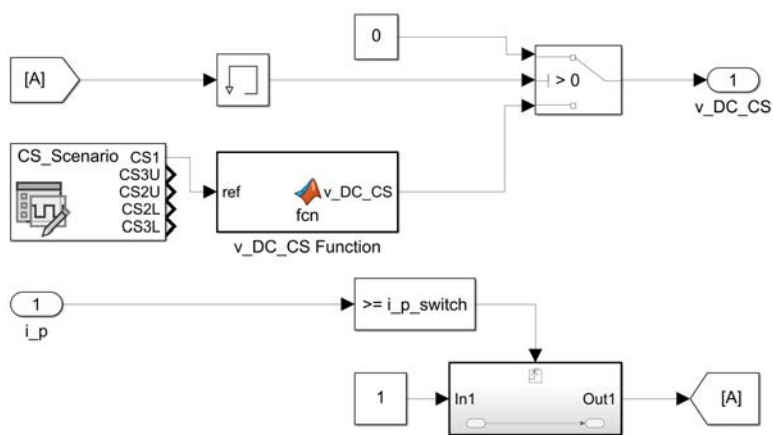
Figure 4.5: Simulink® subsystem utilized to build equivalent voltage controlled source of multi-turns side
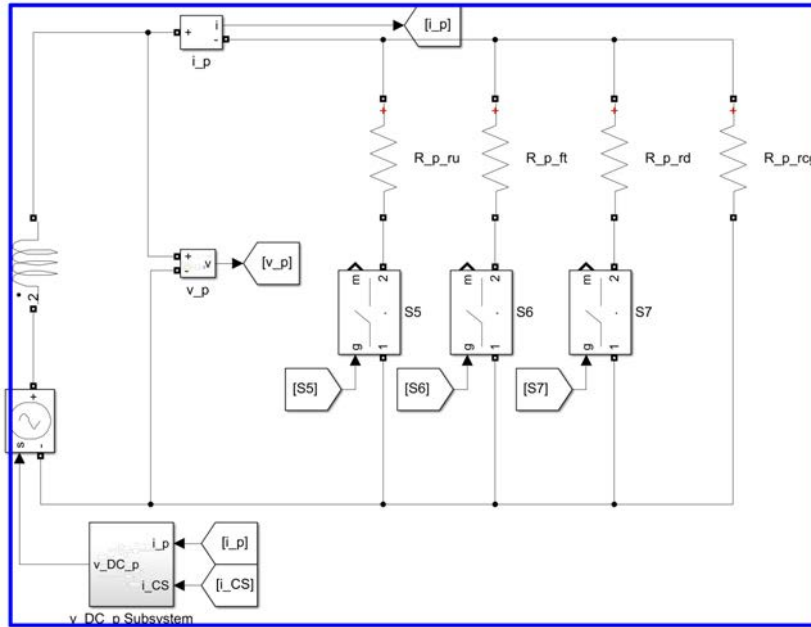
Figure 4.6: Simulink® plasma model and equivalent voltage controlled source of single-turn side
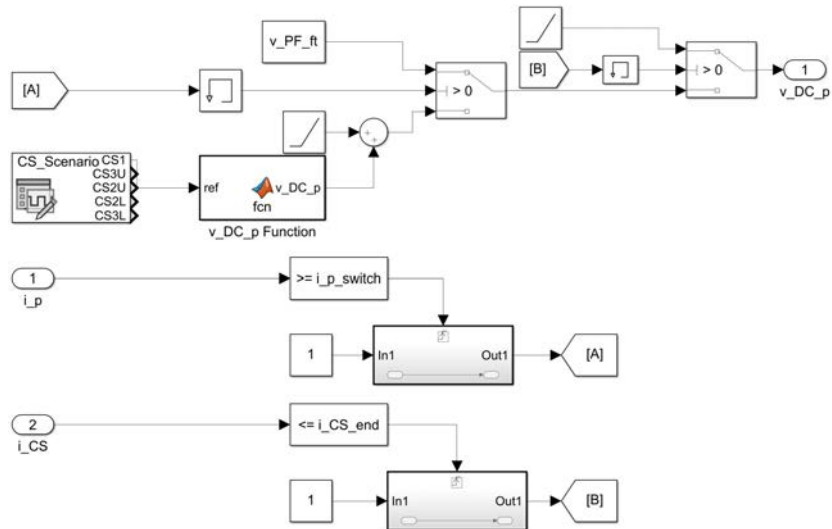
Figure 4.7: Simulink® subsystem utilized to build equivalent voltage controlled source of single-turn side
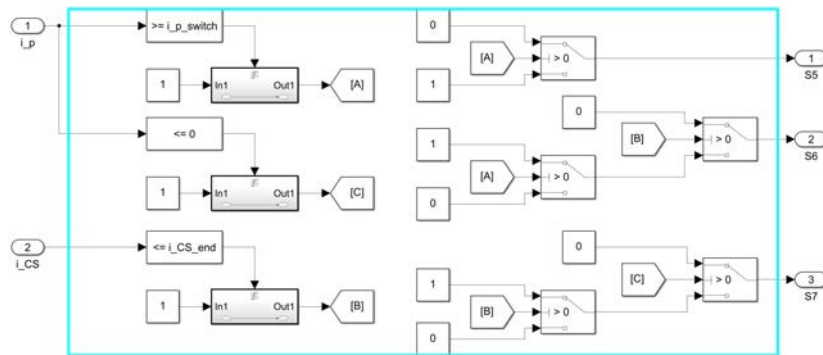
Figure 4.8: Simulink® subsystem utilized to build switches signals for plasma resistances

To evaluate the frequency of simulations utilizing S1 and S2 signals and time vector taken from Simulink®, a Matlab® script is built and is the following:

```matlab
function[F,T]=frequency(signal,time)
a=size(time,1);
kk=1;
T=0;
x=1;
for k=1:a-1
        if signal(k)==signal(k+1)
        else
                T(kk+1,1)=time(k,1)-sum(T);
                x(kk+1,1)=k;
                kk=kk+1;
        end
end
b=floor((size(T,1)-1)/2);
f=zeros(b,1);
for kk=1:b
        f(kk,1)=1/(T(2*kk,1)+T(2*kk+1,1));
end
F=zeros(a,1);
F(1:x(3,1),1)=f(1,1);
for ii=2:b
        F(x(2*ii-1,1)+1:x(2*ii+1,1),1)=f(ii,1);
end
end
```

Values of inductances and resistances are taken from DEMO pre-conceptual design and are shown in table 4.1. Values of reference parameters are shown in table 4.2. For flat-top (which takes 7200 seconds, 2 hours), capacitance is set to a bigger value (10 F) to have a lower switching frequency that allows a shorter acceptable simulation time. Indeed with $C = 40{,}3 \cdot 10^{-3}$ F, simulation time of FT would be almost 3 hours. The correct frequency (with the right capacitance value) is calculated by multiplying the ratio between fictitious and real capacitance and the equation 3.17 due to the fact that f and C are linearly proportional.

Data of i_{CS} derivative are not given directly, but they can be extrapolated using individual points provided by the files in appendix A and considering that voltage from one point to another is constant (so that current variation on inductance is linear). Another essential data for simulations are initial values, which depend on what coil you chose to simulate. To verify the feasibility of MEST on DEMO coils, CS1 references for the whole impulse are given and moreover PF2 references will be simulated during BD to verify the applicability. Initial condition, which is common to all simulations with CS1, is $i_{TC} = 41$ kA because it provides, initially, to satisfy the mandatory condition $i_{TC} \geq i_{CS}$. To carry out any other simulations, needed values are in the appendix A. Breakdown simulations are run with a fixed b (whose value is used in the capacitance design), and with a b% which means that the hysteresis band depends on the voltage requested to MEST.

Other voltages must be calculated due to the fact that data are not complete. Voltage of flat top and dwell time are not defined yet but using other phases conditions they can be obtained. Indeed assuming that FT voltage is constant and taking into account final RU current condition of i_{CS} and initial RD current condition of i_{CS}, FT voltage is easily calculated with inductor component equation (. A similar procedure is used for DT voltage, utilizing final RD condition and initial RU condition. So that, for second equation of 3.8, FT and DW voltages are obtained by considering that $di_p/dt = 0$ and so that $v_{CS} = L_{CS} di_{cs}/dt$. Therefore resulting values are:

$$v_{CS,FT} = L_{CS}\frac{di_{CS}}{dt} = 5.716\frac{(-40.11 + 18.98) \cdot 10^3}{7200} = -16.77\,\text{V}$$

$$v_{CS,DT} = L_{CS}\frac{di_{CS}}{dt} = 5.716\frac{(-30.03 - 41) \cdot 10^3}{-600} \approx 670\,\text{V}$$

inductances				resistances				
L_{CS} [H]	L_{TC} [H]	L_p [μH]	M [mH]	R_{ru} [nΩ]	R_{ft} [nΩ]	R_{rd} [nΩ]	R_{rch} [Ω]	C [mF]
5.716	5.716	1.127	1.4	22.5	2.92	225	1	40.3

Table 4.2: Reference parameters for simulations

v_C references							half band width	
v_{ru}	V_{ft} [V]	v_{rd} [V]	V_{rchg} [V]	$V_{DC_{PS}}$ [V]	$\frac{di_p}{dt}$ [MA/s]	f_{max}[Hz]	b_{fix} [V]	$b_\%$
appendix A	16.77	appendix A	-670	13.67	0.1	500	300	10%

Simulations will be divided into breakdown, ramp-up, flat-top, ramp-down, recharge phases. This necessity is due to the fact that different simulation steps have to be used. Indeed in BD, RU and RD small time-step is required to obtain a capacitor voltage acceptable otherwise upper and lower limit of hysteresis band would be greatly overcame with different values so that mean value of v_C would not be equal to the reference. Instead on FT a greater time-step is possible due to the fact that a bigger capacitance is used and so that a reduced simulation time is achieved. Using one single simulation step on all the phases would have taken very long time to be computed. In next section, simulations of MEST model will be carried out and presented.

4.3 SIMULATIONS RESULTS

4.3.1 BREAKDOWN PHASE

During the breakdown phase, two magnets, CS1 and PF2, are taken into consideration, those with more consistent voltage variations. Indeed, in less than a 0.1 seconds the voltage of CS1 goes from -10 kV to $+10$ kV, while the voltage of PF2 goes from $+9$ kV to 0 in less than 0.5 seconds. Two CS1 simulations are produced, one with $b_\%$ and one with b_{fix} to see how the frequency varies in the two cases. Two simulation of PF2 are made to see how the difference between i_{TC} and i_{CS} influences rapidity of variation of MEST.

Figures 4.9a and 4.9c show CS1 BD phase with fixed Hysteresis Band (HB). Initial conditions are: $i_{TC} = 41 \cdot 10^3$, $i_{CS} = 40 \cdot 10^3$ and $i_p = 0$. It can be noted that the frequency remains far below 500 Hz. Indeed its maximum is 125 Hz and this is due to the fact that initial currents of tank coil and central solenoid are very close to each other and so the differ-

ence is small (equation 3.17). It is important to underline that the current difference in state [1001] and [0110] is i_C, which affects significantly the rapidity of MEST. With $i_{CS} > 0$ if i_C is small, the decrease is slow (see in figure 4.9b how much it takes to reach lower bond the first time). With $i_{CS} < 0$ if i_C is small, the increase is slow. The high variation of frequency is due to the fact that the reference voltage is stepped and if the switching takes place during one edge, the next commutation is faster or slower than those nearby. If the reference had been without discontinuity, the frequency would probably have been more linear.

Figures 4.9b and 4.9d show CS1 BD phase with percentage hysteresis band, which means that UB and LB are calculated by multiplying reference value with $1 \pm b_\%$. Initial condition are the same of previous simulation. It can be noticed how the frequency goes from values below 100 Hz (most of the time) to values over 500 Hz, reaching the maximum at ≈ 900 Hz. This happens when the reference value is near to zero, so that HB is very thin.

A hysteresis band which would combine the two methods would be more efficient: with high reference voltage (use of percentage until fixed band value is reached), frequency would be small, instead with low reference voltage (fixed band), frequency would be that used for MEST components design.

Figures 4.10 show PF2 coil voltage trends and frequency. Initial conditions are: $i_{TC} = 1 \cdot 10^3$ for first simulation, $i_{TC} = 1{,}5 \cdot 10^3$ for second one, $i_{CS} = 9{,}038 \cdot 10^3$ and $i_p = 0$. Differences between figures 4.10b and 4.10a can be noticed at the beginning and in the end of simulations and are due to the same cause: different value of $i_{TC} - i_{CS}$ influence the behaviour and dynamic of MEST. In 4.10a decrease of v_C is too slow to follow the reference but the frequency is lower (its maximum value is 133 Hz and the mean value is 73 Hz). In 4.10b v_C can follow the reference waveform without any delay but the frequency is higher (its maximum is 208 Hz and the mean is 135 Hz).

This results show that the initial TC current value has to be carefully evaluated, such that the dynamic of MEST is the one required by the tokamak.
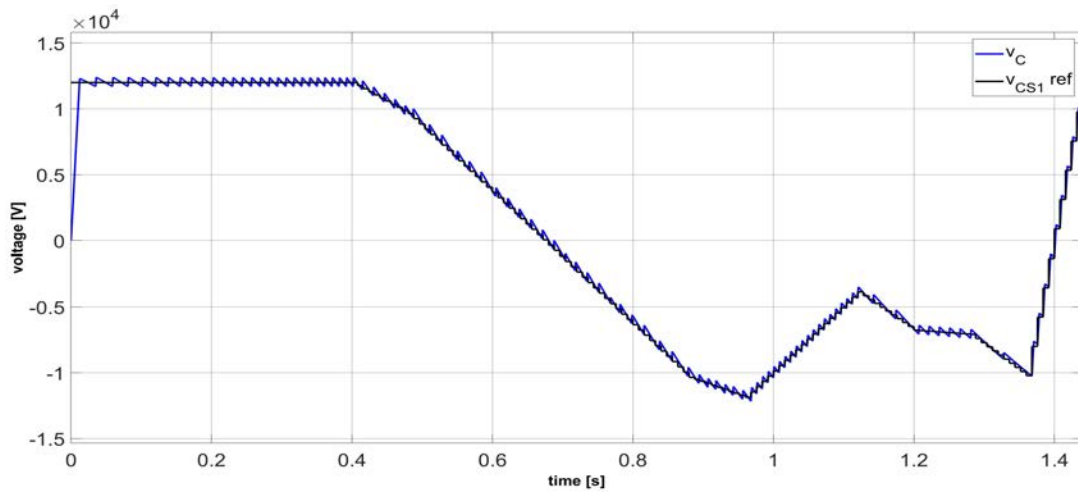
(a) v_C and CS1 reference voltage in BD phase with fixed HB
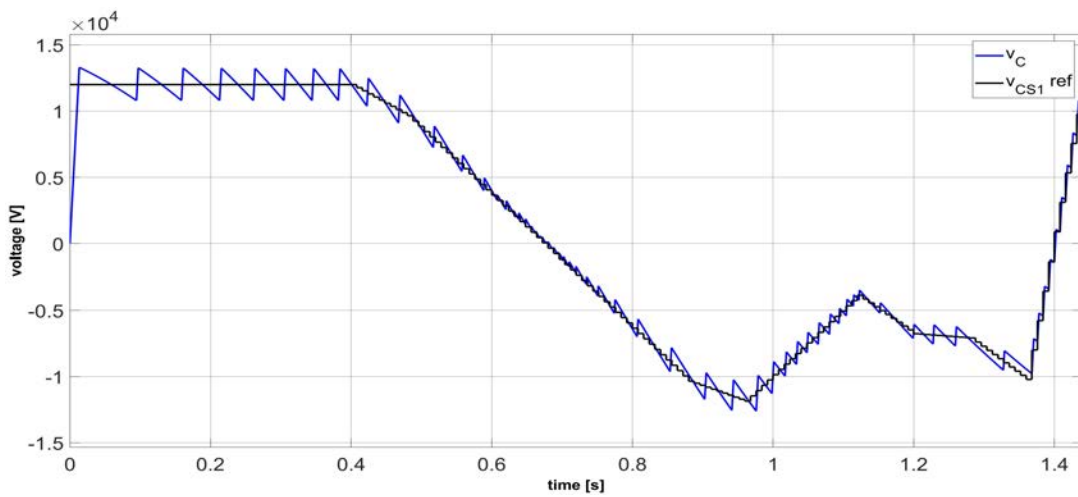
(b) v_C and CS1 reference voltage in BD phase with percentage HB
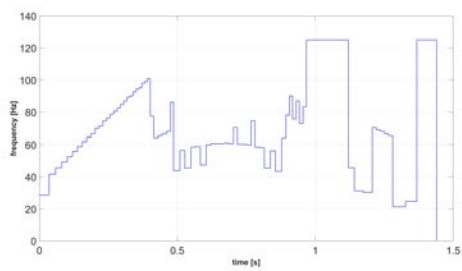
(c) Switching frequency with fixed HB
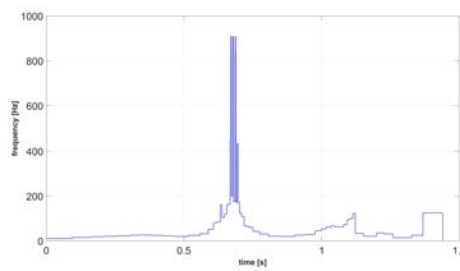
(d) Switching frequency with percentage HB

Figure 4.9: Voltage trends and frequency with different HB with CS1 voltage reference
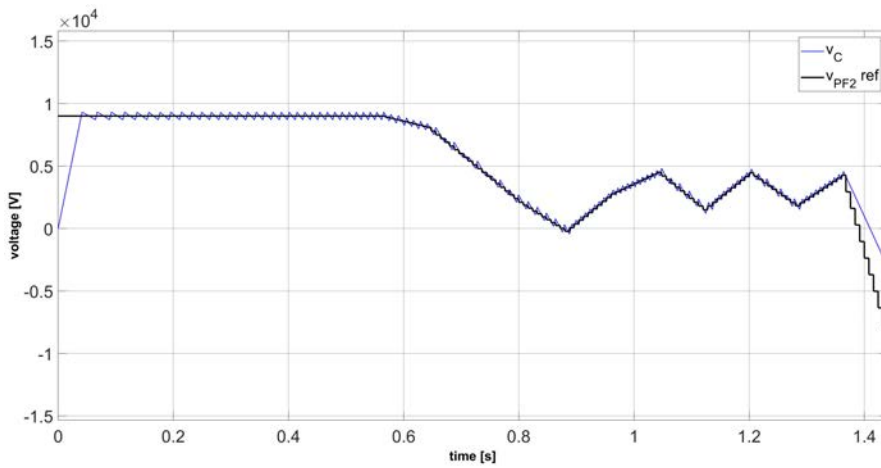
(a) v_C and P2 reference voltage in BD phase with fixed HB with $i_{TC}(0) = 1 \cdot 10^4$
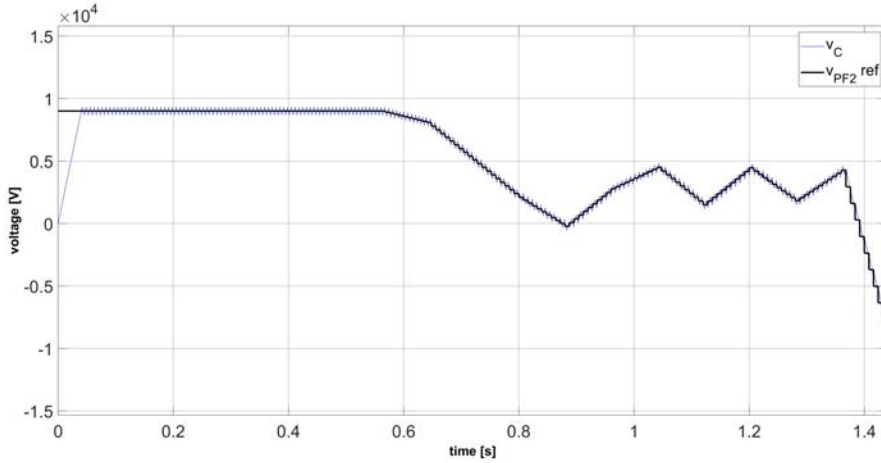
(b) v_C and P2 reference voltage in BD phase with fixed HB with $i_{TC}(0) = 1{,}5 \cdot 10^4$
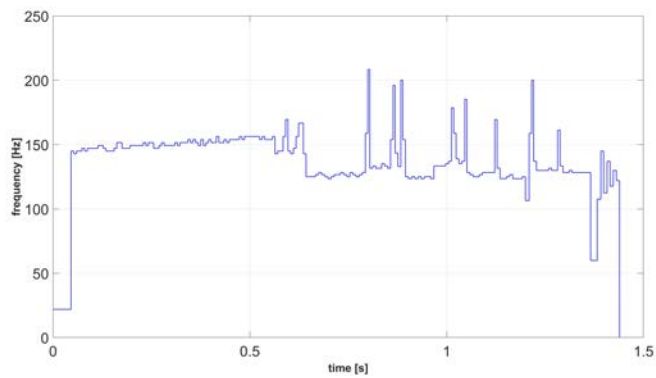
(c) Switching frequency with fixed HB with $i_{TC}(0) = 1{,}5 \cdot 10^4$

Figure 4.10: Simulations of P2 breakdown phase

4.3.2 RAMP-UP PHASE

Simulation of ramp-up phase is shown in figures 4.11 and the most significant variables are presented. Initial conditions are: $i_{TC} = 41 \cdot 10^3$, $i_{CS} = 23{,}98 \cdot 10^3$ and $i_p = 5 \cdot 10^6$. Regarding v_C, you immediately notice that the voltage values required by the coil are significantly lower than in the BD phase. This is because breakdown phase is a crucial phase, in which plasma current has to be triggered and high variation of magnetic flux is required; instead ramp-up phase serves to increase plasma current to the maximum value in a relatively long time (with respect to the BD) and so it does not need an high induced electromotive force. Looking at figure 4.11a one would expect, with an hysteresis control, an output voltage having a fixed band whose average value is the reference value. In the figure this does not happen because of the sampling step which is not sufficiently small, but, however, it can not be further reduced because the simulation would take place in extremely long times (with this sampling - $100\ \mu s$ - it lasted about 10 minutes to simulate 146 seconds). At about 90 seconds, the switching frequency is near zero, since the i_{CS} cross 0: from equation 3.17 if $i_{CS} = 0$ also $f = 0$, as you can see in figure 4.11c. Moreover about frequency, it remains always below 500 Hz (as it should be by the design). Its maximum is 460 Hz and it happens when passage from RU to FT occurs. In this moment hysteresis limits change and lower limit of RU and upper limit of FT are closer than other instant, therefore recharge time of capacitor is shorter and switching frequency is higher. Regarding currents, i_p starts at 5 MA due to the fact that in BD phase plasma current reaches that value; i_{TC} grows up until its maximum when i_{CS} crosses zero and then it decreases, as specified in section 3.2. Simulation time is 145.1, similar to time of scenario waveform that is 146; the difference is probably due to the complexity of plasma and coupling which are not represented carefully in MEST model and due to the fact that mean value of v_C is not the same as the reference.
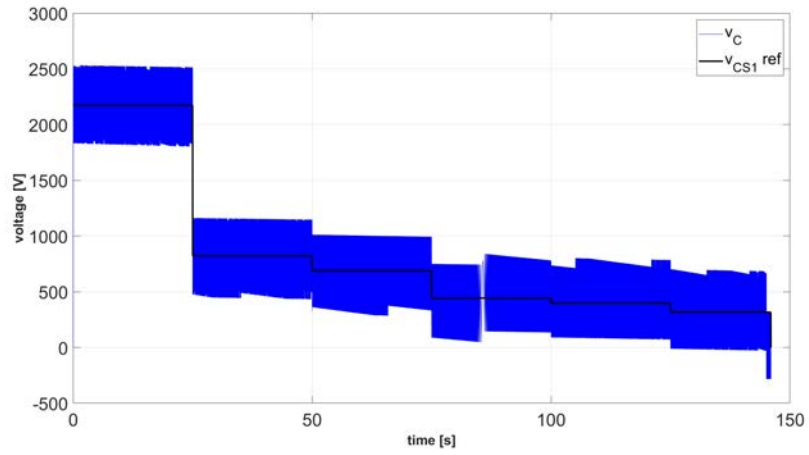
(a) v_C trend and CS1 voltage reference
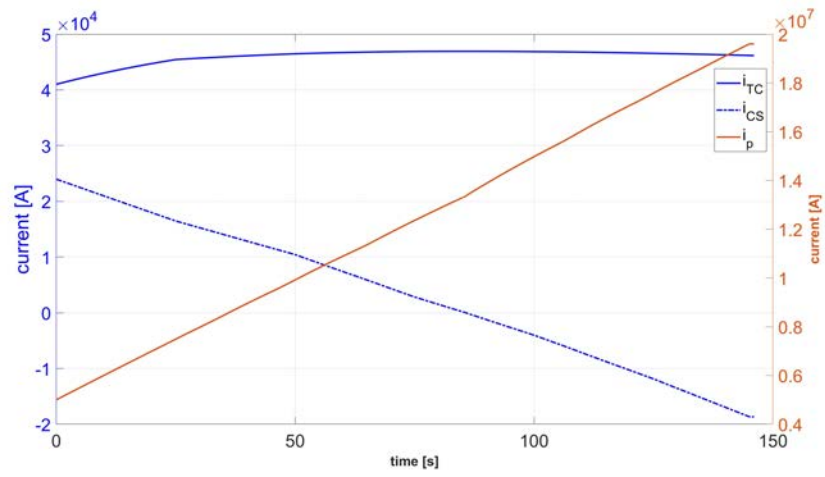
(b) i_{TC}, i_{CS} and i_p trends
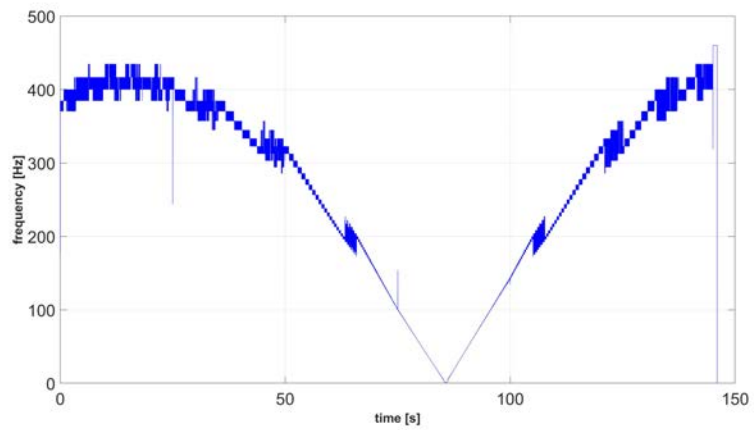
(c) Switching frequency

Figure 4.11: CS1 ramp-up simulation

65

4.3.3 Flat-top phase

At the moment the flat top phase is not available in the scenario waveform. The only points available are the initial CS current value (which corresponds to the final value in the RU) and its final value (which corresponds to the initial value for the RD). As far as, the voltage controlled source which compensates other coils influence is set to 0 in one side of model (multi-turns, $V_{eq_{CS}} = 0$). Voltage applied to the capacitor as reference is obtained by the third equation of system 3.7a.

The flat top phase lasts 7200 seconds, as fixed by DEMO operation, but capacitance is increased to 10 F so that simulation can be carried out with acceptable time, as explained in section 4.2. Initial conditions are: $i_{TC} = 46,19 \cdot 10^3$, $i_{CS} = -18,98 \cdot 10^3$ and $i_p = 19,6 \cdot 10^6$. The notable things are: the reference voltage is extremely small (16.77 V) because the resistance of plasma to be compensated is very small, so that voltage drop is very modest; plasma current is not a constant value because, being affected by di_{CS}/dt which depends on L_{TC} and C, sinusoidal waveform of circuit LC makes i_p swing; current of tank coil, instead of decreasing as previously mentioned, increases because the power supply charges the tank coil more than CS discharges it (figure 4.12, if there had not been PS i_{TC} would have decreased); maximum frequency, once corrected to take into account the correct capacitance value, is 500 Hz, according to the design.
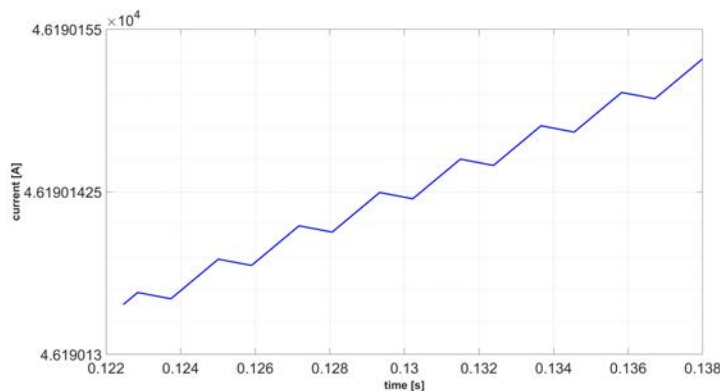
Figure 4.12: i_{TC} in a very small scale
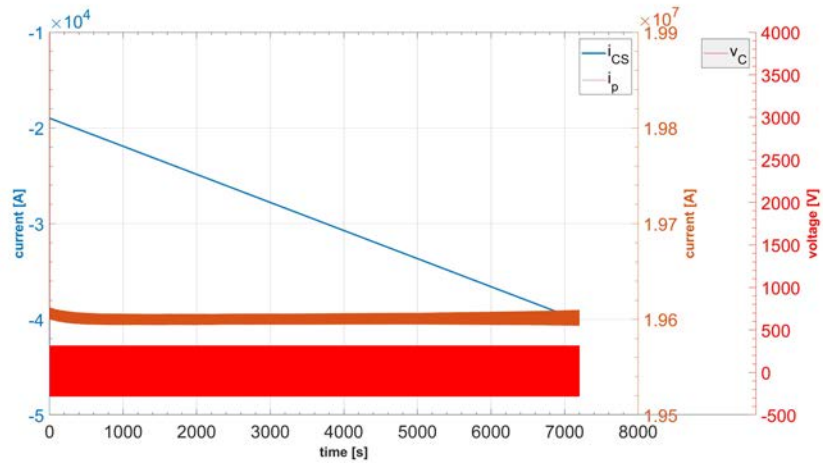
(a) i_{CS}, i_p and v_C trends
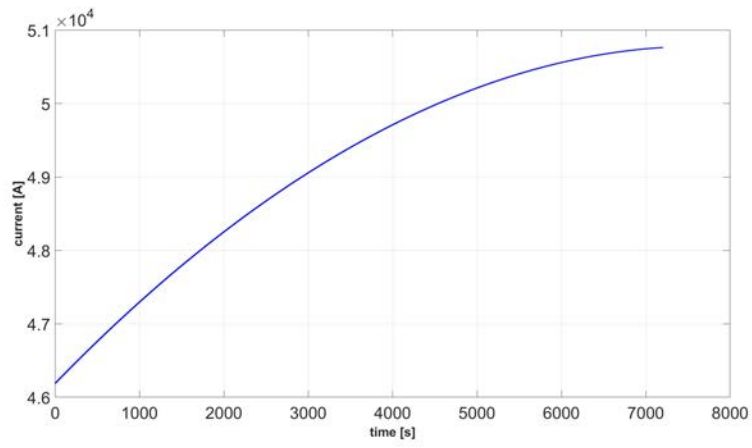
(b) i_{TC} trend
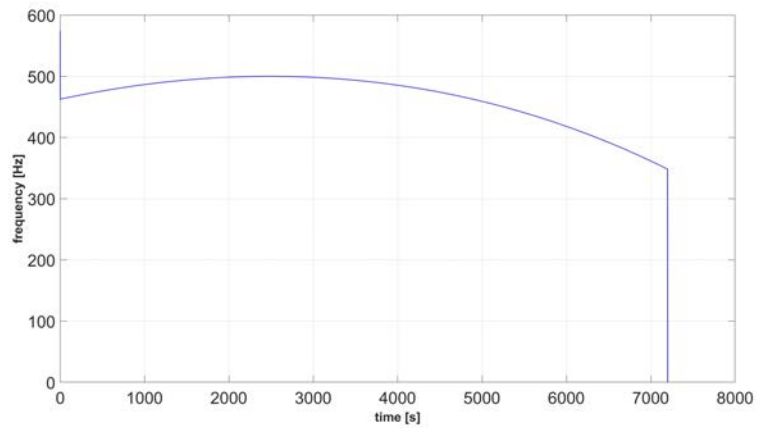
(c) Switching frequency

Figure 4.13: CS1 flat-top simulation

67

Ramp-down simulation is shown in figures 4.14. Initial conditions are: $i_{TC} = 50{,}77 \cdot 10^3$, $i_{CS} = -40{,}11 \cdot 10^3$ and $i_p = 19{,}6 \cdot 10^6$. It is necessary to have a negative voltage on the CS to obtain controlled decrease of the plasma current. Having i$_{CS}$ and v$_C$ reference negative in the period from 25 and 146 seconds, energy goes from CS to the tank coil. This means that TC current increases as you can see from figure 4.14b. Also CS current increases due to energy transfer from plasma and due to negative voltage reference. Simulation stops with $i_p = 5$ MA because the scenario data does not provide any other values. Frequency graph (figure 4.14c) is very interesting to analyse. Indeed hysteresis band and capacitance value remain the same as in other phases, but frequency goes over 500 Hz and reaches its maximum at 588 Hz. That is due to the coils currents, $i_{CS} \pm i_{TC}$ ($\pm$ depends on which switches are closed and i$_{CS}$ has to be taken with its sign). Indeed frequency, from equation 3.17, depends on i$_{TC}$ and i$_{CS}$: greater is the difference between currents, higher is the switching frequency. In this phase the difference between coils currents is so big that frequency overcomes the imposed technological limit.

An alternative use of power supply can solve this problem and can reduce greatly frequency value. Since i$_{TC}$ must be greater than i$_{CS}$ otherwise MEST switch control does not work, PS can be used to provide the right voltage to maintain the different between i_{TC} and i_{CS} constant and this happens if TC current varies with the opposite derivative of i$_{CS}$ (figure 4.15b). The voltage is calculated by using Kirchhoff's voltage law and, as there are two different states of switches for $i_{CS} < 0$, two equations are utilized, that are:

$$\text{State } [1010] \quad v_{PS} = v_{TC} = L_{TC} \frac{di_{CS}}{dt}$$

$$\text{State } [0110] \quad v_{PS} = v_{TC} + v_C = L_{TC} \frac{di_{CS}}{dt} + v_C$$

where v_{PS} is power supply voltage, v_C is capacitor voltage reference and di_{CS}/dt is given by the scenario.

Frequency is obtained analytically by imposing the difference taking into account the mandatory constraint of coils currents. By the 3.17, fixing $i_{TC} - i_{CS} = 20\%$ it results:

$$f = \frac{|i_{CS}|(1.2|i_{CS}| - i_{CS})}{1.2i_{CS} * 2Cb} = \frac{|i_{CS}|}{12Cb}$$

The model was run with this different PS control and the resulting waveforms are shown in figure 4.15. You can notice that frequency (figure 4.15c) is far below the limit and its maximum is 400 Hz and its mean value is 301 Hz.

However this method requires lot of power (peak is 116.6 MW) and it goes contrary to the operation of MEST, *i.e.* to reduce peak active power for DEMO. Other methods can be implemented to manage the PS and they will be discussed in next section.
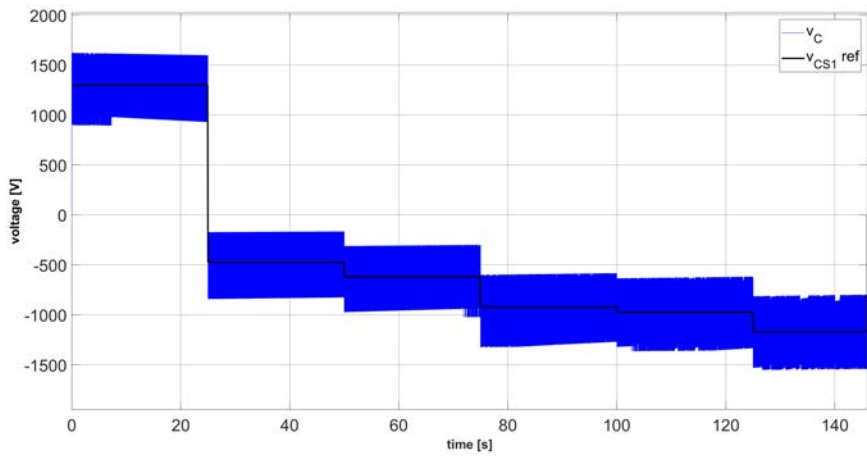
(a) v_C trend and CS1 voltage reference
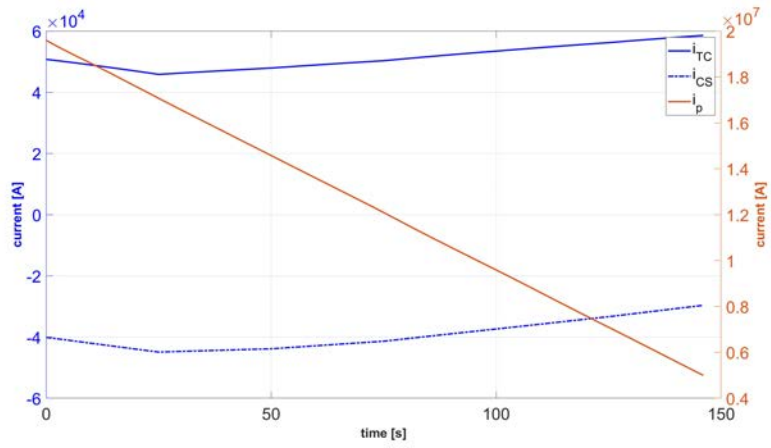
(b) i_{TC}, i_{CS} and i_p trends
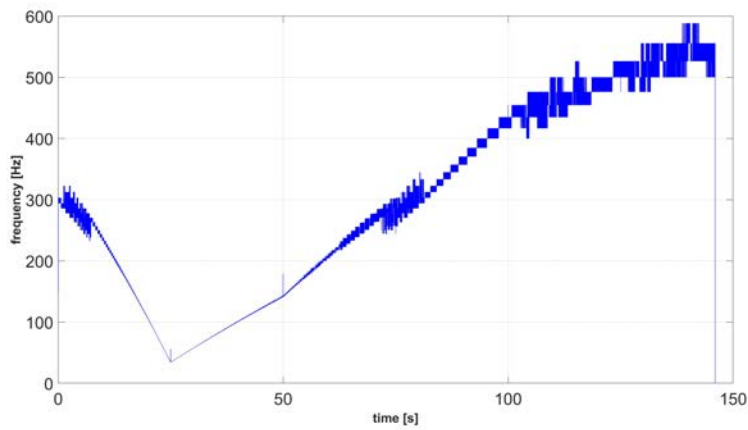
(c) Switching frequency

Figure 4.14: CS1 ramp-down simulation
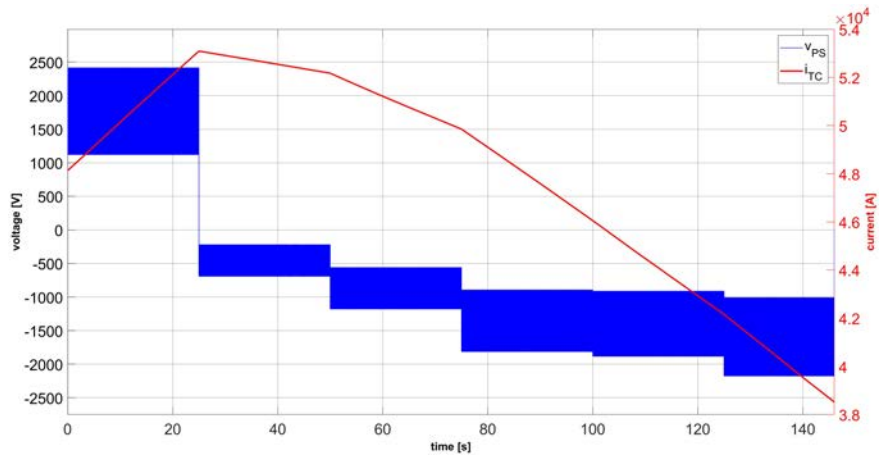
(a) v_{PS} and i_{TC} trends
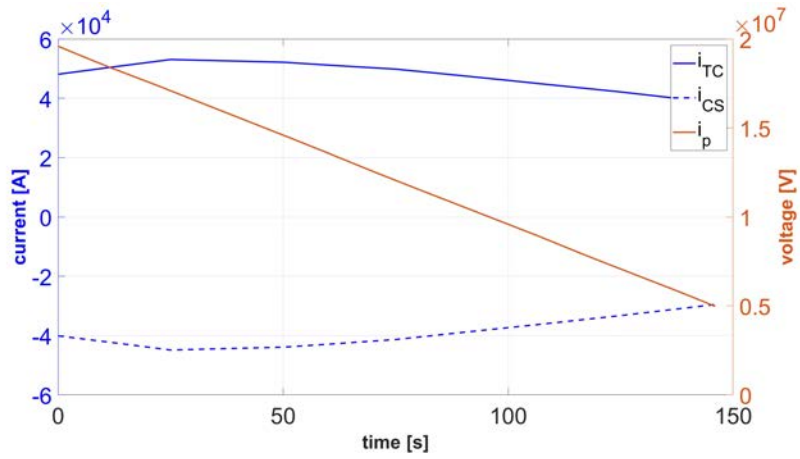
(b) i_{TC}, i_{CS} and i_p trends
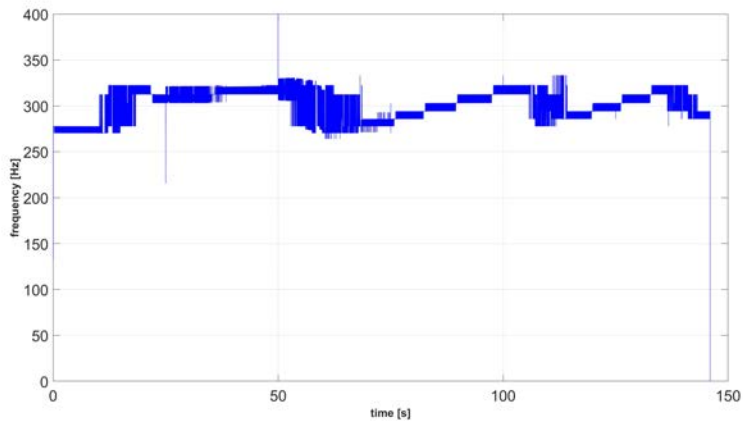
(c) Switching frequency

Figure 4.15: CS1 ramp-down simulation with alternative use of power supply

71

4.3.5 Dwell time

Dwell time (or recharge) phase is shown in figure 4.16. Initial conditions are: $i_{TC} = 58,44 \cdot 10^3$, $i_{CS} = -30 \cdot 10^3$ and $i_p = 0$. In this phase with the use of power supply described in section 3.4, i_{TC} reaches the maximum value ($65,69 \cdot 10^3$ A) which would be used to design tank coil conductors. Moreover the currents on TC and CS do not have the same value at the end of the simulation, therefore it means that the energy stored in TC is larger than that required by MEST for the next pulse. Indeed initial condition of i_{TC} of ramp-up or breakdown is different from final one ($i_{TC,begin} = 41 \cdot 10^3$ and $i_{TC,final} = 51,85 \cdot 10^3$). Also switching frequency is higher than the imposed limit of 500 Hz because difference between currents is considerable (its maximum is 618 Hz).

Using the alternative control of PS, figures 4.17 are obtained. CS current is the same of previous simulation because it has its shape to follow; TC current is very different, it decreases until i_{CS} reaches zero then it increases. This means that initially CS and TC provide energy to PS and the grid and when $i_{CS} > 0$ PS and TC supply CS. As you can notice from figure 4.17c, capacitor current switches from i_{CS} value to a constant value: that is because when state [1010] and [0101] occur $i_C = i_{CS}$ instead when state [1001] and [0110] occur $i_C = i_{TC} - |i_{CS}|$ (which is constant). Switching frequency is very low and its maximum is 211 Hz.

Again as in ramp-down, this method requires the grid to accept high active power and its feasibility has to be verified. Other strategy will be discuss further on.
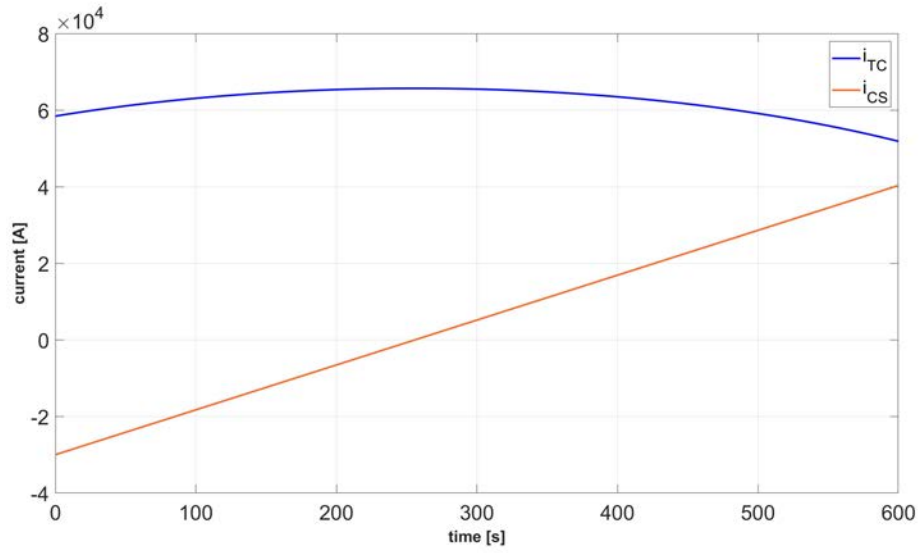
(a) i_{CS} and i_{TC} trends
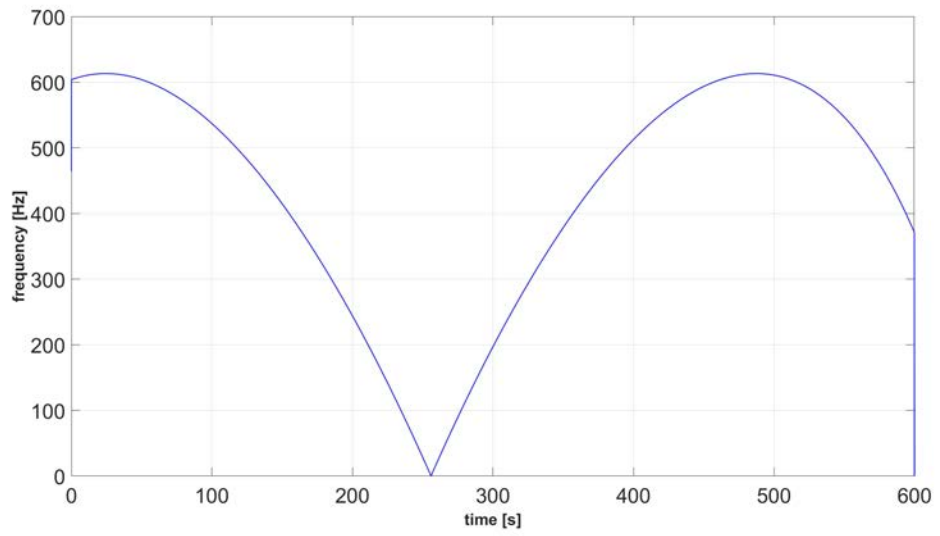
(b) Switching frequency

Figure 4.16: CS1 dwell time simulation
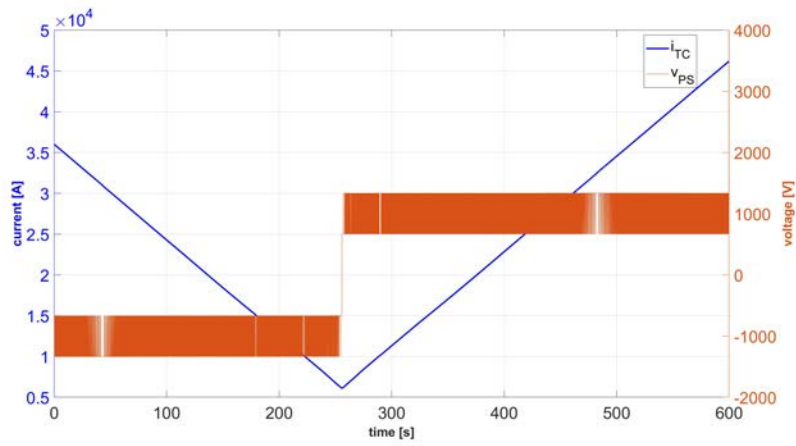
(a) v_{PS} and i_{TC} trends with alternative control of PS
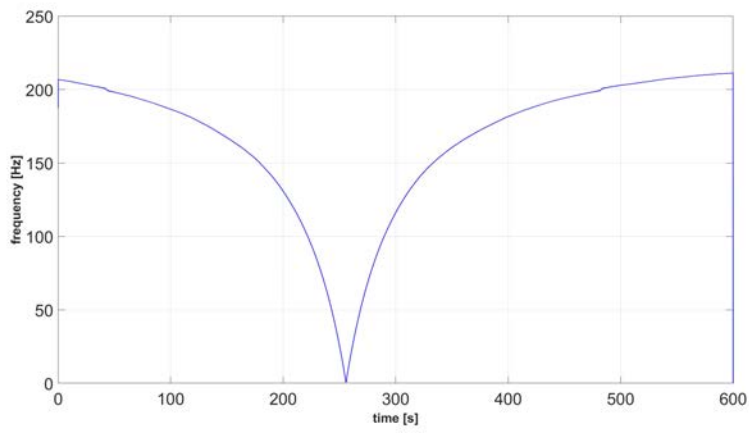
(b) Switching frequency with alternative control of PS
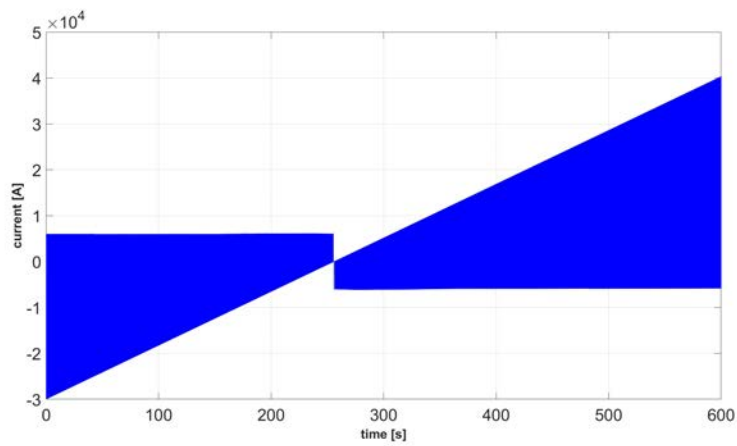
(c) Capacitor current with alternative control of PS

Figure 4.17: CS1 dwell time simulation with alternative control of PS

From the explanation of operation and the proposed simulations, it is noted that the pillars on which MEST concept is based, are the capacitance and current of the capacitor, in addition to the constraint on tank coil and central solenoid currents. It is not surprising that these are the fundamental parameters because they affect the derivative of capacitor voltage, voltage that controls energy exchange between TC and CS, and thus the switching frequency of MEST. In this section the critical issues discussed in the previous paragraphs will be examined and possible solutions will be presented.

The system is designed for the highest mandatory value of energy requested in tank coil, so that what happens in second half-part of ramp-down and in dwell time are over of design limits, both in switching frequency and in maximum current value.

As for frequency, a solution is to accept those values: consequences are that more switches have to be added in parallel for maximum current and that losses increase and so efficiency decreases. This method is not suitable compared with other solutions.

Another approach could be the insertion of an additional capacitance in parallel to the main one. Knowing that $m_{max} = |i_{CS}|(i_{TC} - i_{CS})/i_{TC} = 14{,}83 \cdot 10^3$ A (m is defined in section 3.3.2) from the previous simulation, additional capacitor is obtained by finding new total capacitance with the equation 3.17 and by considering that two capacitances in parallel are equal to the sum, so:

$$C_{add} = \frac{m}{2fb} - C_{main} = 9{,}17 \cdot 10^{-3} \approx 10 \cdot 10^{-3} \text{ F}$$

This solution will reduce switching frequency but additional needed capacitance has its cost in terms of both money and space. Moreover maximum current issue would not be solved. Another method could be increasing hysteresis band. By equation 3.17 it results:

$$b_{new} = \frac{14.83 \cdot 10^3}{2fC} = 368 \approx 370\text{V}$$

and therefore the band would be $2b = 740$ V. Increasing hysteresis band would not cost and would not affect in any case currents. However problem of high current value would remain.

Two solutions would influence both issues and they are: a bigger tank coil and an alternative control strategies of power supply.

Increasing inductance of TC means that, fixing magnetic stored energy, current will be lower than with a smaller inductance. Thus with the same simulations, the tank coil current would be reduced and also the difference $i_{TC} - |i_{CS}|$, so that switching frequency would decrease. Another advantage is that with high inductance higher voltage is necessary to produce the same current variation. In MEST operation it means that the constraint of $i_{TC} > |i_{CS}|$ could be solved without energy exchange with the grid because TC current would remain almost constant and higher than maximum absolute value of i_{CS}. Disadvantages of this solution are the design of such inductor, its cost and the cost of occupied space.

The alternative control strategies of PS diversify from each other based on how you want to distribute energy over the different phases. The simplest strategy is described in section 3.2 and it consists in having a constant voltage to compensate losses. Another one is described in ramp-down and recharge simulations and it consists in maintaining a constant difference between currents. Both of these control strategies are not suitable for MEST.

A third solution could be to control PS to maintain constant i_{TC}: the advantages are those of having a bigger inductance but, as disadvantage, there is a continuous exchange of power between tank coil and the grid. This gets to a more sophisticate control of power supply because with different states, exchanged energy must vary and moreover an analysis of power flow in bars of plant electrical system must be carried out. To reduce exchanges between PS and TC which could create difficulties in PES for the amount of power, a hysteresis band on i_{TC} could be utilized, where the lower limit would be the minimum of i_{CS} and the upper limit would be design on how PES could manage the exchanges.

Finally it would be possible to implement the strategy used to design the capacitor adding a negative PS voltage during ramp-down and dwell time, so that in a first phase (flat-top) PS requests power from the grid and in the next one (RD and DT) power would be reintroduced into the grid or into PES for other loads. In this way the maximum TC current would be the mandatory one reached in the end of flat-top and the switching frequency would be reduced in RD and DT phases. Moreover energy exchange would be fixed and a power flow analysis would be easier.

4.5 Power Comparison with different power supplies

In this section comparison between power requested by PS with MEST system and by thyristors converter for CS1 sector are carried out. In figure 4.18 are shown active and reactive power in different phases of thyristors converter (figure 4.18a BD, 4.18b RU and 4.18c RD)

and of PS with MEST system (figure 4.18d FT). Data of power are taken from [26] for thyristors technology and from simulation with numerical model for MEST.

As for thyristors converter, breakdown phase is the most expensive in terms of active power demand (max 450 MW) to respect of other phases (RU max 52.1 MW; RD max 39.4 MW); regarding reactive power all phases are quite similar in terms of amplitude (BD max 567 MVAR; RU max 346 MVAR; RD 631 MVAR).

As for active power with MEST system, it is easily calculated by $P_{PS}(t) = V_{PS}i_{TC}(t)$ and it reaches its maximum (0.694 MW) in the end of FT. Regarding reactive power, it depends on which PS technology converter is utilized and so some considerations have to be done. Firstly it is essential to rememberer that PS is used as explained in section 3.4 and that voltage is constant. This could bring to choose a diode rectifier. Its advantage is that no reactive power would be requested from the grid, but in other hand it provides only one direction for power, that means that TC could not give back to the grid the magnetic stored energy. Another converter that could be chosen is thyristors converter. It can operate in four-quadrant, energy could flow from/to the grid; it can regulate the voltage (if necessary) but it requires reactive power. A brief example is achieved to estimate reactive power in an hypothetical situation.

In section 2.2 it has been described PES of DEMO in which a LV level of 400 V is present. Considering 400 V as voltage line-to-line Root Mean Square (rms), $V_{LL,rms}$, and considering 14 V as mean value on TC, $V_{mean,\alpha}$, obtained by the delay angle α, from [27] the equation to find the delay angle is:

$$V_{mean,\alpha} = 0.9V_{LL,rms} \cos \alpha \;\rightarrow\; \alpha = \arccos \frac{V_{mean,\alpha}}{0.9V_{LL,rms}} = 87,77°$$

and to calculate reactive power for the first harmonic is:

$$Q_1 = 0.9V_{LL,rms}I_{DC} \sin \alpha \tag{4.1}$$

where I_{DC} is the current in DC side (in this case is i_{TC}). As i_{TC} varies during time, reactive power is evaluated for the worst case so that when TC current is maximum ($I_{DC} = 50,77 \cdot 10^3$ A): with equation 4.1 it results $Q_1 = 18,26 \cdot 10^6$ VAR.

In conclusion it is clearly noted that power (both active and reactive) requested by PS with MEST system is extremely smaller than that provided without any ESS with thyristors converter.
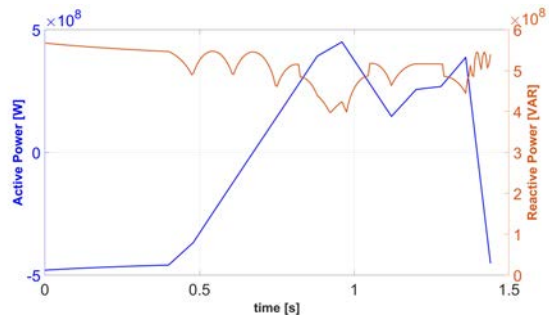
(a) Active and reactive power of PS in BD phase with thyristors converter
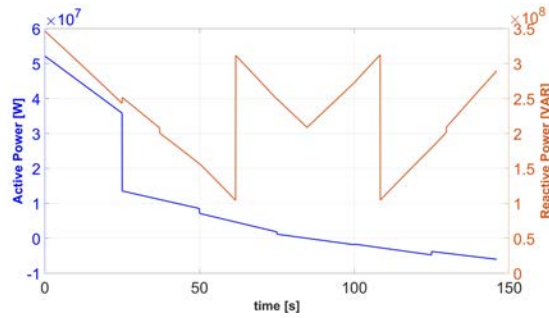
(b) Active and reactive power of PS in RU phase with thyristors converter
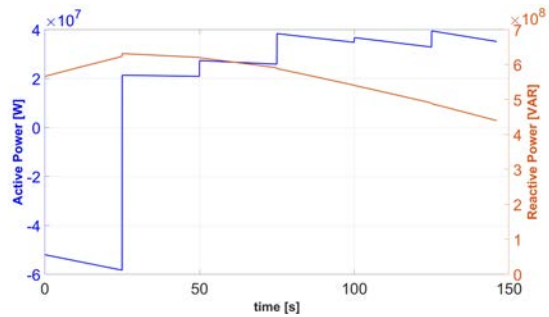
(c) Active and reactive power of PS in RD phase with thyristors converter
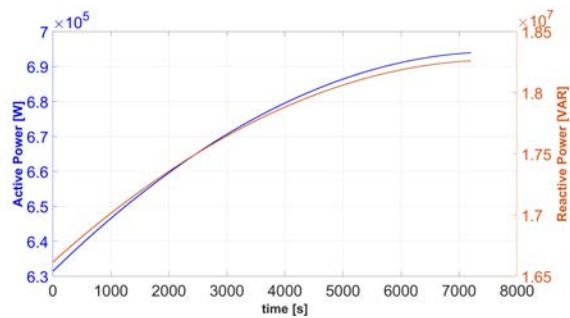
(d) Active and fictitious reactive power of PS in FT phase with MEST system

Figure 4.18: Comparison of active and reactive power of PS with different technologies

5

Conclusion

In the first part of this thesis European DEMOnstration Fusion Reactor has been presented underlining that the magnets (to confine and to maintain the equilibrium of plasma) require a very huge amount of active power and, using thyristors converters as power supply, also a big quantity of reactive power. A brief presentation of thyristor converter design for DEMO has been explained. These issues justify a study on new type of Coils Power Supply System (CPSS).

In the second part alternative solution for DEMO coils power supply has been outlined. Principle of operation of Magnetic Energy Storage and Transfer system has been described dividing up the description into two parts: the first one represents a central solenoid sector or a poloidal field coil without plasma coupling, in which use of switches (with hysteresis control) and the energy transfer have been illustrated; the second one represents the first part but with plasma and other coils coupling defining how to model the plasma and the magnetic coupling to the others coils. Then analytical study has been carried out, solving the differential equations for all states of switches. Furthermore a evaluation of frequency has been calculated due to its importance as it is a technological limit and is related to losses. Then components design has been carried out: firstly power supply voltage, then the capacitance the tank coil inductance and the number of switches and finally the reference voltages of flat-top and dwell time.

In the last part Simulink® model of MEST and implemented Matlab® functions have been shown. With these tools, with data provided by the scenario, which proposes voltage wave-

forms for correct reactor functioning, and with components design, simulations of all phases of DEMO operation have been performed. Results have been presented and discussed with the following conclusions:

- MEST can follow very fast reference (in other words, reference with high derivative) with the right combination of $i_{TC} - |i_{CS}|$ and capacitance;

- Switching frequency has a crucial role and many components (PS voltage, C, L_{TC}, difference between i_{TC} and i_{CS}) affect it, and this makes the frequency be adjustable in a easy way;

- Main issues, that MEST system presents, are high frequency and high tank coil current.

Multiple solutions have been introduced to reduce MEST problems and the increasing of L_{TC} and the proposed strategy of power supply, in which the highest current value of TC is at the end of FT, seem to be the most interesting and the most suitable for a realization. Moreover a power comparison between first design approach (thyristors converter) and MEST system applied to DEMO has been achieved, concluding that MEST would reduce greatly active power peak and could nullify (or reduce) reactive power, separating the grid from the magnets. In this way alternative design for CPSS would make the requested power acceptable for the grid.

Further studies should be realized to improve this system which presents good characteristics to be used as CPSS. Future studies could be focused on which type of power supply is more suitable for a fixed control strategy (for example diode bridge or thyristors converter or others) and on the protection of magnets (with the integration of FDUs) and of tank coil (with the integration of crowbars). Together with PS, it is very important switches choice because they imposed frequency limits and losses (future improvements could change the reachable maximum ratings). Also an optimization on number of capacitances in parallel (one, two or more capacitors) and on number of TC and its inductance value should be studied. Moreover, an analysis should be realized on power flow in busbars of PES because the possibility to move back and forth energy between different coils or other loads is very important.

In near future the construction of a prototype with reduced ratings has been started with the help of industry.

Acknowledgments

È giunto il momento di concludere definitivamente questa tesi e il mio percorso universitario, che mi ha portato grandi soddisfazioni e un bel po' di stress, ringraziando coloro i quali hanno permesso tutto ciò.

Innanzitutto vorrei ringraziare il professor Paolo Bettini che mi ha fatto conoscere il mondo della fusione nucleare, complicato ma molto interessante, e l'Ing. Elena Gaio che è stata punto di riferimento e guida eccellente. In particolar modo vorrei rigraziare affettuosamente il Dott. Ing. Alberto Maistrello che ha avuto la pazienza e gentilezza di rispondere sempre a tutte le mie domande e che mi ha seguito passo per passo in ogni momento, dall'inizio alla fine di questa tesi. Ringrazio Francesco Lunardon che ha sopportato le mie richieste d'aiuto sui blocchi di Simulink®.

Ai miei genitori voglio dire un immenso grazie perché il loro essere, con i difetti e con i pregi, mi ha insegnato a vivere e mi ha fatto diventare quello che sono ora. Ringrzio i miei fratelli, Mattia e Camilla, perché so che, anche nel caso in cui il mondo cascasse, saremmo sempre tutti lì, insieme, a sostenerci l'un l'altro. Ringrazio i miei nonni a cui voglio tanto bene e soprattutto le nonne per tutti i pranzi e le cene che mi hanno mantenuto giovane e sano.

Infine, ringrazio te, Roberta, che sei qui accanto a me ormai da sette anni e che sei già diventata il mio bastone della vecchiaia, mi sorreggi, mi stabilizzi, mi accompagni ad ogni mio passo. Si sa che il futuro è sempre incerto e non è mai come uno se lo immagina, ma qui, ora e sempre, comunque vada, dirò che ne è valsa la pena di stare con te.

References

[1] I. P. C. C., *Chapter 10: Detection and Attribution of Climate Change.* Cambridge university press, 2016.

[2] I. E. A., *World Energy Outlook 2016.* International Energy Agency, 2016.

[3] J. Freidberg, *Plasma Physics and Fusion Energy.* Cambridge university press, 2007.

[4] T. Donné, W. Morris *et al.*, *European Research Roadmap to the Realisation of Fusion Energy.* EUROfusion, 2018.

[5] S. Ciattaglia, G. Federici, L. Barucca, A. Lampasi, S. Minucci, and I. Moscato, "The european DEMO fusion reactor: Design status and challenges from balance of plant point of view," *2017 IEEE International Conference on Environment and Electrical Engineering and 2017 IEEE Industrial and Commercial Power Systems Europe (EEEIC / I&CPS Europe),* 2018. [Online]. Available: https://ieeexplore.ieee.org/document/7977853

[6] M. Mattei, R. Ambrosino, and R. Albanese, "EM investigations of dynamic phases in DEMO," 2017, EUROfusion.

[7] A. Ferro and E. Gaio, "DEMO electrical system configuration and circuits."

[8] J. Tao, I. Benfatto, K. J. Goff, F. Mankani, A Milani, I. Song, H. Tan, and J. Thomsen, "ITER coil power supply and distribution system," *IEEE/INPSS 24th Symposium on Fusion Engineering,* 2011.

[9] E. Dick and C. Dustmann, "Inductive energy transfer using flying capacitor," *Proc. of Int. Conf. on Energy Storage, Compression, and Switching,* no. 485-89, 1976.

[10] H. Peterson, N. Mohan, W. Young, and R. Boom, "Superconductive inductor-converter units for pulsed power loads," *Proc. of Int. Conf. on Energy Storage, Compression, and Switching,* no. 485-89, 1976.

[11] R. Piovan, E. Gaio, F. Lunardon, and A. Maistrello, "MEST: a new Magnetic Eenergy Storage and Transfer system for improving the power handling in fusion experiments."

[12] G. Federici, "DEMO design activity in europe: Progress and updates," *Fusion Engineering and Design*, 2018. [Online]. Available: https://doi.org/10.1016/j.fusengdes.2018.04.001

[13] A. Ferro, F. Lunardon, S. Ciattaglia, and E. Gaio, "The reactive power demand in DEMO: estimations and study of mitigation via a novel design approach for base converters," *in press*, 2018.

[14] J. W. Tester, *Sustainable Energy*. The MIT press, 2004.

[15] ITER heating system. [Online]. Available: https://www.iter.org/mach/Heating

[16] J. You, E. Visca, C. Bachmann *et al.*, "European DEMO divertor target: operational requirements and material-design interface," 2016.

[17] M. Abdou, N. B. Morley, S. Smolentsev *et al.*, "Blanket/first wall challenges and required R&D on the pathway to DEMO," 2015.

[18] F. Cismondi, L. Boccaccini, G. Aiello *et al.*, "Progress in EU breeding blanket design and integration," 2018.

[19] T. N. Todd, "Pulsed DEMO design assessment studies," *EURATOM/CCFE Fusion Association, Culham Science Centre, Abingdon UK*, 2013.

[20] A. Lampasi *et al.*, "First switching network unit for the JT-60SA superconducting central solenoid," *Fusion Engineering and Design*, 2015.

[21] F. Burini, M. Pretelli, G. Taddia, S. Tenconi, A. Lampasi, and P. Zito, "Switching network units for high currents and voltages for plasma applications," *Proceedings of RuPAC2016, St. Petersburg, Russia*, 2016.

[22] A. Roshal *et al.*, "Design and analysis of switching network units for the ITER coil power supply system," *Fusion Engineering and Design*, 2011.

[23] F. Milani, A. Roshal, I. Benfatto, I. Song, and J. Thomsen, "System integration of the ITER switching network, fast discharge units and busbars," 2011.

[24] A. D. Mankani, I. Benfatto, J. Tao, J. Goff, J. Hourtoule, and J. Gascon, "The ITER Reactive Power Compensation and Harmonic Filtering (RPC & HF) System: Stability & Performance," *2011 IEEE/INPSS 24th Symposium on Fusion Engineering*, 2011.

[25] M. Guarnieri and A. Stella, *Principi e applicazioni di elettrotecnica*, terza ed.   Progetto Padova, 2004.

[26] F. Lunardon, "Studies on the reactive power demand in DEMO and mitigation strategies," 2017/2018, Tesi di laurea, Università degli Studi di Padova.

[27] N. Mohan, T. M. Undeland, and W. P. Robbins, *Elettronica di Potenza*, Hoepli, Ed., 2003.

Appendix A

All following data are taken from relation [6].

Table 5.1: Breakdown voltages of Central Solenoid sectors

t [s]	CS3U [V]	CS2U [V]	CS1 [V]	CS2L [V]	CS3L [V]
0,00	6000,00	-6000,00	12000,00	-6000,00	6000,00
0,01	6000,00	-5539,22	12000,00	-5698,72	6000,00
0,02	6000,00	-5078,44	12000,00	-5397,44	6000,00
0,02	6000,00	-4617,66	12000,00	-5096,16	6000,00
0,03	6000,00	-4156,88	12000,00	-4794,88	6000,00
0,04	6000,00	-3696,10	12000,00	-4493,60	6000,00
0,05	6000,00	-3235,32	12000,00	-4192,32	6000,00
0,06	6000,00	-2774,55	12000,00	-3891,04	6000,00
0,06	6000,00	-2313,77	12000,00	-3589,76	6000,00
0,07	6000,00	-1852,99	12000,00	-3288,48	6000,00
0,08	6000,00	-1392,21	12000,00	-2987,20	6000,00
0,09	6000,00	-1192,21	12000,00	-2787,20	6000,00
0,10	6000,00	-992,21	12000,00	-2587,20	6000,00
0,10	6000,00	-792,21	12000,00	-2387,20	6000,00
0,11	6000,00	-592,21	12000,00	-2187,20	6000,00
0,12	6000,00	-392,21	12000,00	-1987,20	6000,00
0,13	6000,00	-192,21	12000,00	-1787,20	6000,00
0,14	6000,00	7,79	12000,00	-1587,20	6000,00
0,14	6000,00	207,79	12000,00	-1387,20	6000,00
0,15	6000,00	407,79	12000,00	-1187,20	6000,00
0,16	6000,00	607,79	12000,00	-987,20	6000,00
0,17	6000,00	807,79	12000,00	-787,20	6000,00
0,18	6000,00	1007,79	12000,00	-587,20	6000,00
0,18	6000,00	1207,79	12000,00	-387,20	6000,00

Table 5.1 continued from previous page

0,19	6000,00	1407,79	12000,00	-187,20	6000,00
0,20	6000,00	1607,79	12000,00	12,80	6000,00
0,21	6000,00	1807,79	12000,00	212,80	6000,00
0,22	6000,00	2007,79	12000,00	412,80	6000,00
0,22	6000,00	2207,79	12000,00	612,80	6000,00
0,23	6000,00	2407,79	12000,00	812,80	6000,00
0,24	6000,00	2607,79	12000,00	1012,80	6000,00
0,25	6000,00	2807,79	12000,00	1212,80	6000,00
0,26	6000,00	3007,79	12000,00	1412,80	6000,00
0,26	6000,00	3207,79	12000,00	1612,80	6000,00
0,27	6000,00	3407,79	12000,00	1812,80	6000,00
0,28	6000,00	3607,79	12000,00	2012,80	6000,00
0,29	6000,00	3807,79	12000,00	2212,80	6000,00
0,30	6000,00	4007,79	12000,00	2412,80	6000,00
0,30	6000,00	4207,79	12000,00	2612,80	6000,00
0,31	6000,00	4407,79	12000,00	2812,80	6000,00
0,32	6000,00	4607,79	12000,00	3012,80	6000,00
0,33	5945,34	4547,01	12000,00	3212,80	6000,00
0,34	5890,68	4486,23	12000,00	3412,80	6000,00
0,34	5836,02	4425,45	12000,00	3612,80	6000,00
0,35	5781,36	4364,68	12000,00	3812,80	6000,00
0,36	5726,70	4303,90	12000,00	4012,80	6000,00
0,37	5672,04	4243,12	12000,00	4212,80	6000,00
0,38	5617,38	4182,34	12000,00	4412,80	6000,00
0,38	5562,72	4121,56	12000,00	4612,80	6000,00
0,39	5508,06	4060,78	12000,00	4812,80	6000,00
0,40	5453,40	4000,00	12000,00	5012,80	6000,00
0,41	5253,40	3800,00	11764,92	5086,60	6000,00
0,42	5053,40	3600,00	11529,84	5160,39	6000,00
0,42	4853,40	3400,00	11294,76	5234,18	6000,00
0,43	4653,40	3200,00	11059,69	5307,98	6000,00
0,44	4453,40	3000,00	10824,61	5381,77	6000,00
0,45	4253,40	2800,00	10589,53	5455,57	6000,00

Table 5.1 continued from previous page

0,46	4053,40	2600,00	10354,45	5529,36	6000,00
0,46	3853,40	2400,00	10119,37	5603,15	6000,00
0,47	3653,40	2200,00	9884,29	5676,95	6000,00
0,48	3453,40	2000,00	9649,22	5750,74	6000,00
0,49	3253,40	1800,00	9249,22	5550,74	6000,00
0,50	3053,40	1600,00	8849,22	5350,74	6000,00
0,50	2853,40	1400,00	8449,22	5150,74	6000,00
0,51	2653,40	1200,00	8049,22	4950,74	6000,00
0,52	2453,40	1000,00	7649,22	4750,74	6000,00
0,53	2253,40	800,00	7249,22	4550,74	6000,00
0,54	2053,40	600,00	6849,22	4350,74	6000,00
0,54	1853,40	400,00	6449,22	4150,74	6000,00
0,55	1653,40	200,00	6049,22	3950,74	6000,00
0,56	1453,40	0,00	5649,22	3750,74	6000,00
0,57	1253,40	-200,00	5249,22	3550,74	6000,00
0,58	1053,40	-400,00	4849,22	3350,74	6000,00
0,58	853,40	-600,00	4449,22	3150,74	6000,00
0,59	653,40	-800,00	4049,22	2950,74	6000,00
0,60	453,40	-1000,00	3649,22	2750,74	6000,00
0,61	253,40	-1200,00	3249,22	2550,74	6000,00
0,62	53,40	-1400,00	2849,22	2350,74	6000,00
0,62	-146,60	-1600,00	2449,22	2150,74	6000,00
0,63	-346,60	-1800,00	2049,22	1950,74	6000,00
0,64	-546,60	-2000,00	1649,22	1750,74	6000,00
0,65	-746,60	-2200,00	1249,22	1550,74	5800,00
0,66	-946,60	-2400,00	849,22	1350,74	5600,00
0,66	-1146,60	-2600,00	449,22	1150,74	5400,00
0,67	-1346,60	-2800,00	49,22	950,74	5200,00
0,68	-1546,60	-3000,00	-350,78	750,74	5000,00
0,69	-1746,60	-3200,00	-750,78	550,74	4800,00
0,70	-1946,60	-3400,00	-1150,78	350,74	4600,00
0,70	-2146,60	-3600,00	-1550,78	150,74	4400,00
0,71	-2346,60	-3800,00	-1950,78	-49,26	4200,00

Table 5.1 continued from previous page

0,72	-2546,60	-4000,00	-2350,78	-249,26	4000,00
0,73	-2746,60	-4200,00	-2750,78	-449,26	3800,00
0,74	-2946,60	-4400,00	-3150,78	-649,26	3600,00
0,74	-3146,60	-4600,00	-3550,78	-849,26	3400,00
0,75	-3346,60	-4800,00	-3950,78	-1049,26	3200,00
0,76	-3546,60	-5000,00	-4350,78	-1249,26	3000,00
0,77	-3746,60	-5200,00	-4750,78	-1449,26	2800,00
0,78	-3946,60	-5400,00	-5150,78	-1649,26	2600,00
0,78	-4146,60	-5600,00	-5550,78	-1849,26	2400,00
0,79	-4346,60	-5800,00	-5950,78	-2049,26	2200,00
0,80	-4546,60	-6000,00	-6350,78	-2249,26	2000,00
0,81	-4691,94	-6000,00	-6750,78	-2449,26	1800,00
0,82	-4837,28	-6000,00	-7150,78	-2649,26	1600,00
0,82	-4982,62	-6000,00	-7550,78	-2849,26	1400,00
0,83	-5127,96	-6000,00	-7950,78	-3049,26	1200,00
0,84	-5273,30	-6000,00	-8350,78	-3249,26	1000,00
0,85	-5418,64	-6000,00	-8750,78	-3449,26	800,00
0,86	-5563,98	-6000,00	-9150,78	-3649,26	600,00
0,86	-5709,32	-6000,00	-9550,78	-3849,26	400,00
0,87	-5854,66	-6000,00	-9950,78	-4049,26	200,00
0,88	-6000,00	-6000,00	-10350,78	-4249,26	0,00
0,89	-6000,00	-6000,00	-10501,57	-4424,33	-200,00
0,90	-6000,00	-6000,00	-10652,35	-4599,41	-400,00
0,90	-6000,00	-6000,00	-10803,13	-4774,48	-600,00
0,91	-6000,00	-6000,00	-10953,91	-4949,56	-800,00
0,92	-6000,00	-6000,00	-11104,69	-5124,63	-1000,00
0,93	-6000,00	-6000,00	-11255,47	-5299,70	-1200,00
0,94	-6000,00	-6000,00	-11406,25	-5474,78	-1400,00
0,94	-6000,00	-6000,00	-11557,03	-5649,85	-1600,00
0,95	-6000,00	-6000,00	-11707,81	-5824,93	-1800,00
0,96	-6000,00	-6000,00	-11858,60	-6000,00	-2000,00
0,97	-6000,00	-6000,00	-11458,60	-6000,00	-2200,00
0,98	-6000,00	-6000,00	-11058,60	-6000,00	-2400,00

Table 5.1 continued from previous page

0,98	-6000,00	-6000,00	-10658,60	-6000,00	-2600,00
0,99	-6000,00	-6000,00	-10258,60	-6000,00	-2800,00
1,00	-6000,00	-6000,00	-9858,60	-6000,00	-3000,00
1,01	-6000,00	-6000,00	-9458,60	-6000,00	-3200,00
1,02	-6000,00	-6000,00	-9058,60	-6000,00	-3400,00
1,02	-6000,00	-6000,00	-8658,60	-6000,00	-3600,00
1,03	-6000,00	-6000,00	-8258,60	-6000,00	-3800,00
1,04	-6000,00	-6000,00	-7858,60	-6000,00	-4000,00
1,05	-6000,00	-6000,00	-7458,60	-6000,00	-4200,00
1,06	-6000,00	-6000,00	-7058,60	-6000,00	-4400,00
1,06	-6000,00	-6000,00	-6658,60	-6000,00	-4600,00
1,07	-6000,00	-6000,00	-6258,60	-6000,00	-4800,00
1,08	-6000,00	-6000,00	-5858,60	-6000,00	-5000,00
1,09	-6000,00	-6000,00	-5458,60	-6000,00	-5200,00
1,10	-6000,00	-6000,00	-5058,60	-6000,00	-5400,00
1,10	-6000,00	-6000,00	-4658,60	-6000,00	-5600,00
1,11	-6000,00	-6000,00	-4258,60	-6000,00	-5800,00
1,12	-6000,00	-6000,00	-3858,60	-6000,00	-6000,00
1,13	-6000,00	-6000,00	-4149,18	-6000,00	-6000,00
1,14	-6000,00	-6000,00	-4439,77	-6000,00	-6000,00
1,14	-6000,00	-6000,00	-4730,36	-6000,00	-6000,00
1,15	-6000,00	-6000,00	-5020,94	-6000,00	-6000,00
1,16	-6000,00	-6000,00	-5311,53	-6000,00	-6000,00
1,17	-6000,00	-6000,00	-5602,12	-6000,00	-6000,00
1,18	-6000,00	-6000,00	-5892,70	-6000,00	-6000,00
1,18	-6000,00	-6000,00	-6183,29	-6000,00	-6000,00
1,19	-6000,00	-6000,00	-6473,88	-6000,00	-6000,00
1,20	-6000,00	-6000,00	-6764,46	-6000,00	-6000,00
1,21	-6000,00	-6000,00	-6796,52	-6000,00	-6000,00
1,22	-6000,00	-6000,00	-6828,58	-6000,00	-6000,00
1,22	-6000,00	-6000,00	-6860,64	-6000,00	-6000,00
1,23	-6000,00	-6000,00	-6892,70	-6000,00	-6000,00
1,24	-6000,00	-6000,00	-6924,76	-6000,00	-6000,00

Table 5.1 continued from previous page

1,25	-6000,00	-6000,00	-6956,82	-6000,00	-6000,00
1,26	-6000,00	-6000,00	-6988,89	-6000,00	-6000,00
1,26	-6000,00	-6000,00	-7020,95	-6000,00	-6000,00
1,27	-6000,00	-6000,00	-7053,01	-6000,00	-6000,00
1,28	-6000,00	-6000,00	-7085,07	-6000,00	-6000,00
1,29	-6000,00	-6000,00	-7398,32	-6000,00	-6000,00
1,30	-6000,00	-6000,00	-7711,58	-6000,00	-6000,00
1,30	-6000,00	-6000,00	-8024,84	-6000,00	-6000,00
1,31	-6000,00	-6000,00	-8338,10	-6000,00	-6000,00
1,32	-6000,00	-6000,00	-8651,36	-6000,00	-6000,00
1,33	-6000,00	-6000,00	-8964,61	-6000,00	-6000,00
1,34	-6000,00	-6000,00	-9277,87	-6000,00	-6000,00
1,34	-6000,00	-6000,00	-9591,13	-6000,00	-6000,00
1,35	-6000,00	-6000,00	-9904,39	-6000,00	-6000,00
1,36	-6000,00	-6000,00	-10217,65	-6000,00	-6000,00
1,37	-6000,00	-6000,00	-7995,88	-6000,00	-6000,00
1,38	-6000,00	-6000,00	-5774,12	-6000,00	-6000,00
1,38	-6000,00	-6000,00	-3552,35	-6000,00	-6000,00
1,39	-6000,00	-6000,00	-1330,59	-6000,00	-6000,00
1,40	-6000,00	-6000,00	891,18	-6000,00	-6000,00
1,41	-6000,00	-6000,00	3112,94	-6000,00	-6000,00
1,42	-6000,00	-6000,00	5334,71	-6000,00	-6000,00
1,42	-6000,00	-6000,00	7556,47	-6000,00	-6000,00
1,43	-6000,00	-6000,00	9778,24	-6000,00	-6000,00
1,44	-6000,00	-6000,00	12000,00	-6000,00	-6000,00

Table 5.2: Breakdown voltages of Poloidal Field coils

t [s]	PF1 [V]	PF2 [V]	PF3 [V]	PF4 [V]	PF5 [V]
0,00	6000,00	9000,00	9000,00	9000,00	9000,00
0,01	6000,00	9000,00	9000,00	9000,00	9000,00
0,02	6000,00	9000,00	9000,00	9000,00	9000,00
0,02	6000,00	9000,00	9000,00	9000,00	9000,00
0,03	6000,00	9000,00	9000,00	9000,00	9000,00
0,04	6000,00	9000,00	9000,00	9000,00	9000,00
0,05	6000,00	9000,00	9000,00	9000,00	9000,00
0,06	6000,00	9000,00	9000,00	9000,00	9000,00
0,06	6000,00	9000,00	9000,00	9000,00	9000,00
0,07	6000,00	9000,00	9000,00	9000,00	9000,00
0,08	6000,00	9000,00	9000,00	9000,00	9000,00
0,09	6000,00	9000,00	9000,00	9000,00	9000,00
0,10	6000,00	9000,00	9000,00	9000,00	9000,00
0,10	6000,00	9000,00	9000,00	9000,00	9000,00
0,11	6000,00	9000,00	9000,00	9000,00	9000,00
0,12	6000,00	9000,00	9000,00	9000,00	9000,00
0,13	6000,00	9000,00	9000,00	9000,00	9000,00
0,14	6000,00	9000,00	9000,00	9000,00	9000,00
0,14	6000,00	9000,00	9000,00	9000,00	9000,00
0,15	6000,00	9000,00	9000,00	9000,00	9000,00
0,16	6000,00	9000,00	9000,00	9000,00	9000,00
0,17	6000,00	9000,00	9000,00	9000,00	9000,00
0,18	6000,00	9000,00	9000,00	9000,00	9000,00
0,18	6000,00	9000,00	9000,00	9000,00	9000,00
0,19	6000,00	9000,00	9000,00	9000,00	9000,00
0,20	6000,00	9000,00	9000,00	9000,00	9000,00
0,21	6000,00	9000,00	9000,00	9000,00	9000,00
0,22	6000,00	9000,00	9000,00	9000,00	9000,00
0,22	6000,00	9000,00	9000,00	9000,00	9000,00
0,23	6000,00	9000,00	9000,00	9000,00	9000,00
0,24	6000,00	9000,00	9000,00	9000,00	9000,00

Table 5.2 continued from previous page

0,25	6000,00	9000,00	9000,00	9000,00	9000,00
0,26	6000,00	9000,00	9000,00	9000,00	9000,00
0,26	6000,00	9000,00	9000,00	9000,00	9000,00
0,27	6000,00	9000,00	9000,00	9000,00	9000,00
0,28	6000,00	9000,00	9000,00	9000,00	9000,00
0,29	6000,00	9000,00	9000,00	9000,00	9000,00
0,30	6000,00	9000,00	9000,00	9000,00	9000,00
0,30	6000,00	9000,00	9000,00	9000,00	9000,00
0,31	6000,00	9000,00	9000,00	9000,00	9000,00
0,32	6000,00	9000,00	9000,00	9000,00	9000,00
0,33	6000,00	9000,00	9000,00	9000,00	9000,00
0,34	6000,00	9000,00	9000,00	9000,00	9000,00
0,34	6000,00	9000,00	9000,00	9000,00	9000,00
0,35	6000,00	9000,00	9000,00	9000,00	9000,00
0,36	6000,00	9000,00	9000,00	9000,00	9000,00
0,37	6000,00	9000,00	9000,00	9000,00	9000,00
0,38	6000,00	9000,00	9000,00	9000,00	9000,00
0,38	6000,00	9000,00	9000,00	9000,00	9000,00
0,39	6000,00	9000,00	9000,00	9000,00	9000,00
0,40	6000,00	9000,00	9000,00	9000,00	9000,00
0,41	5800,00	9000,00	8728,99	9000,00	9000,00
0,42	5600,00	9000,00	8457,97	9000,00	9000,00
0,42	5400,00	9000,00	8186,96	9000,00	9000,00
0,43	5200,00	9000,00	7915,95	9000,00	9000,00
0,44	5000,00	9000,00	7644,93	9000,00	9000,00
0,45	4800,00	9000,00	7373,92	9000,00	9000,00
0,46	4600,00	9000,00	7102,91	9000,00	9000,00
0,46	4400,00	9000,00	6831,90	9000,00	9000,00
0,47	4200,00	9000,00	6560,88	9000,00	9000,00
0,48	4000,00	9000,00	6289,87	9000,00	9000,00
0,49	3800,00	9000,00	5989,87	9000,00	9000,00
0,50	3600,00	9000,00	5689,87	9000,00	9000,00
0,50	3400,00	9000,00	5389,87	9000,00	9000,00

Table 5.2 continued from previous page

0,51	3200,00	9000,00	5089,87	9000,00	9000,00
0,52	3000,00	9000,00	4789,87	9000,00	9000,00
0,53	2800,00	9000,00	4489,87	9000,00	9000,00
0,54	2600,00	9000,00	4189,87	9000,00	9000,00
0,54	2400,00	9000,00	3889,87	9000,00	9000,00
0,55	2200,00	9000,00	3589,87	9000,00	9000,00
0,56	2000,00	9000,00	3289,87	9000,00	9000,00
0,57	1800,00	8909,43	2989,87	9000,00	9000,00
0,58	1600,00	8818,86	2689,87	9000,00	9000,00
0,58	1400,00	8728,29	2389,87	9000,00	9000,00
0,59	1200,00	8637,72	2089,87	9000,00	9000,00
0,60	1000,00	8547,15	1789,87	9000,00	9000,00
0,61	800,00	8456,58	1489,87	9000,00	9000,00
0,62	600,00	8366,01	1189,87	9000,00	9000,00
0,62	400,00	8275,44	889,87	9000,00	9000,00
0,63	200,00	8184,87	589,87	9000,00	9000,00
0,64	0,00	8094,30	289,87	9000,00	9000,00
0,65	-200,00	7794,30	-10,13	9000,00	9000,00
0,66	-400,00	7494,30	-310,13	9000,00	9000,00
0,66	-600,00	7194,30	-610,13	9000,00	9000,00
0,67	-800,00	6894,30	-910,13	9000,00	9000,00
0,68	-1000,00	6594,30	-1210,13	9000,00	9000,00
0,69	-1200,00	6294,30	-1510,13	9000,00	9000,00
0,70	-1400,00	5994,30	-1810,13	9000,00	9000,00
0,70	-1600,00	5694,30	-2110,13	9000,00	9000,00
0,71	-1800,00	5394,30	-2410,13	9000,00	9000,00
0,72	-2000,00	5094,30	-2710,13	9000,00	9000,00
0,73	-2200,00	4794,30	-3010,13	8700,00	9000,00
0,74	-2400,00	4494,30	-3310,13	8400,00	9000,00
0,74	-2600,00	4194,30	-3610,13	8100,00	9000,00
0,75	-2800,00	3894,30	-3910,13	7800,00	9000,00
0,76	-3000,00	3594,30	-4210,13	7500,00	9000,00
0,77	-3200,00	3294,30	-4510,13	7200,00	9000,00

Table 5.2 continued from previous page

0,78	-3400,00	2994,30	-4810,13	6900,00	9000,00
0,78	-3600,00	2694,30	-5110,13	6600,00	9000,00
0,79	-3800,00	2394,30	-5410,13	6300,00	9000,00
0,80	-4000,00	2094,30	-5710,13	6000,00	9000,00
0,81	-4200,00	1862,44	-5490,32	6092,82	9000,00
0,82	-4400,00	1630,57	-5270,50	6185,64	9000,00
0,82	-4600,00	1398,71	-5050,69	6278,45	9000,00
0,83	-4800,00	1166,84	-4830,88	6371,27	9000,00
0,84	-5000,00	934,98	-4611,06	6464,09	9000,00
0,85	-5200,00	703,11	-4391,25	6556,91	9000,00
0,86	-5400,00	471,24	-4171,44	6649,72	9000,00
0,86	-5600,00	239,38	-3951,62	6742,54	9000,00
0,87	-5800,00	7,51	-3731,81	6835,36	9000,00
0,88	-6000,00	-224,35	-3511,99	6928,18	9000,00
0,89	-6000,00	75,65	-3211,99	6628,18	9000,00
0,90	-6000,00	375,65	-2911,99	6328,18	9000,00
0,90	-6000,00	675,65	-2611,99	6028,18	9000,00
0,91	-6000,00	975,65	-2311,99	5728,18	9000,00
0,92	-6000,00	1275,65	-2011,99	5428,18	9000,00
0,93	-6000,00	1575,65	-1711,99	5128,18	9000,00
0,94	-6000,00	1875,65	-1411,99	4828,18	9000,00
0,94	-6000,00	2175,65	-1111,99	4528,18	9000,00
0,95	-6000,00	2475,65	-811,99	4228,18	9000,00
0,96	-6000,00	2775,65	-511,99	3928,18	9000,00
0,97	-6000,00	2948,21	-211,99	3770,54	9000,00
0,98	-6000,00	3120,76	88,01	3612,89	9000,00
0,98	-6000,00	3293,32	388,01	3455,25	9000,00
0,99	-6000,00	3465,88	688,01	3297,61	9000,00
1,00	-6000,00	3638,44	988,01	3139,97	9000,00
1,01	-6000,00	3811,00	1288,01	2982,33	9000,00
1,02	-6000,00	3983,56	1588,01	2824,69	9000,00
1,02	-6000,00	4156,12	1888,01	2667,05	9000,00
1,03	-6000,00	4328,68	2188,01	2509,41	9000,00

Table 5.2 continued from previous page

1,04	-6000,00	4501,24	2488,01	2351,77	9000,00
1,05	-5940,93	4201,24	2788,01	2651,77	9000,00
1,06	-5881,86	3901,24	3088,01	2951,77	9000,00
1,06	-5822,79	3601,24	3388,01	3251,77	9000,00
1,07	-5763,72	3301,24	3688,01	3551,77	9000,00
1,08	-5704,65	3001,24	3988,01	3851,77	9000,00
1,09	-5645,58	2701,24	4288,01	4151,77	9000,00
1,10	-5586,51	2401,24	4588,01	4451,77	9000,00
1,10	-5527,43	2101,24	4888,01	4751,77	9000,00
1,11	-5468,36	1801,24	5188,01	5051,77	9000,00
1,12	-5409,29	1501,24	5488,01	5351,77	9000,00
1,13	-5209,29	1796,41	5188,01	5336,03	9000,00
1,14	-5009,29	2091,58	4888,01	5320,29	9000,00
1,14	-4809,29	2386,75	4588,01	5304,55	9000,00
1,15	-4609,29	2681,92	4288,01	5288,81	9000,00
1,16	-4409,29	2977,09	3988,01	5273,07	9000,00
1,17	-4209,29	3272,27	3688,01	5257,33	9000,00
1,18	-4009,29	3567,44	3388,01	5241,59	9000,00
1,18	-3809,29	3862,61	3088,01	5225,85	9000,00
1,19	-3609,29	4157,78	2788,01	5210,11	9000,00
1,20	-3409,29	4452,95	2488,01	5194,37	9000,00
1,21	-3254,27	4189,51	2273,97	5067,95	9000,00
1,22	-3099,26	3926,08	2059,94	4941,54	9000,00
1,22	-2944,24	3662,64	1845,91	4815,12	9000,00
1,23	-2789,22	3399,20	1631,88	4688,71	9000,00
1,24	-2634,20	3135,76	1417,84	4562,29	9000,00
1,25	-2479,18	2872,32	1203,81	4435,87	9000,00
1,26	-2324,16	2608,88	989,78	4309,46	9000,00
1,26	-2169,14	2345,44	775,75	4183,04	9000,00
1,27	-2014,13	2082,01	561,71	4056,63	9000,00
1,28	-1859,11	1818,57	347,68	3930,21	9000,00
1,29	-2059,11	2062,86	647,68	4082,76	9000,00
1,30	-2259,11	2307,16	947,68	4235,31	9000,00

Table 5.2 continued from previous page

1,30	-2459,11	2551,46	1247,68	4387,86	9000,00
1,31	-2659,11	2795,75	1547,68	4540,41	9000,00
1,32	-2859,11	3040,05	1847,68	4692,96	9000,00
1,33	-3059,11	3284,35	2147,68	4845,51	9000,00
1,34	-3259,11	3528,64	2447,68	4998,07	9000,00
1,34	-3459,11	3772,94	2747,68	5150,62	9000,00
1,35	-3659,11	4017,24	3047,68	5303,17	9000,00
1,36	-3859,11	4261,53	3347,68	5455,72	9000,00
1,37	-4073,20	2935,38	3912,91	4010,14	9000,00
1,38	-4287,29	1609,23	4478,15	2564,57	9000,00
1,38	-4501,38	283,07	5043,38	1119,00	9000,00
1,39	-4715,46	-1043,08	5608,61	-326,57	9000,00
1,40	-4929,55	-2369,23	6173,84	-1772,14	9000,00
1,41	-5143,64	-3695,39	6739,07	-3217,71	9000,00
1,42	-5357,73	-5021,54	7304,30	-4663,29	9000,00
1,42	-5571,82	-6347,69	7869,54	-6108,86	9000,00
1,43	-5785,91	-7673,85	8434,77	-7554,43	9000,00
1,44	-6000,00	-9000,00	9000,00	-9000,00	9000,00

Table 5.3: Ramp-up currents of plasma and Central Solenoid sectors

Time [s]	Ipl [MA]	ICS3U [kA]	ICS2U	ICS1	ICS2L	ICS3L
0	5	28,79	27,63	23,98	26,40	38,15
25	7,5	28,23	20,15	16,46	17,66	34,52
50	10	28,48	14,19	10,35	12,19	33,10
75	12,5	28,27	7,39	2,65	6,65	31,01
100	15	28,53	1,20	-4,16	2,37	30,10
125	17,5	29,24	-4,36	-11,91	-2,86	29,05
146	19,6	29,53	-9,47	-18,98	-7,83	27,68

Table 5.4: Ramp-up voltages of Central Solenoid sectors

Time [s]	CS3U [V]	CS2U	CS1	CS2L	CS3L
0	-415,51	-925,25	-2174,16	-1063,21	-586,54
25	-128,72	-345,91	-821,85	-339,39	-151,02
50	-116,45	-279,96	-687,13	-261,38	-137,77
75	-65,85	-182,03	-443,95	-153,36	-68,33
100	-44,76	-141,15	-399,59	-145,62	-64,51
125	-41,41	-113,66	-317,01	-119,74	-58,49
146					

Table 5.5: Ramp-down currents of plasma and Central Solenoid sectors

Time [s]	Ipl [MA]	ICS3U [kA]	ICS2U	ICS1	ICS2L	ICS3L
0	19,6	-3,71	-37,61	-40,11	-39,30	-16,71
25	17,5	7,44	-45,00	-45,00	-34,05	-17,73
50	15,0	-11,10	-35,43	-44,05	-24,43	-29,74
75	12,5	-14,67	-30,79	-41,61	-19,31	-37,31
100	10,0	-25,83	-24,73	-37,71	-15,96	-40,73
125	7,5	-17,86	-18,54	-33,73	-14,95	-41,21
146	5,0	-27,57	-5,43	-30,03	-10,28	-41,71

Table 5.6: Ramp-down voltages of Central Solenoid sectors

Time [s]	CS3U [V]	CS2U	CS1	CS2L	CS3L
0	579,49	-619,67	-1297,12	215,99	-83,12
25	-1118,23	304,67	474,24	446,32	-716,72
50	-192,23	297,29	620,81	258,56	-464,35
75	-636,10	304,84	921,68	269,36	-187,52
100	470,93	669,86	973,23	176,05	-4,65
125	-549,08	840,48	1169,50	458,08	73,04
146					